THE DEVELOPMENT OF PRECISION STATEMENTS FOR SEVERAL ASTM TEST METHODS

MAY 1963

NO. 12

Joint Highway Research Project

PURDUE UNIVERSITY
LAFAYETTE INDIANA

by

S.J. HANNA

and

J.F. McLAUGHLIN

Technical Paper

THE DEVELOPMENT OF PRECISION STATEMENTS FOR SEVERAL ASTM TEST METHODS

TO: K. B. Woods, Director
Joint Highway Research Project

May 8, 1963

FROM: H. L. Michael, Associate Director
Joint Highway Research Project

File: 5-15-1
Project: C-36-65A

Attached is a Technical Paper entitled "The Development of Precision Statements for Several ASTM Test Methods" by S. J. Hanna and J. F. McLaughlin.

This paper is a summary of the final report of the same title which was presented to the Board several months ago. The paper is to be presented at the Annual Meeting of the American Society for Testing and Materials.

The paper is presented to the Board for the record with the recommendation that publication by the American Society for Testing and Materials be authorized.

Respectfully submitted,

Harold L. Michael/kmc

Harold L. Michael, Secretary

HLM:kmc

Attachment

Copy:

F. L. Ashbaucher
J. R. Cooper
W. L. Dolch
W. H. Goetz
F. F. Havey
F. S. Hill
G. A. Leonards
J. F. McLaughlin
R. D. Miles
R. E. Mills
M. B. Scott
J. V. Smythe
J. L. Waling
E. J. Yoder

Technical Paper

THE DEVELOPMENT OF PRECISION STATEMENTS FOR SEVERAL ASTM TEST METHODS

by

S. J. Hanna

and

J. F. McLaughlin

Joint Highway Research Project
File No: 5-15-1
Project No: C-36-65A

Purdue University
Lafayette, Indiana

May 8, 1963

INTRODUCTION

Many standard methods of test for concrete and concrete aggregates contain little or no information that will give the user of the test method a quantitative indication of how well individual test results of a series ought to agree with each other or how well test results from different laboratories, on supposedly "identical" samples, ought to agree. Such a statement might be called a "precision statement." It has been suggested that some form of precision statement be included in ASTM Test Methods.

In a recent report to Subcommittee II-a (Evaluation of Data) of ASTM Committee C-9 (14)* it was suggested that ASTM designations be divided into four classes or groups. They are as follows:

Group I - Methods of tests for which it appears possible to obtain a measure of repeatability and reproducibility having little or no sample variance either by repeating the test on the same sample or by making synthetic samples.

Group II - Methods for which the measure of repeatability and reproducibility will necessarily include a component of variability introduced by sampling. That is, the method cannot be applied a number of times to the same sample and it does not appear that synthetic samples can be made.

Group III - Methods of test in which multiple specimens are required. These methods might possibly be

* Numbers in parenthesis refers to references listed in the bibliography.

classified with those of Group II but some differences should be recognized.

Group IV - Specifications and miscellaneous designations for which no statement of precision is needed.

In any test method there are many variables, some of which are inherent in the method itself and others that are the result of outside influence. Several of the components of variance that are present can be easily noted. There may be within-laboratory variance caused by differences in equipment, operators, etc. There may be between-laboratory variance and variance caused by sample-to-sample differences. Finally there is the variability introduced by the method itself and that due to differences in materials.

Not every ASTM designation requires precision statements of the type under consideration. It is those "... methods-of-test specifications wherein apparatus and procedure is defined for evaluating a magnitude or a property that precision statements are needed. Such precision statements should define, within stated confidence limits, the maximum and the normal deviation between test results that may be expected of the test method in question when performed by experienced operators." (5). The ASTM Manual on Quality Control of Material (2) contains a section entitled "Presenting ± Limits of Uncertainty of an Observed Average." The necessary components of a precision statement can be determined using these two references as a basis. They seem to be: The ± limits for a variable, the confidence level at which these limits apply, and the degrees of freedom associated with the determination of the limits. Since these limits are determined by statistical analysis

of the data and sample statistics are used it is necessary to use the "Student's t" in determining confidence limits. This is mentioned by Kaplan (11) in his analysis and is generally discussed in detail in most statistical texts (i.e. 15).

A precision statement can be of great value to the user of the test. The limits provide a range of values in which the results of a duplicate test should lie with a certain probability. The operator is given a criterion for deciding if something has gone wrong. The variability of the test results, when compared with the expected variability, can give an indication of how well the test is being performed. That is, is the operator using the proper techniques and is he being accurate enough and careful enough in his measurements?

If the repeatability and reproducibility of the test method is known, it is then possible to compare results of different operators and laboratories on a rational basis. Errors that are not within the inherent error of the process or method can be discerned and with a knowledge that excessive errors are present the situation can be analyzed accordingly.

PURPOSE AND SCOPE

The primary purpose of this investigation was to illustrate an experimental design with appropriate analyses by which data could be collected to formulate precision statements for certain classes of ASTM Test Methods. A secondary purpose or a result deriving from the primary purpose was the development of precision statements for the specific methods selected for illustration. Detailed procedures are given which illustrate the general approach.

Statistical analyses of the data were made and from these, confidence limits and control limits were determined at the 95 and 99 percent confidence levels. The investigation was intended to determine the within-laboratory precision of the test methods for different operators following exactly the procedures for the methods as given in the ASTM Standards. During the testing a careful analysis of the testing procedure was made to determine if the method is adequate and if the desired results are achieved by the procedure.

Since precision statements (as they have been defined) contain confidence intervals and degrees of freedom it was necessary to evaluate the means and variances of the test results. From these, limits on the sample statistics were determined for the two confidence levels.

Three ASTM Test Methods falling in Group I (as previously defined) were used, namely;

1. C 117-49 Test for Amount of Material Finer than No. 200 Sieve in Aggregate
2. C 127-59 Test for Specific Gravity and Absorption of Coarse Aggregate
3. C 128-57 Test for Specific Gravity and Absorption of Fine Aggregates.

STATISTICAL PROCEDURES

To accomplish the stated objective there are, generally speaking, many experimental designs that could be used. The choice of the model must be made by the experimentor but the choice will necessarily be influenced by the information being sought, the flexibility and the economy of the model. Careful study of the problem before testing has begun will eliminate the gathering of data that will be useless for the testing of the experimentor's hypothesis.

In keeping with this line of thought, each test method was examined to determine variables present and a model for each method was selected so as to give the desired information. For the three methods investigated, the use of factorial models seemed to be advantageous. Ostle, (12) in his discussion of factorial models states the following advantages and disadvantages:

Advantages:

1. Greater efficiency in the use of available experimental resources is achieved.
2. Information is obtained about the various interactions.

3. The experimental results are applicable over a wider range of conditions; that is, due to the combining of the various factors in one experiment the results are of a more comprehensive nature.
4. There is a gain due to the hidden replication arising from the factorial arrangement.

Disadvantages:

1. The experimental setup and the resulting statistical analysis are more complex.
2. With a large number of treatment combinations the selection of homogeneous experimental units becomes more difficult.
3. Certain of the treatment combinations may be of little or no interest; consequently, some of the experimental resources may be wasted.

It appeared that the advantages far outweigh the disadvantages.

In this investigation sampling variation was eliminated by performing the test on the same sample a number of times. Since different operators would be using the test method, operators were included as a random variable. Type of material was also included as a random variable. In addition, the amount of minus 200 material was included as a variable for test method C 117-49. The range from 1% to 10% minus 200 material was chosen as being of primary importance and four levels were selected within this range. This

variable was determined to be a fixed variable since the extremes were represented and two other levels covered the range sufficiently.

The following is the mathematical model for Test Method C 117-49. The mathematical models for C 127-59 and C 128-57 are similar to this model except that there are two main effects rather than three. This naturally eliminates all terms containing the main effect symbol. The experimental error is then a function of three terms (replicates, main effect 1, and main effect 2).

Mathematical Model for C 117-49

$$Y_{ijkl} = \mu + \rho_i + \alpha_j + \beta_k + \gamma_l + (\alpha\beta)_{jk} + (\alpha\gamma)_{jl} + (\beta\gamma)_{kl} + (\alpha\beta\gamma)_{jkl} + \epsilon_{ijkl}$$

Y_{ijkl} = an individual observation in the ith replicate, in the jth level of factor a, in the kth level of factor b, and in the lth level of factor c

μ = the true mean value

ρ_i = effect of the ith replicate

α_j = effect of the jth level of factor a (material)

β_k = effect of the kth level of factor b (amount)

γ_l = effect of the lth level of factor c (operators)

$(\alpha\gamma)_{jl}$ = effect of the interaction of the jth level of factor a with the lth level of factor c

$(\alpha\beta)_{jk}$ = effect of the interaction of the jth level of factor a with the kth level of factor b

$(\beta\gamma)_{kl}$ = effect of the interaction of the kth level of factor b with the lth level of factor c

$(\alpha\beta\gamma)_{jkl}$ = effect of interaction of the three levels of factors

ϵ_{ijkl} = effect of the experimental unit in the ith replicate

to which the (jkl)th treatment combination has been randomly assigned,

and the terms α_j, γ_1, $(\alpha\gamma)_{j1}$ and ϵ_{ijkl} are assumed to be independently normally distributed with expected values of 0 and variances σ_α^2, σ_γ^2, $\sigma_{\alpha\gamma}^2$, and σ^2 respectively,

and $\sum_{i=1}^{r} \rho_i = \sum_{k=1}^{4} \beta_k = \sum_{k=1}^{4} (\alpha\beta)_{jk} = \sum_{k=1}^{4} (\beta\gamma)_{kl} = \sum_{k=1}^{4} (\alpha\beta\gamma)_{jkl} = 0$

Prior to testing, an Analysis of Variance Table (ANOV) was formulated for each type method and the expected mean squares (EMS) were determined.

A Type I error, usually denoted by α, is committed if the hypothesis is rejected when it is actually true. Obviously one wishes to choose a test in which the probability of an error of this kind is small. It has been found generally acceptable in practice to use an α-level of 0.05, although this depends on the type of problem under consideration. For this study an α-level of 0.05 was used in performing F-tests.

The following equation was used in calculating the variance used in computing the control limits.

$$\text{Variance } (\bar{Y}_{jkl}) = n_\alpha^2 + n_\beta^2 + n_{\alpha\beta}^2 + n_\rho^2 + n_\epsilon^2$$

where:

σ_α^2 = Variance component due to α

σ_β^2 = Variance component due to β

σ_ρ^2 = Variance component due to ρ

$\sigma_{\alpha\beta}^2$ = Variance component due to the interaction of α and β

σ_ϵ^2 = Variance component due to experimental error

and,

n_α = number of a's = a

n_β = number of b's = b

$n_{\alpha\beta}$ = a times b

n_ρ = number of replicates = r

n_ϵ = total number of observations used to estimate variance ($\bar{Y}_{jkl}$), in this case abr.

The Variance ($\bar{Y}_{jkl}$) is used in computing control limits which are placed on the "grand" mean. If control limits are placed on means which are averaged over only one of the variables then the appropriate variance ($\bar{Y}_{\alpha}$) must be used. For example, if control limits are placed on means averaged over replicates only, the variance would be: Variance $(\bar{Y}_\rho) = \frac{\sigma_\rho^2}{n_\rho} + \frac{\sigma_\epsilon^2}{n_\epsilon}$. Where n is equal to the number of observations used to estimate the variance, in this case $n_\epsilon = n_\rho = r$.

PROCEDURES

The procedures detailed in the ASTM Standards were followed exactly by the operators when performing the tests. Two operators, acting independently, performed ten replicates for each test method investigated. The operators performed several practice tests to familiarize themselves with the method and test procedures before actual testing began.

From the data collected by the operators, sample means and sample variances were calculated. A statistical analysis was made on the data for each test method. Confidence limits were determined for 95 and 99 percent confidence levels. From the statistical analysis of the data, precision statements of various kinds could be formulated for each test method studied.

Test Method C 117-49

The purpose of C 117-49 is to determine the amount of material finer than the No. 200 sieve size in aggregate. Briefly the test

consists of washing a tared sample of aggregate over a No. 200 sieve and then drying it to a constant weight and determining, by weight, the percentage lost.

The material used in the performance of this test was local concrete sand of glacial origin. The sand was prepared by washing it over a No. 200 sieve several times to eliminate all material finer than that sieve size. The sand was dried to a constant weight and material finer than the No. 200 sieve was added to batches of it in amounts so as to produce 500.0 gram samples containing one, four, seven, and ten percent material finer than the No. 200 sieve.

Two types of minus 200 material were used in the investigation. In one series limestone dust, obtained from commercial limestone filler, was used. In the other series, a limestone-residual clay soil was the source of the fine material.* The limestone dust was chosen so as to represent a non-cohesive fine material and the clay was chosen so as to represent a very cohesive fine material.

For each replicate, eight samples were prepared and tested in random order. Each replicate contained samples representing the two material types and the four levels of each material. A table of random numbers was used to achieve the random order. This precaution was taken to eliminate any bias which might occur due to an ordered procedure of preparing and testing the samples. Replicates were made on different days to prevent any undue influence from the operator's "mood" on any one particular day from influencing the final results.

---

* Unified Soil Classification, CH.

Test Method C 127-59

The purpose of C 127-59 is to determine the twenty-four hour absorption and specific gravity of coarse aggregate. Briefly the test consists of immersing an oven dried sample of coarse aggregate in water for twenty-four hours, then determining its weight in water and its weight (SSD) in air. The sample is then dried to a constant weight and weighed. The absorption and specific gravity are then calculated.

Two materials were used in this experiment. One was a crushed limestone from a quarry near Bloomington, Indiana, the other was a local gravel. The coarse aggregates were graded so as to have equal amounts of material retained on the 1, 3/4, 1/2, 3/8 inch, and No. 4 sieves. They were sieved, washed and dried to a constant weight, then the various fractions were combined to form a 5000.0 gram sample.

For each replicate the two samples were tested by each operator. Replicate determinations were made on different days to prevent bias. Upon completion of the testing the two samples were again sieved and any change in weight of each fraction was noted.

Test Method C 128-57

The purpose of C 128-57 is to determine the twenty-four hour absorption and specific gravity of fine aggregate. Briefly the method consists of soaking a tared sample for twenty-four hours and at the end of this period drying the sample to a saturated surface dry condition where upon a 500.0 gram sample is immediately placed in a 500 ml flask. Enough water is added to bring the volume to 500 ml and the weight of water added is determined. The specific gravities and absorptions are calculated.

The material used for this was local concrete sand. The sand was washed to remove material finer than the No. 200 sieve, dried to a constant weight, and separated into various fractions using a logrithmic series of sieves. Sand from these fractions was then recombined to form samples having two gradations, one with a fineness modulus of 2.40 and the other a fineness modulus of 3.00. Each sample weighed 1000.0 grams.

Each of the two samples was then washed for absorption and specific gravity following the procedures outlined in test method C 128-57. One procedure not specifically stated in ASTM standards was used, however. When the sample was removed from the volumetric flask, the water was removed by decanting the sample. The sand plus the filter paper was then placed in the drying oven together and the dry weight obtained. The filter paper was oven dried prior to testing to a constant weight and its dry weight determined and subtracted from this weight from the combined dry weight the sample dry weight was obtained. This procedure was used to speed drying time and while the method does not explicitly state that the procedure should be followed, the wording does not preclude its use.

The portion of the sand not used in the flask was placed in a separate container and dried to a constant weight along with the sample from the flask. After the dry weights were determined the portions were recombined for the next replicate. As before, two operators acting independently performed ten replicates on each sample. One hundred percent ethanol was used in minor amounts to reduce foaming in the flask.

Upon completion of testing the [illegible] samples were [illegible] and the change in weight of each [illegible] during [illegible] the [illegible]

[illegible]

[illegible] results [illegible] have [illegible] the [illegible] of [illegible] [illegible] the [illegible] and [illegible] application [illegible] and [illegible] with the analysis of [illegible] the [illegible]

[illegible]

[illegible] for [illegible] and [illegible]

[illegible] that the within-sample [illegible] variances for two materials [illegible] being equal at an α-level of 0.0[illegible] [illegible] conclusion was reached for the within-sample variances [illegible] However, a B[illegible] test over the entire table of data [illegible] operators) resulted in the rejection of the hypothesis that all within-sample variances were equal at the 0.05 α-level.

With the problem of non-homogeneous variance present, it was deemed advisable to analyze the results of Operator A and Operator B separately since one of the assumptions underlying the analysis of variance is that variances are homogeneous (10). Analyzing the data for Operator A and Operator B separately eliminated the operator variable and hence changed the statistical model from a 3-factor factorial to two 2-factor factorial models similar to the model for analysis of test method C 127-59.

The calculations for the sum of squares for the analysis of variance tables followed the procedure presented in Ostle (12) page 351.

Table 1 is the Analysis of Variance Table for Operator A, Test Method C 117-49. The estimate of experimental error, σ^2, is shown to be 0.0124. This mean square is used in testing hypotheses in regard to the effect of replicates, materials, and the operator-material interaction. The mean square for amounts was, as would be expected, very large, 296.1773, in comparison to the variance which was used to test the hypothesis that $\sigma_\beta^2 = 0$ (amount effect). This effect must be tested using the mean square for amount-material interaction since the expected mean square for amount includes σ^2 and $\sigma_{\alpha\beta}^2$.

F-tests performed on the data from the analysis of variance indicated that materials and amounts were significant. That is that one cannot, at the 0.05 α-level accept the hypothesis that $\sigma_\alpha^2 = 0$ (material effect) and that $\sigma_\beta^2 = 0$ (amount effect). The results of the F-tests indicated further that one can accept the hypothesis that $\sigma_r^2 = 0$ (replicate effect) and $\sigma_{\alpha\beta}^2 = 0$ (material-amount interaction).

TABLE 1

ANALYSIS OF VARIANCE TABLE

TEST METHOD C 117-49: OPERATOR A

Source of Variation	Degrees of Freedom	Sum of Squares	Mean Square	Expected Mean Square
Replicates	$(r-1) = 9$	$R_{yy} = 0.1819$	0.0202	$\sigma^2 + ab\,\sigma_\rho^2$
α	$(a-1) = 1$	$R_{yy} = 0.0594$	0.0594	$\sigma^2 + rb\,\sigma_\alpha^2$
β	$(b-1) = 3$	$B_{yy} = 888.5318$	296.1773	$\sigma^2 + r\,\sigma_{\alpha\beta}^2 + ra\sum_{K=1}^{K=4}\frac{\sigma_K^2}{(b-1)}$
$\alpha\beta$	$(a-1)(b-1) = 3$	$(AB)_{yy} = 0.0609$	0.0203	$\sigma^2 + r\,\sigma_{\alpha\beta}^2$
Experimental Error	$(r-1)(ab-1) = 63$	$E_{yy} = 0.7851$	0.0124	σ^2
Total	$(rab-1) = 79$			

TABLE 2

ANALYSIS OF VARIANCE TABLE

TEST METHOD C 117-49: OPERATOR B

Source of Variation	Degrees of Freedom	Sum of Squares	Mean Square	Expected Mean Square
Replicates	$(r-1) = 9$	$R_{yy} = 0.0490$	0.0054	$\sigma^2 + ab\,\sigma_\rho^2$
α	$(a-1) = 1$	$A_{yy} = 0.0003$	0.0003	$\sigma^2 + rb\,\sigma_\alpha^2$
β	$(b-1) = 3$	$B_{yy} = 896.4696$	298.8232	$\sigma^2 + r\sigma_{\alpha\beta}^2 + ra\sum_{i=1}^{i=10} \frac{\beta_k^2}{(b-1)}$
$\alpha\beta$	$(a-1)(b-1) = 3$	$(AB)_{yy} = 0.0075$	0.0025	$\sigma^2 + r\,\sigma_{\alpha\beta}^2$
Experimental Error	$(r-1)(ab-1) = 63$	$E_{yy} = 0.1738$	0.0028	σ^2
Total	$(rab-1) = 79$			

Table 2 presents a similar Analysis of Variance Table for Operator B, Test Method C 117-49. The estimate of experimental error was 0.0028. Since the expected mean squares for this design model are the same as those for the previously discussed model the same procedures of hypothesis testing were followed. As before the mean square for amounts were very large, 298.8232, with respect to the mean square used in testing the hypothesis that $\sigma_\beta^2 = 0$, namely $\sigma^2 + \sigma_{\alpha\beta}^2$.

F-tests performed on the data from the analysis of variance of the data for Operator B indicated that amounts were significant, $\sigma_\beta^2 \neq 0$, at 0.05 α-level.

Amounts would be expected to be significant since their means were chosen to be different. The fact that the material effect was significant for Operator A indicated that the type of minus 200 material has some effect on the results obtained. An examination of the means for Operator A indicates that generally a higher percentage of minus 200 material was determined for the finely ground limestone than for minus 200 clay material (Table 3).

TABLE 3

MEANS DETERMINED FOR DATA OF OPERATOR A

Material	Limestone				Clay			
Percent Added	1	4	7	10	1	4	7	10
Percent Determined by C 117-49	1.066	4.052	7.006	10.030	1.080	3.912	6.952	9.988

The fact that material was found not significant for the data of Operator B, coupled with the fact that the variances of Operator A and Operator B were found to be different, indicates that the results obtained using this test method are highly sensitive to the skill of the operator performing the test. Another factor lends some support to this suggestion. Operator B was an "experienced" operator while Operator A was not (even though he was given a reasonable "break-in" or learning period). Therefore, the results obtained by Operator B may be indicative of results obtained when the test method is performed by an experienced laboratory technician, while the results obtained by Operator A may be indicative of results obtained when the test method is performed by a person not trained in laboratory techniques of this nature.

The problem of establishing an acceptable range within which results of duplicate determination should agree, or establishing an interval, within which one expects, with some given probability, the population parameter being estimated to lie, was complicated by the non-homogeneity of variance encountered.

Another factor that arises is selecting the type of limits to be set, i.e. confidence limits or control limits. Confidence limits on a mean or observation provide a range that, with a given probability, include the true mean, μ. Control limits on the other hand provide limits in which a certain percent of the sample statistics should fall in the long run. A set of data that has a number of observations outside the control limits (greater than that amount determined by choice of an α-level) is said to be out of control. Several factors may account for the data being out of control. One can be the fact

that some assignable cause had led to discrepancies between observations, but another is that the precision of the test method or process is incapable of producing results of the quality required.

For the purpose of this study it seems appropriate to present both confidence limits and control limits. These limits are presented for the data Operator A and Operator B separately.

Confidence Limits for Operator A

$s^2 = 0.0124$ from Table 1, therefore $s = 0.111$.

Ninety-five percent confidence limits on the mean of n observations made to determine the amount of material finer than No. 200 sieve are $\pm t_{.05} \frac{s}{\sqrt{n}}$, where t is based on the chosen α-level (0.05 in this case) and the degrees of freedom associated with s. In this case the number of degrees of freedom is 63. For these conditions, the value of t is 1.998 and the limits are $\pm \frac{0.222}{\sqrt{n}}$.

If, for example, three observations are made the confidence limits placed on the average of the three is $\bar{\bar{Y}} \pm \frac{0.222}{\sqrt{3}} = \bar{\bar{Y}} \pm 0.128$. The interpretation that is placed on these limits is that one is 95% confident that the true mean, μ, lies within the limits established by, $\bar{\bar{Y}} \pm 0.128$ where $\bar{\bar{Y}}$ is the observed mean.

Control Limits for Operator A

The establishment of control limits for a measurement process can give a basis for determining whether observations are made within the limits of variability allowable or inherent in the process. The control limits were placed on individual observations. Since both material and amount were determined significant, the limits were placed about the average of ten replicates. The limits, placed on

individual observations are wider than limits placed on means. The limits are indicative of how well an operator may repeat his measurements.

The limits are as follows:

$$\text{Estimate of variance} = \sigma^2_{\bar{Y}_{jr}} = \frac{\sigma_{\rho}^2}{1} + \frac{\sigma^2}{1} = 0.0134$$

For 0.05 α-level based on n observation, where n equals ten replicates, $t_{.05} = 2.262$. The control limits are then equal to:

$\pm$ 2.262 $\sqrt{0.0134}$ = $\pm$ 0.262%.

For 0.01 α-level, t = 3.25 and the control limits are:

$\pm$ 3.25 $\sqrt{0.0134}$ = $\pm$ 0.376%.

A plot of the observations in each replicate and the control limits as determined above are shown in Figure 1 for the clay material. A similar chart can be constructed for the limestone material except that the mean, $\bar{\bar{X}}$, would be shifted.

Confidence Limits for Operator B

$s^2 = 0.0028$ from Table 2. Therefore, s = 0.0548.

95% confidence limits equal: $\pm \frac{0.110}{\sqrt{n}}$ following the same procedures shown in the determination of confidence limits for Operator A.

Control Limits for Operator B

Control limits for data of Operator B were placed on individual observations. The limits were plotted about means averaged over replicates and materials since amounts were significant. The procedures followed in determining these limits were the same as those used for determining control limits for the data of Operator A except that, obviously a different variance was used, that associated with Operator B. The limits are:

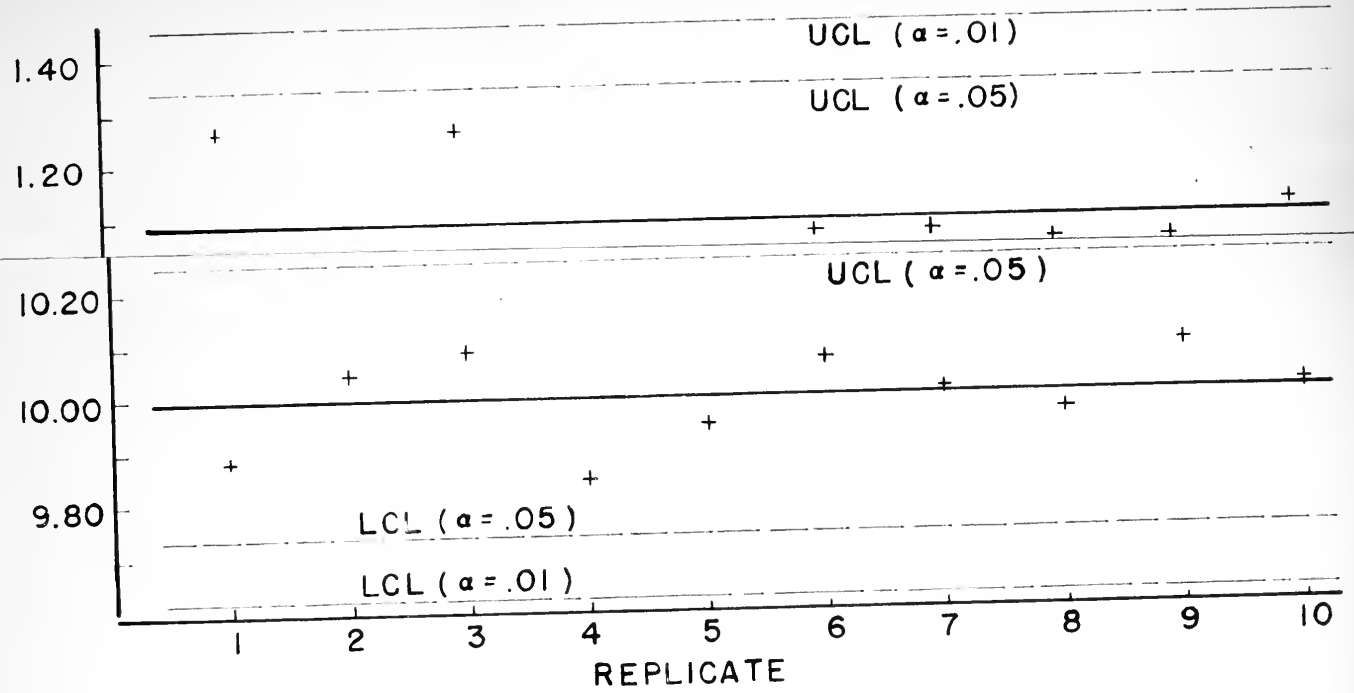

FIG. 1 CONTROL CHARTS FOR OPERATOR A
TEST METHOD C 117-49

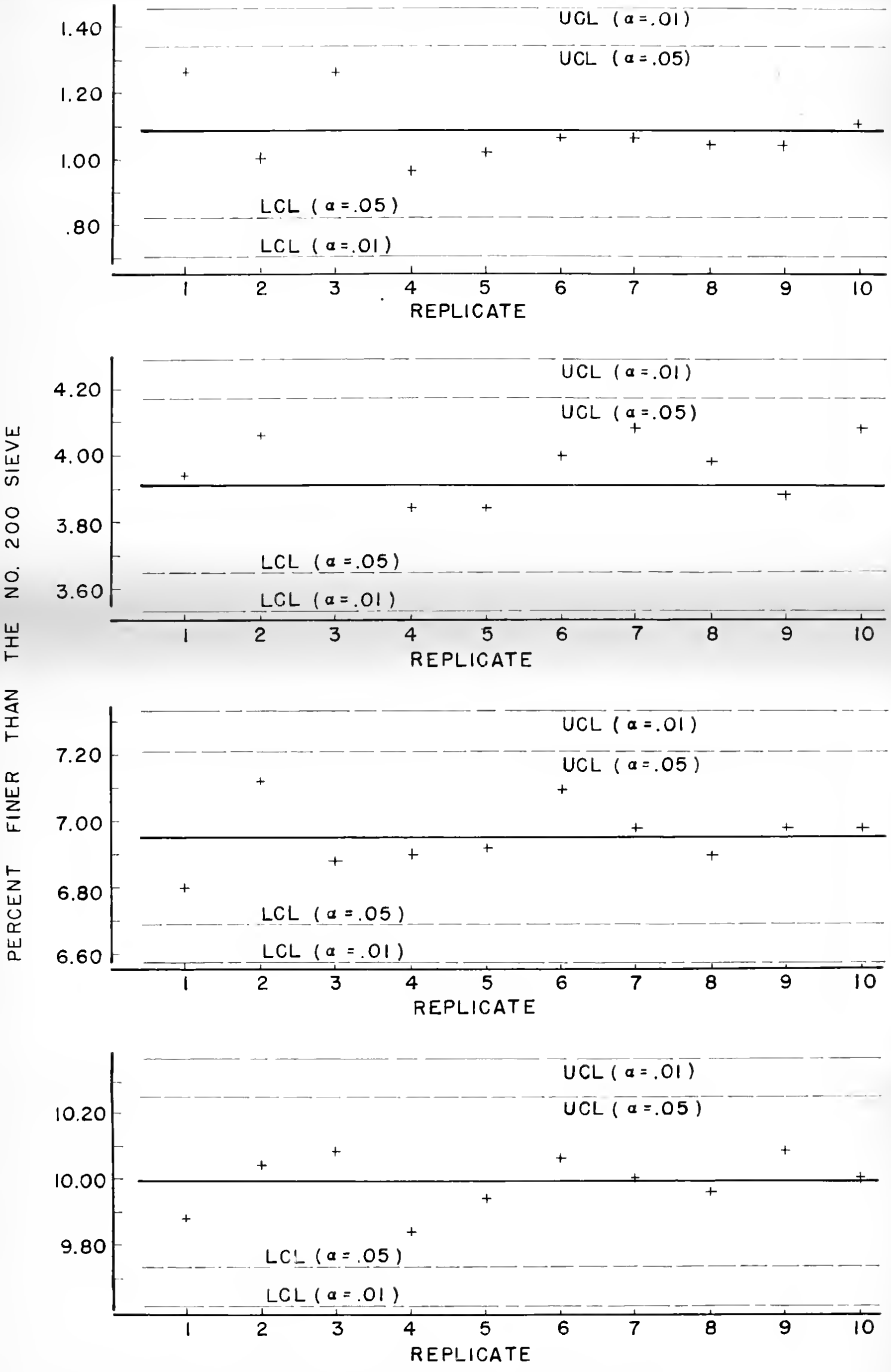

FIG. 1 CONTROL CHARTS FOR OPERATOR A
TEST METHOD C 117-49

$\pm$ 0.116% for an α-level of 0.05

$\pm$ 0.159% for an α-level of 0.01

Figure 2 shows the observations and the control limits as determined above.

General Observations

Figure 1 and Figure 2 give an indication of how wide the limits are and how some of the data were scattered. This scattering could be due to several factors (e.g. a variable which was not controlled, such as laboratory humidity, may be significant). It is of interest to note that the ASTM Committee responsible for this test method has revised it* so that the weight determination and calculation of percent finer than No. 200 sieve is made to the nearest 0.1 percent instead of the nearest 0.02 percent. The remainder of the revision appears to be in keeping with procedures followed during this study. If the percent finer than No. 200 sieve was determined to the nearest 0.1 percent, the variances are, for practical purposes, zero for the data of Operator B. The situation is then similar to the situation encountered for the specific gravity data of Test Method C 127-59. Namely, the data are insensitive to statistical analyses and practical limits of $\pm$ 0.1 percent seem appropriate. Noting what happened in the case of Operator A the placement of these "practical" limits may not be justified.

Results of Test Method C 127-59

Prior to testing, the variables present were determined and a 2-factor factorial model was chosen for the analysis of absorption and specific gravity data.

---

* Accepted as a tentative, C 117-61T, in 1961.

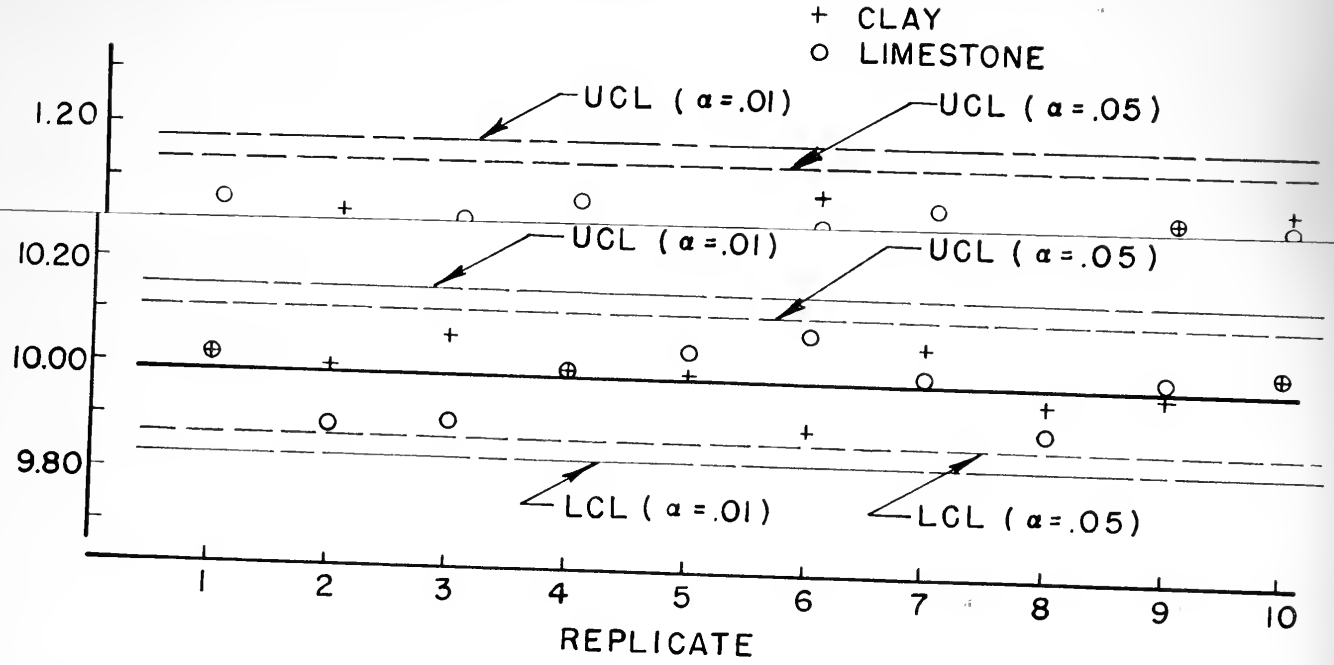

FIG. 2 CONTROL CHARTS FOR OPERATOR B
TEST METHOD C 117-49

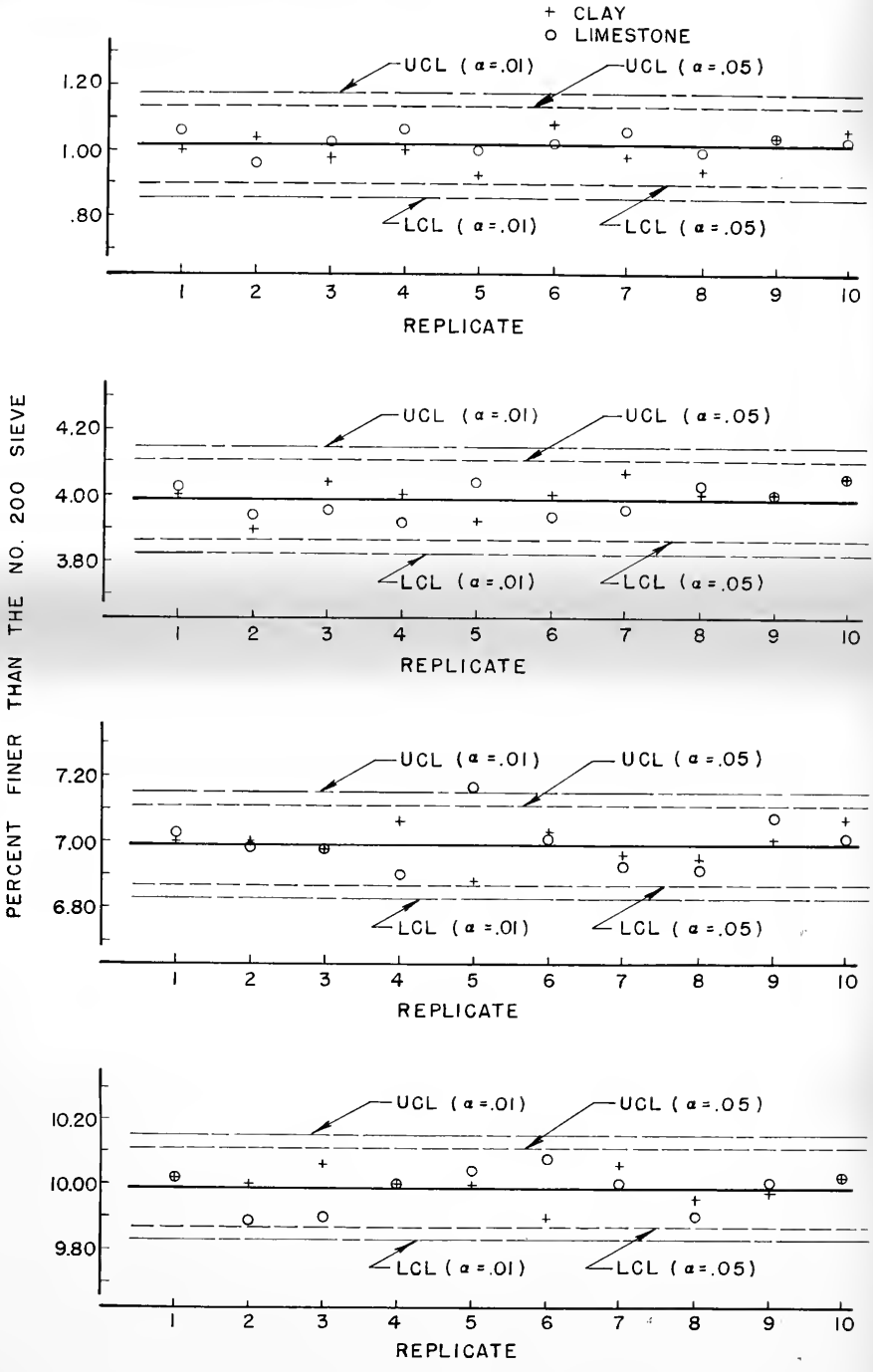

FIG. 2 CONTROL CHARTS FOR OPERATOR B
TEST METHOD C 117-49

Absorption

A Bartlett test for homogeneity of variance was performed and resulted in accepting the hypothesis that within-sample variances were equal at the 0.05 α-level. With these variances determined equal, it was then possible to proceed with the analysis of the data using the factorial model.

The sums of squares and the mean squares were calculated according to the procedures for 2-factor factorial models. These sums of squares and mean squares are shown in Table 4.

F-tests performed on the data from the analysis of variance indicated that there was a significant interaction between materials and operators, i.e. $\sigma_{\alpha\beta}^2 \neq 0$. Replicates and operators were not significant. The F-tests also indicated that materials were not significant, $\sigma_{\alpha}^2 = 0$. Materials were expected to be significant since aggregates having different absorptions were deliberately selected. The significant interaction can be logically explained. One operator may be more experienced, or more familiar, with one material than the other and this could conceivably influence his results.

With estimates of the variance components available, limits were determined. As before, both confidence limits and control limits were determined. Control limits were placed on individual observations.

The calculation of the components of variance results in $\sigma_{\epsilon}^2 = 0$. The sum of squares for replicates and experimental error were pooled to form a better estimate of the population variance. This variance was determined to be 0.00145 with 36 degrees of freedom. The control limits for $\alpha = 0.05$ and $\alpha = 0.01$ are indicated below.

TABLE 4

ANOV TABLE FOR ABSORPTION DATA

TEST METHOD C 127-59

Source of Variation	Degrees of Freedom	Sum of Squares	Mean Square	Expected Mean Square
Replicates	$(r-1) = 9$	$R_{yy} = 0.0128$	0.00142	$\sigma^2 + ab\sigma_\rho^2$
α	$(a-1) = 1$	$A_{yy} = 1.4745$	1.47450	$\sigma^2 + r\sigma_{\alpha\beta}^2 + rb\sigma_\alpha^2$
β	$(b-1) = 1$	$B_{yy} = 0.0084$	0.00840	$\sigma^2 + r\sigma_{\alpha\beta}^2 + ra\sigma_\beta^2$
$\alpha\beta$	$(a-1)(b-1) = 1$	$(AB)_{yy} = 0.0130$	0.01300	$\sigma^2 + r\sigma_{\alpha\beta}^2$
Experimental Error	$(r-1)(ab-1) = 27$	$E_{yy} = 0.0394$	0.00146	σ^2
Total	$(rab-1) = 39$			

For $\alpha = 0.05$.

$t_{0.05,\ 9 \text{ degrees of freedom}} = 2.262$

$$\text{control limits} = \pm 2.262 \sqrt{\frac{0.00145}{1}} = \pm 0.086\%$$

For $\alpha = 0.01$.

$t_{0.01,\ 9 \text{ degrees of freedom}} = 3.250$

$$\text{control limits} = \pm 3.250 \sqrt{\frac{0.00145}{1}} = \pm 0.133\%$$

Confidence limits were determined as follows. $\sigma^2 = 0.00145$ (pooled), therefore $\sigma = 0.038$. For this case, t equals 2.029 based on 0.05 α-level and 36 degrees of freedom. The confidence limits are therefore, $\pm 2.029 \frac{0.038}{\sqrt{n}} = \pm \frac{0.077}{\sqrt{n}}$.

Control limits were also determined for "between operators." These limits were determined as follows.

The estimate of variance, $\sigma^2_{\bar{y}_j}$, equals 0.000073. The limits are $\pm t \sqrt{0.000073}$. For an α-level of 0.05 and 27 degrees of freedom, t equals 2.052 and the limits are $\pm 0.018\%$. For an α-level of 0.01 and 27 degrees of freedom, t equals 2.771 and the limits are $\pm 0.024\%$.

These limits are narrower than the control limits determined for a single operator and are applicable to situations where one is interested in making comparisons between operator means.

Specific Gravity

A statistical analysis of the specific gravity data was not warranted since the range in values for each type of specific gravity never exceeded 0.02 and the variances were, for practical purposes, zero. The practical control limits for this case, therefore, are ± 0.01. These limits would also apply to between-operators since a check of

the data indicated almost identical specific gravity determinations by each operator.

A precision statement as it might appear in the test method would be as follows: Duplicate determinations made by the same, or by different operators, should lie within the range determined by $\bar{Y} \pm 0.01$, where $\bar{Y}$ is the observed average of the specific gravity determinations.

One particular point was noted during the course of the study of Test Method C 127-59. This was that care should be taken, when submersing the sample into the water for the weight determination in water, to place the sample in the water in such a manner as to prevent as much as possible the entrapment of air. Possibly some reference in the test method is warranted.

Results of Test Method C 128-57

Prior to testing, the variables present were determined and a 2-factor factorial model was chosen for the analysis of absorption and specific gravity data.

Absorption

A Bartlett test for homogeneity of variance was performed on the data. The test resulted in accepting the hypothesis that within-sample variances were equal at the 0.05 α-level. With these variances determined equal, it was then possible to proceed with the analysis of the data using the factorial model.

The sums of squares and the mean squares were calculated according to the procedures for 2-factor factorial models. These sums of squares and mean squares are shown in Table 5. The estimate of experimental error is 0.02258 as determined by the ANOV.

TABLE 5

ANALYSIS OF VARIANCE TABLE FOR ABSORPTION DATA

TEST METHOD C 128-57

Source of Variation	Degrees of Freedom	Sum of Squares	Mean Square	Expected Mean Square
Replicates	(r-1) = 9	R_{yy} = 0.0896	0.00995	$\sigma^2 + ab\sigma_\rho^2$
α	(a-1) = 1	A_{yy} = 0.2657	0.2657	$\sigma^2 + r\sigma_{\alpha\beta}^2 + rb\,\sigma_\alpha^2$
β	(b-1) = 1	B_{yy} = 0.5108	0.5108	$\sigma^2 + r\sigma_{\alpha\rho}^2 + ra\,\sigma_\beta^2$
$\alpha\beta$	(a-1)(b-1) = 1	$(AB)_{yy}$ = 0.0029	0.0029	$\sigma^2 + r\sigma_{\alpha\beta}^2$
Experimental Error	(r-1)(ab-1) = 27	E_{yy} = 0.6096	0.02258	σ^2
Total	(rab-1) = 39			

F-tests performed on the data from the analysis of variance indicated that operator effect was significant, $\sigma_\beta^2 \neq 0$, and also the material effect was significant, $\sigma_\alpha^2 \neq 0$. Replicate effect and the operator-material interaction were determined to be not significant.

Materials might be expected to be significant. Different fineness modulus (different gradations) were deliberately chosen. Since the material used was a natural sand of a heterogeneous nature, it is not unusual to find different size fractions having different absorptions.

It is interesting to note that operator effect was significant, indicating the sensitivity of the test method to this variable. The procedure involved requires judgment as to when a saturated surface dry condition has been obtained and it also involves some amount of skill on the part of the operator in placing 500.0 grams of material into the flask quickly. It should be noted that only two operators were used in this study and therefore it is difficult to make generalities about the whole population of operators with confidence. This study does give an indication as to what might be expected.

With estimate of the variances components available, confidence and control limits were determined. To obtain an estimate of the precision of an operator the control limits were placed on the individual observations. The procedures followed in determining the control limits were the same as those used in determining the control limits for absorption data of Test Method C 127-59. For this case a pooled estimate of σ^2 was determined as 0.0190. Since $\sigma_\rho^2 = 0$ and $\sigma_{\alpha\beta}^2 = 0$ these were used with σ^2 to determine a pooled estimate of σ^2.

The pooled estimate of the variance σ^2 equals 0.0190 with 37 degrees of freedom. The control limits were determined as noted below.

For $\alpha = 0.05$

$$\text{Control limits} = \pm 2.262 \sqrt{\frac{0.0190}{1}} = \pm 0.312\%$$

For $\alpha = 0.01$

$$\text{Control limits} = \pm 3.25 \sqrt{\frac{0.0190}{1}} = \pm 0.448\%$$

Confidence limits were determined as follows. The pooled estimates of variance equal 0.0190, therefore σ equals 0.138. The 95% confidence limits are, $\bar{Y} \pm 2.028 \frac{0.138}{\sqrt{n}} = \bar{Y} \pm \frac{0.280}{\sqrt{n}}$. The 99% confidence limits are, $\bar{Y} \pm 2.716 \frac{0.138}{\sqrt{n}} = \bar{Y} \pm \frac{0.375}{\sqrt{n}}$.

Control limits were also determined for "between operators." These limits were determined calculating the variance and the degrees of freedom. The Satterwaithe equation was used to determine the degrees of freedom, which for this case was one. The control limits were determined as $\pm t \sqrt{\sigma^2_{\bar{Y}_j}}$. The $\sigma^2_{\bar{Y}_j}$ for this case was equal to 0.01325. The limits were then $\pm t \sqrt{0.01325}$ where t was based on the chosen α-level and the degrees of freedom determined, which was one. For an α-level of 0.05 the control limits are $\pm 12.706 \sqrt{0.01325} = \pm 1.46\%$. These limits from a practical viewpoint are far too high. This points up the problems associated with trying to make generalities over a whole population with only one degree of freedom associated with the variance component due to operators. It should be further noted that the operator effect was determined significant, as previously mentioned, and fact would tend to indicate that the control limits would be wider for this case.

A comparison of the error variances of this test method with that determined for Test Method C 127-59 shows that this test method has a much higher component of variance due to experimental error than did Test Method C 127-59. These error variances were 0.0226 and 0.00146, respectively.

Specific Gravity

Results of the analyses of variance performed on the data for the three types of specific gravity indicated that all have approximately the same magnitude of experimental error, namely $\sigma^2 = 0.0001$. However, the estimate of this was difficult since the magnitude of computational figures are small and the factor of significant figures reduces the precision of the analysis. This estimate of σ^2 however, if used in setting control limits on means of duplicate determination, replicates, gives $\pm$ 0.01. This is the same as the practical limits determined for the specific gravities of coarse aggregate determined by Test Method C 127-59. The specific gravities of fine aggregate as determined by Test Method C 128-57 are more variable than those of coarse aggregates as determined by Test Method C 127-59.

The variances associated with the specific gravity data were small but some general observations may be made. Bulk specific gravity had more variance associated with it and is more sensitive to the operator variable and to the material variable than bulk specific gravity (SSD). Bulk gravity (SSD) in turn is more sensitive to the operator variable and the material variable than is apparent specific gravity. In fact, this study indicated no variance component due to the operator effect.

General Observations

In the course of this study, it was noted that certain factors in Test Method C 128-57 could be improved or elaborated upon. The temperature bath specification contains no provision for any variance about 20°C. The time specified for the sample to remain in the bath also has no tolerance associated with it. The flask specified, 500 ml, is actually too small for the size of sample being tested.

The flask is not large enough to allow the sand to be mixed by the rolling action to remove entrapped air. It was noted that it was very difficult to remove the air entrapped in the sand at the bottom of the flask due to the fact that no mixture was achieved by the rolling action. A larger flask would provide sufficient room for the sample to be mixed with the water and the entrapped air released.

No provision is made for the counter-action of foaming that may occur during the removal of air by the procedure specified.

Results Applicable to the Development of Precision Statements

Both confidence limits and control limits were computed in the statistical analysis of the test data. Control limits define a range in values within which, in the long run, the sample statistics will fall a certain percentage of the time. Confidence limits define a range around the sample statistic that, with a given probability, will include the true value of the population parameter. Further, control limits indicate how well an operator is performing the test. If the operator's results are "out of control" some assignable cause may be the reason (e.g. the operator may not be following exactly the test procedures specified).

For inclusion in a precision statement, control limits are superior to confidence limits since they provide more information relative to the actual performance of the test method.

There are many forms which a precision statement may take. The following are examples of several types that seem worthy of consideration for use.

1. A simple statement of the repeatability and reproducibility determined for the test method.

   Example: Duplicate determinations should check to the nearest 0.02 in the case of a single operator and to the nearest 0.05 for between-operators.

2. A statement giving the estimate of experimental error determined for the test method, the estimate of each variance component, and the degrees of freedom associated with each.

   Example: The experimental error for the test method is 0.0015 with 27 degrees of freedom. The components of variance for replicates, operators, and materials are 0.0014 with 9 degrees of freedom, 0.008 with 1 degree of freedom, and 1.47 (highly significant) with 1 degree of freedom, respectively.

3. A statement giving the estimate of experimental error and the expression for computing control limits (e.g. UCL = $\bar{Y} + t\sqrt{\sigma_{\bar{Y}}^2}$, LCL = $\bar{Y} - t\sqrt{\sigma_{\bar{Y}}^2}$ where $\bar{Y}$ = the sample mean and $\sigma_{\bar{Y}}^2$ = the variance about the mean). The degrees of freedom and the α-levels to be used with t must also be noted.

   Example: The experimental error for the test method is 0.0015. Control limits are to be computed by $\bar{Y} \pm t\sqrt{\sigma_{\bar{Y}}^2}$, where $\sigma_{\bar{Y}}^2 = \sigma_{\epsilon}^2$ and t is based on an α-level of 0.05 and 9 degrees of freedom.

4. A statement giving the control limits for a single operator performing the test a number of times and the control limits for between-operators. The degrees of freedom and the α-level for determining t should also be given.

Example: Control limits for a single operator performing the test are $\bar{Y} \pm 0.03$, with 27 degrees of freedom associated with the estimate of experimental error and t based on 9 degrees of freedom and an α-level of 0.05. Control limits for between-operators are the same as for a single operator.

Example 4 provides the optimum information and seems to be the best for inclusion in test methods of the type considered in this study.

SUMMARY

The results of this study indicate that it is essential to determine the variables for a test method and to develop a statistical model before actual testing begins. The estimate of error variance and other variance components can be determined from an analysis of variance. With this information available, significance test can then be made. Control limits can be placed on the data of a single operator and on data for between-operators.

In addition it was found that:

a) the experimental designs used produce information useful in determining control limits applicable to individual observations of the attribute being measured.

b) control limits on individual observations form the basis for useful precision statements.

c) the data collected are also useful in the evaluation of the test method itself.

Precision Statements for Test Methods Studied

The following are examples of the form that precision statements might take using the results of this study. These statements are based on the previous assumptions and include components of variance due to replicates, operators, and material. This study specifically eliminated the component of variance due to sampling and other variables not mentioned. The precision statements are for test data when the tests are performed by experienced personnel following exactly the procedures as outlined in the ASTM Standards for the test method.

Test Method C 117-49: Test for Material Finer than the No. 200 Sieve in Aggregate

Control limits for a single operator performing the test are $\bar{Y} \pm 0.12$ percent, with 63 degrees of freedom associated with the estimate of experimental error and t based on 9 degrees of freedom and an α-level of 0.05.

Test Method C 127-59: Test for Specific Gravity and Absorption of Coarse Aggregate

Absorption. Control limits for a single operator performing the test are $\bar{Y} \pm 0.09$ percent, with 27 degrees of freedom associated with the estimate of experimental error and t based on 9 degrees of freedom and an α-level of 0.05. Control limits for between-operators are the same.

Specific Gravity. Practical control limits for both a single operator and between-operators are $\bar{Y} \pm 0.01$, based on 40 observations.

Test Method C 128-57: Test for Specific Gravity and Absorption of Fine Aggregate

Absorption. Control limits for a single operator performing the test are $\bar{Y} \pm 0.31$ percent, with 27 degrees of freedom associated with the estimate of experimental error and t based on 9 degrees of freedom and an α-level of 0.05.

Specific Gravity. Practical control limits for both a single operator and between-operators are $\bar{Y} \pm 0.01$, based on 40 observations.

BIBLIOGRAPHY

1. ASTM Committee E-11 on Quality Control of Materials, Recommended Procedure for Conducting on Interlaboratory Study of a Test Method, June, 1961.

2. ASTM Manual on Quality Control of Materials, Special Technical Publication 15-C, American Society for Testing Materials, 1951.

3. ASTM Standards 1958, Part 4.

4. ASTM Proceedings, p 379, Appendix IV, 1953.

5. Brown, A. B., Precision of Present ASTM Tests on Bitumens and Bituminous Materials, ASTM Special Technical Publication No. 252.

6. Burr, I. W., Engineering Statistics and Quality Control, McGraw-Hill Book Company, Inc., New York, 1953, Chapter 15.

7. Cochran, W. G., Some Consequences when the Assumptions for Analysis of Variance are Not Satisfied, Biometrics, Vol. 3, No. 1, March, 1947.

8. Conner, W. S., How to Evaluate Precision, Material Research and Standards, Vol. 1, No. 4, April, 1961, pp. 272.

9. Crandall, J. R. and Blaine, R. L., Statistical Evaluation of Inter-laboratory Cement Tests, ASTM Proceedings, Vol. 59, 1959, pp. 1129.

10. Eisenhart, Churchill, The Assumptions Underlying the Analysis of Variance, Biometrics, Vol. 3, No. 1, March 1947.

11. Kaplan, M. F., The Reproducibility of Flexure and Compression Tests for Determining the Strength of Cement, ASTM Proceedings, Vol. 60, 1960, pp. 1006.

12. Ostle, B., Statistics in Research, The Iowa State College Press, Ames, Iowa, 1954.

13. Report of Committee D-6 on Paper Products, Sixty-third Annual Meeting of the American Society for Testing Materials, 1960.

14. Report to Subcommittee II-a of ASTM Committee C-9 on the Present Status and Need for Precision Statements in Methods of Test, 1960.

15. Steel, R. G. D. and Torrie, J. H., Principles and Procedures of Statistics, McGraw-Hill Book Company, Inc., New York, 1960.

16. Supplement to Book of ASTM Standards, Part 4, 1959.

17. Terry, M. E., On the Analysis of Planned Experiments, Materials Research and Standards, Vol. 1, No. 4, April, 1961, pp. 273.

18. Youden, W. J., Experimental Designs and ASTM Committees, Materials Research and Standards, Vol. 1, No. 11, November, 1961, p. 862.

19. Youden, W. J., How to Evaluate Accuracy, Materials Research and Standards, Vol. 1, No. 4, April, 1961, p. 272.

20. Youden, W. J., Statistical Aspects of the Cement Testing Program, ASTM Proceedings, Vol. 59, 1959, p. 1120.

STRESS & DEFLECTION IN AN ELASTIC MASS UNDER SEMIELLIPSOIDAL LOADS

MAY 1963
NO. 13

Joint Highway Research Project

by

J.L. SANBORN

PURDUE UNIVERSITY
LAFAYETTE INDIANA

Informational Report

STRESS AND DEFLECTION IN AN ELASTIC MASS
UNDER SEMIELLIPSOIDAL LOADS

TO: K. B. Woods, Director
Joint Highway Research Project

May 8, 1963

FROM: H. L. Michael, Associate Director
Joint Highway Research Project

File: 6-20-6
Project: C-36-52F

Attached is an informational report entitled "Stress and Deflection in an Elastic Mass Under Semiellipsoidal Loads" which has been prepared by Mr. John L. Sanborn a member of the staff of the School of Civil Engineering. The research reported was the thesis of Mr. Sanborn for the MSCE degree and was performed under the direction of Professor E. J. Yoder.

The research reported is concerned with the estimation of stresses and deflections at points within a pavement due to applied wheel loads. Specifically the report describes the application of numerical integration, by means of a high speed digital computer, to the solution of elastic stress and deflection equations for a semiellipsoidal load at the surface of a uniform, semi-infinite mass having a plane boundary.

The research was financed by the School of Civil Engineering and the University and is presented to the Board for information.

Respectfully submitted,

Harold L. Michael, Secretary

HLM:kmc

Attachment

Copy:

F. L. Ashbaucher
J. R. Cooper
W. L. Dolch
W. H. Goetz
F. F. Havey
F. S. Hill
G. A. Leonards
J. F. McLaughlin
R. D. Miles
R. E. Mills
M. B. Scott
J. V. Smythe
J. L. Waling
E. J. Yoder

Informational Report

STRESS AND DEFLECTION IN AN ELASTIC MASS UNDER SEMIELLIPSOIDAL LOADS

by

John L. Sanborn
Research Assistant

Joint Highway Research Project
File No: 6-20-6
Project No: C-36-52F

Purdue University
Lafayette, Indiana

May 8, 1963

ACKNOWLEDGMENTS

The author expresses his deep appreciation to the many people who gave support, encouragement and advice throughout the conduct of this study.

Especial thanks is extended to Professor E. J. Yoder who served as the author's major professor. Professor Yoder provided the original suggestion for the study and contributed much through his continuous interest and encouragement, as well as his reviews of the several stages of the work.

Thanks is expressed also to Professor T. J. Herrick and the School of Aeronautical and Engineering Sciences for guidance and for use of a computer during initial studies, and to the Computer Sciences Center for funds, services and equipment to carry out the project.

TABLE OF CONTENTS

	Page
LIST OF ILLUSTRATIONS	iv
ABSTRACT	v
INTRODUCTION	1
PURPOSE AND SCOPE	3
REVIEW OF LITERATURE	5
PROCEDURE	7
Computer Program	7
Program Logic	7
Input	15
Output	16
Curves	17
SUMMARY AND CONCLUSION	30
Summary	30
Recommendations	30
BIBLIOGRAPHY	32
APPENDIX A	34
Fortran Program for IBM 7090 Computer	34
APPENDIX B	37
Example Determination of Stress and Deflection	37

LIST OF ILLUSTRATIONS

Figure		Page
1.	Stresses on an Element Due to a Concentrated Load at the Surface	8
2.	A Distributed Load Illustrating Terminology Used in Fortran Program	11
3.	Flow Diagram	12
4.	Maximum Contact Pressure at Center of Tire	19
5.	Contact Area and Pressure Distribution	20
6.	Vertical Stress, σ_z. Transverse Plane	24
7.	Vertical Deflection, Δ. Transverse Plane	25
8.	Vertical Stress, σ_z. Diagonal Plane ($\theta = 68.2^\circ$)	26
9.	Vertical Deflection, Δ. Diagonal Plane ($\theta = 68.2^\circ$)	27
10.	Vertical Stress, σ_z. Longitudinal Plane	28
11.	Vertical Deflection, Δ. Longitudinal Plane	29
12.	Example Gear Configuration	38

ABSTRACT

Sanborn, John Leonard, MSCE, Purdue University, January 1963. Stress and Deflection in an Elastic Mass Under Semiellipsoidal Loads. Major Professor: Eldon J. Yoder.

A common problem in the design and evaluation of highway and airfield pavements is the estimation of theoretical stresses and deflections at points within the pavement due to applied wheel loads. Elastic stress distribution in a homogeneous mass is generally used for such estimates, but its application in this field has been limited to assumptions of concentrated load or of uniformly distributed circular loads. Formal integration of the expressions for stress and deflection for non-uniform loads is either impossible of impracticable.

This report describes the application of numerical integration, by means of a high speed digital computer, to the solution of elastic stress and deflection equations for a semiellipsoidal load at the surface of a uniform, semi-infinite mass having a plane boundary. Normal stresses are computed by the Boussinesq equations, and the strain due to those stresses determined by accepted elastic theory. Integration is performed by Simpson's Rule. Three sets of curves representing stress and deflection on three planes normal to the surface are included. The curves were compiled from data developed, with the program described, on an IBM 7090 computer.

The actual program, in 7090 Fortran language, and an example of the use of the curves are appended to this report.

INTRODUCTION

One of the most frequently encountered problems in design and evaluation of flexible highway and airfield pavements is the estimation of stresses and deflections at points within the structure and subgrade due to applied wheel loads. Recent studies (19, 21)* have shown, in particular, the importance of determining deflections of various components of pavements in order to evaluate their adequacy or serviceability. In the past, a common approach to this problem has been to consider the pavement and subgrade to act as an elastic mass and to evaluate stresses according to the Boussinesq theory of stress distribution. This approach implies, of course, a significant simplification of the layered systems actually used in pavements. The numerical values of stress and deflection determined from this simplification vary significantly from true values both as a result of the idealization of the structure and of the difficulty of determining elastic properties of the materials. Nevertheless, patterns of measured stress and deflection do follow theoretical values (21). The idealized case may, therefore, be used reasonably to evaluate relative effects of different loads or different pavements. Basic equations for stress due to a concentrated load are integrated over the loaded area to approximate the effect of a wheel load. Strains integrated from any given depth to infinity will give total elastic deflection of the given point.

The major difficulty with such a procedure is that it has been

* Numbers in parentheses refer to references listed in Bibliography.

practically limited to uniform circular loads because of the unmanageable expressions which it is otherwise required to integrate. A partial solution is provided by influence charts (12, 13) prepared by Newmark based on the effects of uniform circular loads. These permit determination of stresses and deflections at any point due to any uniform load. Even this requires different scale drawings for each load at each depth for which stress and/or deflection is required, however. Furthermore, non-uniform loads require superposition of a series of uniform loads to approximate the effect of the actual load.

Curves of stress and deflection have also been produced (4), based on Newmark's influence charts, which are practical to use from a design or investigation standpoint. These, however, serve only the uniform circular load.

It has long been known that wheel loads vary considerably from circular areas of uniform pressure, (7), but no feasible method of evaluating the effect of these loads has been available. With the advent of high speed digital computers, however, numerical methods of integrating any configuration of load are entirely practicable. An important use of this tool is to compare the effects of known load distributions to those of conventionally assumed distributions, and to provide simple and useful techniques for estimating those effects in practice. To this end, the computer program reported here was devised to evaluate vertical stress and deflection according to Boussinesq theory due to semiellipsoidal loads. The completed program was used to prepare curves of stress and deflection which are included herein.

PURPOSE AND SCOPE

The purpose of this study was to devise a numerical solution for theoretical stresses and deflections in a soil mass due to non-circular loads of non-uniform distribution. The analysis was based on accepted theory of elasticity and previous investigations of the configuration of ordinary wheel loads.

The study was composed of two basic parts--(1) to write a program for a digital computer, which could be used directly or with minor modifications for any given load, and (2) to use that program to develop charts of vertical stress and deflection for a reasonable approximation of usual tire loads.

The computer program has been written in the IBM Fortran language which is acceptable to a variety of digital computers readily available to many highway and airfield agencies as well as to most universities and colleges. Variations are easily introduced to provide for different load conditions.

Charts of stress and deflection were developed for a semiellipsoidal load of proportions which approximate contact pressures and areas under some standard tires. The charts are in the form of curves of stress and deflection, respectively, in terms of maximum contact pressure, plotted against depth in terms of size of contact area. Deflection is treated as a factor, since actual deflections depend on the contact area and the elastic modulus of the soil as well as the contact pressure.

Stresses are considered to be distributed according to Boussinesq

theory which assumes a homogeneous, isotropic elastic mass. No attempt is made to account for the effects of the layered structure of flexible pavements. Several investigators have described solutions to two and three layer problems. However, since a primary function of this program is to provide a basis for comparison of effects of non-uniform loads with the conventionally assumed uniform circular loads, the work was restricted to the simpler, homogeneous case which has been the assumption adopted by other investigators in a large portion of the earlier work.

REVIEW OF LITERATURE

A number of investigations have shown that the assumption of elastic behavior is reasonable for the response of flexible pavements to traffic loads. Foster and Fergus (5) compared results of extensive test measurements on a clayey silt subgrade to theoretical stresses and deflections and reported good agreement. Newmark's influence charts (12, 13) have been used extensively, and served as the basis for Foster and Ahlvin's charts (4) of stress and deflection due to a circular load of uniform pressure distribution. The latter charts are commonly used in design and research problems in highway and airfield pavements (20). Palmer and Barber (14) also made use of the assumption of elastic behavior with satisfactory results. Baker and Papazian (1), Walker (19) and Yoder (21) all point out the important contribution of the elastic portion of pavement deflections in determining the performance of pavement.

Burmister (3) has considered the effect of the layered structure of pavements and presented curves of surface deflection at the center of a uniform circular load for the two layer case. Fox (6) extended the work of Burmister to evaluate stresses at various points in the structure. More recently, with the use of a digital computer, Jones (9) has developed tables of stresses for a range of conditions of a three layer structure. These are all based on a uniform circular load at the pavement surface, and are limited to points on the axis of symmetry of the load.

There have been relatively few studies of tire contact areas and pressures. However, results of several studies indicate significant variations from the assumption of a uniform circular load. Among the early investigators were Heldt (7), Teller and Buchanan (17) and McLeod (11), all of whom note the nearly elliptical contact area of truck tires. More recently, Brahma (2) and Lawton (10) have made the same observations with respect to truck and aircraft tires respectively.

Lawton's work is of particular interest in that both contact areas and pressures were determined for loads on a simulated subgrade rather than on a rigid surface. The subgrade used was a mechanical model which has been described in detail by Herner and Aldous (8). The contact areas for a variety of tires and loads were all elliptical and had a reasonably uniform ratio of major to minor axis, averaging about 1.7. Pressure distribution was ellipsoidal for all loads within rated capacities of the tires, and varied to more nearly uniform at overloads.

With respect to numerical methods for calculating stresses and deflections in an elastic mass, Stoll (15) has used a digital computer for calculation of vertical stresses in a foundation soil due to variable and asymmetric column loads. His results indicated that the approach is satisfactory and feasible for use in similar problems.

PROCEDURE

Computer Program

Program Logic

The procedure used in this study was to evaluate stresses in an elastic mass by numerical integration of the Boussinesq equations, and to compute elastic strains resulting from those stresses. The equations attributed to Boussinesq express stress components at any point within a semi-infinite, elastic, isotropic, homogeneous mass due to a single concentrated load on the plane boundary of the mass. With reference to Figure 1, the stress components, as given by Taylor (16), are

$$\sigma_z = \frac{P}{2\pi}\left[\frac{3z^3}{(r^2 + z^2)^{5/2}}\right] \tag{1}$$

$$\sigma_r = \frac{P}{2\pi}\left[\frac{3r^2z}{(r^2 + z^2)^{5/2}} - \frac{(1 - 2\mu)}{r^2 + z^2 + z\sqrt{r^2 + z^2}}\right] \tag{2}$$

$$\sigma_t = -\frac{P}{2\pi}(1 - 2\mu)\left[\frac{z}{(r^2 + z^2)^{3/2}} - \frac{1}{r^2 + z^2 + z\sqrt{r^2 + z^2}}\right] \tag{3}$$

$$\tau_{rz} = \frac{P}{2\pi}\left[\frac{3rz^2}{(r^2 + z^2)^{5/2}}\right] \tag{4}$$

where μ is Poisson's ratio for the elastic mass. A derivation of these equations is presented by Timoshenko and Goodier (18).

The elastic strain of a point subjected to stress is determined from the normal components of stress by the equation

$$\delta_1 = \frac{1}{E}\left[\sigma_1 - \mu\sigma_2 - \mu\sigma_3\right] \tag{5}$$

where μ is Poisson's ratio and E is the modulus of elasticity of the

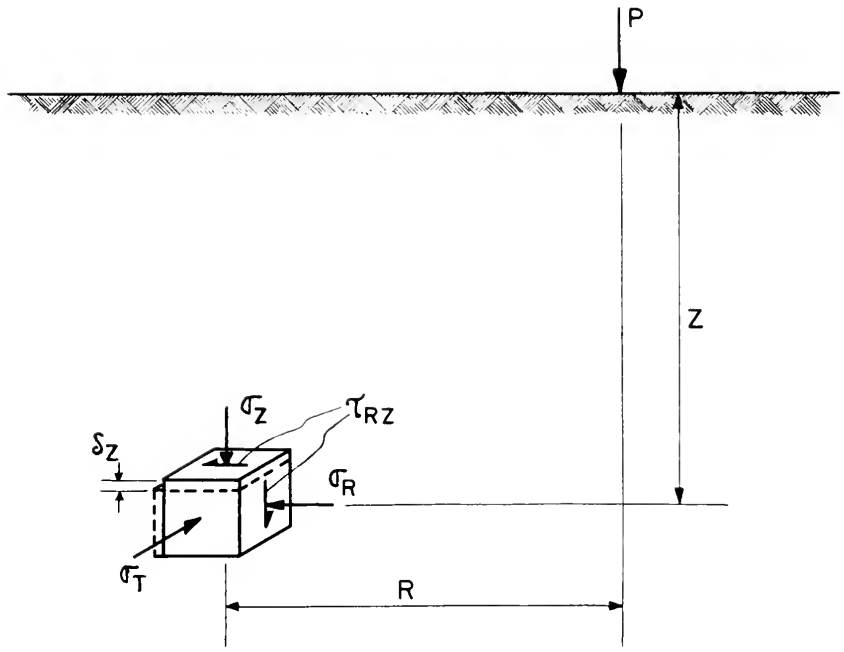

FIGURE 1. STRESSES ON AN ELEMENT DUE TO A CONCENTRATED LOAD AT THE SURFACE

material. Total deflection of a given point depends not only on the strain of that point, but also on strains of other points deeper in the mass. Therefore, to get useful deflections it is necessary to integrate the strains on a vertical line from the given point to infinity. In a numerical procedure the summation is carried out to such depth that the remainder is negligible.

In applying these equations to distributed loads, the basic process is to express the stresses and strain due to an infinitesimal element of the load, treated as a single concentrated load, and to integrate those expressions over the entire loaded area. It is evident that except for symmetrical loads of uniform distribution the formal integration of the expressions is extremely awkward and impractical, even if it is possible, for a given load configuration. A numerical process, however, using a high speed digital computer, is entirely feasible for any load configuration, the only requirement being to define the area of load and the distribution of pressure over that area. In this process, the load is divided into a number of finite elements, each element being treated as a concentrated load, and the numerical integration is carried out in two coordinate directions over the entire loaded area.

The numerical integration used in this program is Simpson's Rule -

$$S = \frac{h}{3}\left[y_0 + 4(y_1 + y_3 + \cdots + y_{n-1}) + 2(y_2 + y_4 + \cdots y_{n-2}) + y_n\right] \quad (6)$$

where y_i are values of the function at equally spaced intervals, h is the spacing and n is the number of spaces (must be even).

Figure 2 illustrates the terminology and arrangement used in development of this program. Plane XY is the boundary of the elastic mass under consideration. Surface ABCDE represents the distributed load

applied to the boundary, and Q, a point in the mass at which it is required to determine stress and deflection. Coordinates G and H locate the vertical line through Q with respect to the coordinate axes XYZ, and point X_{IJ}, Y_{IJ} is any element of the load. P_{MAX} represents the maximum ordinate of the pressure distribution and P_{IJ} the pressure at point X_{IJ}, Y_{IJ}. R_{IJ} is the horizontal distance from the vertical line through Q to point X_{IJ}, Y_{IJ}, and is defined by the equation

$$R_{IJ} = \sqrt{(X_{IJ} - H)^2 + (Y_{IJ} - G)^2}. \tag{7}$$

The program as described here provides for the surface ABCDE to be semiellipsoidal, although the program could be modified to permit any desired load distribution. Vertical stress is determined as a fraction of P_{MAX}, the reference pressure. Deflection is treated as a factor F in the equation

$$\Delta = \frac{P_{MAX}B}{E} F \tag{8}$$

where B is the reference dimension and E is the modulus of elasticity of the soil. Flow of the entire program is shown in block diagram form in Figure 3. A complete Fortran program for the IBM 7090 is given in Appendix A.

The first step in the program is to map the pressure distribution, P_{IJ}, and compute the radial distances R_{IJ} for each element of load, and store these quantities in two arrays in computer memory. It should be noted that for Simpson's Rule to apply an even number of equal intervals, and therefore an odd number of points in the loaded area, is necessary. Computation of stresses and deflection then proceeds along vertical line QS (Figure 2), beginning at the greatest depth used and working upward. This order of computation is used in order to

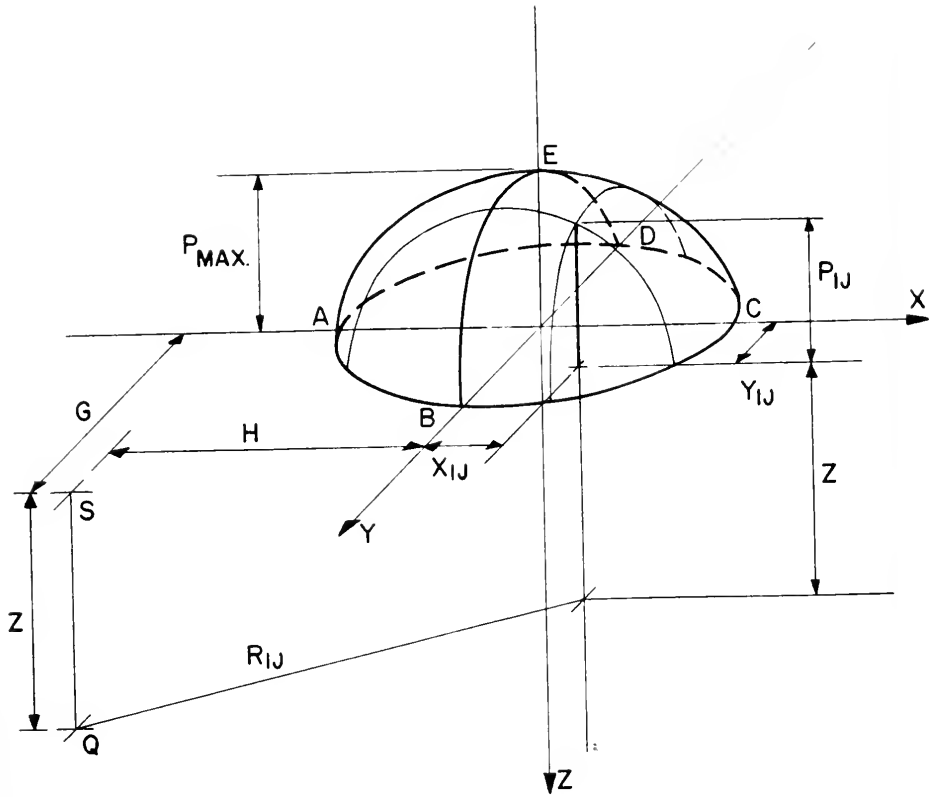

FIGURE 2. A DISTRIBUTED LOAD ILLUSTRATING TERMINOLOGY USED IN FORTRAN PROGRAM

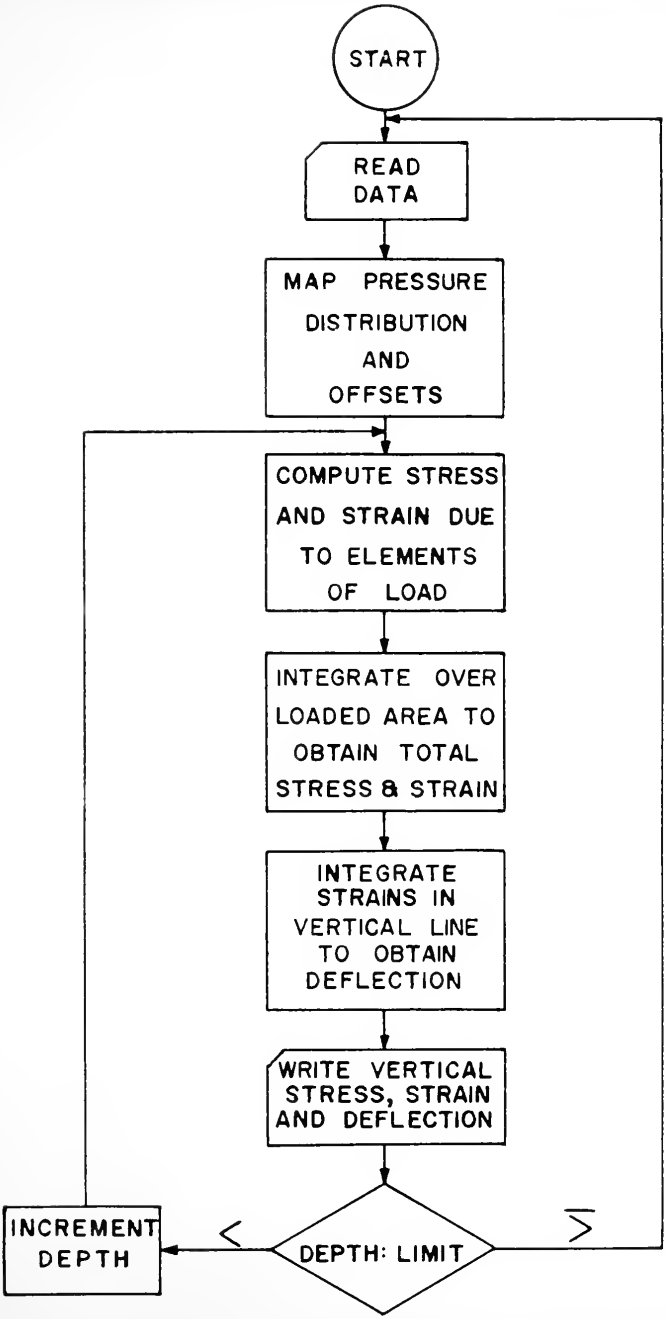

FIGURE 3. FLOW DIAGRAM

facilitate integration of strains and to eliminate the requirement of storing results in memory until a vertical line is completed.

Because the orientation of the point relative to an element of the load is variable, it is necessary to compute strain directly due to each element of the load. The program, therefore, provides for computation of both stresses and strain at a single point of interest due to a single element of load, repeating this routine for each element of load, then sums the results for the given point of interest. Similar computations for successive points along line QS permit the determination of total deflections.

Calculation of stresses for each element of load is according to equations 1, 2, and 3. Shear stress was not included since it has no effect on vertical strain, though it could be included easily provided a computer with adequate memory is available. With normal stresses known it is possible to calculate the factor $\sigma_1 - \mu\sigma_2 - \mu\sigma_3$ in equation 5. This permits the factor 1/E to be applied independently for the soil conditions pertaining in any instance. Because the strain required is that in a vertical direction, the factor becomes

$$\sigma_z - \mu\sigma_r - \mu\sigma_t$$

Having determined stress and the strain factor at Q due to one element of load, these values are stored in computer memory and the routine is repeated for the next element in the array. When all elements in one line of one coordinate direction have been covered, the vertical stress and the strain factor are integrated by equation 6 and the result stored in memory. The same process is used for successive lines across the loaded area. When all lines of load elements have been covered, the

stress and strain factor of the total load is calculated by another application of equation 6 in the second coordinate direction. The total stress and strain factor at the given point are then in computer storage available for printing out.*

Total deflection is, as noted, the sum of all strains along the vertical line through the point in question. Because Simpson's Rule requires an even number of intervals, it is not possible to perform the integration at every point. The computation of deflection factor is, therefore, limited to alternate points on the vertical line. Assuming zero deflection below the point of beginning, an initial deflection is calculated for the first point. Depth, stress, strain and deflection factor are printed out for this point. Depth is then reduced by a predetermined increment and the program returns to the point of computing normal stresses. When stress and strain for this point are computed, they are printed out, with no deflection computation, and depth is incremented again. On completing the third run, deflection is again computed, taking into account strains of all points computed previously, and again, depth, stress, strain and deflection factor are printed out. This process is repeated continuously, computing deflection factor only at alternate points, until depth is essentially zero. No actual result can be calculated for depth equal to zero at points beneath the load, because stress expressions for this case become undefined (i.e., zero divided by zero). End points for the stress curves are known, however, from the load distribution.

* Horizontal components of stress were not stored for summation because of lack of memory in the IBM 1620, on which the original programming was done. It should be noted, however, that these stresses could be retained and printed out with larger machines such as the IBM 7090 by adding subscripts to their notation, reducing to a fixed orientation, and repeating the summation process for these items.

This completes one cycle of program operation. Program control then causes reading of a new data record which defines a new vertical line and may provide new load configuration, grid size and/or Poisson's ratio. The computer is automatically reset to initial conditions and the entire program is repeated. Operation continues until no further data are supplied.

Provision is made in the program for a series of three different depth increments. This is desirable because the curves have relatively sharp curvature near the surface but are nearly straight at considerable depth. Using large increments for the deep points, a minimum of computer runs, and therfore computer time, is required. In areas of sharper curvature, the smaller intervals necessary for proper definition of the curves are used.

Input

Two input formats are required by this program. One provides data relative to the load and the vertical line along which stresses and deflection factors are determined. The second provides the depth boundaries which define the area of computation and the depth increments in each interval.

Data in the first input record are: A, the ratio of major to minor axis of the contact area (this may be unnecessary, or inadequate, for other distributions of load); N and M, the grid size; H and G, the coordinates which locate the vertical line along which computation proceeds; μ, the value of Poisson's ration to be used in the computations; and IDENT, an identification number to control flow of the program. The second input record includes DZ1, DZ2, DZ3, ZF1, ZF2, and ZF3 which

are the increments of depth and limiting depths, respectively, for each of three intervals. Computations begin at ZF3, and depth is incremented by DZ3. When depth ZF2 is reached, the increment is reduced to DZ2, and at depth ZF1 the increment is reduced again to DZ1. The use of two formats permits keeping input to a minimum. Having once established the depth ranges and increments, further data can be processed without redefining these values. On the initial data card a negative digit is punched in the control word IDENT. This digit causes reading of the following card which must contain the depth data in the second format described. Operation then proceeds normally. In successive data records, as long as the depth limits are to remain unchanged, the identification word is left blank. Program operation then by-passes the second input block, proceeding directly with computations for the new line of interest. New depth controls can be introduced for any set of data simply by punching a negative digit in the identification word of that data card and following it with the appropriate depth control data in the specified format.

All linear measurements are in terms of a characteristic dimension of the loaded area. This provides dimensionless results for compilation of general figures. For specific locations or deflections, however, results must be multiplied by the appropriate dimension.

Output

As each set of input data is read, that set of data is printed out for identification of the results which follow it. Each successive computer run through the program results in one line of printed output which represents conditions at a single point of interest. Information

printed includes depth of point as well as vertical stress and vertical strain at that point. Alternate lines also include the total deflection factor for the point. Thus, complete operation on one data set provides in printed output the coordinates of a vertical line relative to the loaded area, and a series of results for points along that line.

When all points defined on a vertical line have been completed, the program automatically reads a new data card representing a new line of interest. The process is repeated continuously as long as data are supplied to the computer.

The vertical stress indicated in the output represents the actual normal component of stress, at the point described, as a fraction of the maximum contact pressure, P_{MAX}. Deflections are expressed as a factor, F, which must be applied in equation 8 to give actual total deflections.

Curves

The second phase of this study, following development of the computer program, was to develop a set of curves of vertical stress and of deflection factor that would be useful both for design application and for further study. A number of difficulties in this aim are immediately evident, among the most important of which are -

1. Every distribution of load will produce a different family of curves;
2. Asymmetric loads will produce a unique family of curves for each vertical plane through any reference point;
3. Curves of deflection will depend on the value of Poisson's ratio used; and

4. Some characteristic pressure must be known as a base for determining actual stress and deflection for any given load.

There is nearly general agreement among investigators that the contact area under wheels on flexible pavements is approximately elliptical. Lawton's work on aircraft tires (10) confirms this and also shows that, for loads within the rated capacity of a tire, the distribution of pressure is essentially semiellipsoidal. The proportions of the contact area are fairly constant, the ratio of major to minor axis ranging generally from 1.6 to 1.8. Maximum pressure depends both on tire pressure and total load.

Typical curves of maximum pressure, P_{MAX}, vs. total load are shown in Figure 4. It can be seen from these curves that at rated load, on most subgrades, P_{MAX} is practically constant at 132 per cent of the average rigid plate contact pressure. In general, the average pressure may be taken as the inflation pressure. Thus, P_{MAX} would be 1.32 times the inflation pressure. For more precision, of course, it may be necessary at times to refer to actual curves of contact pressure vs. inflation pressure and P_{MAX}/p_{ave} vs. load, as presented by Lawton.

On the basis of available information it was decided to construct a set of curves for a semiellipsoidal load, using a ratio of major to minor axis of contact area equal to 1.7. This is shown in Figure 5 where A = 1.7 and B = 1. The equation of the surface which defines the pressure distribution is

$$\frac{X^2}{A^2} + \frac{Y^2}{B^2} + \frac{P^2}{P_{MAX}^2} = 1 \qquad (9)$$

Hence, the pressure at any point, (I, J), on the contact area is:

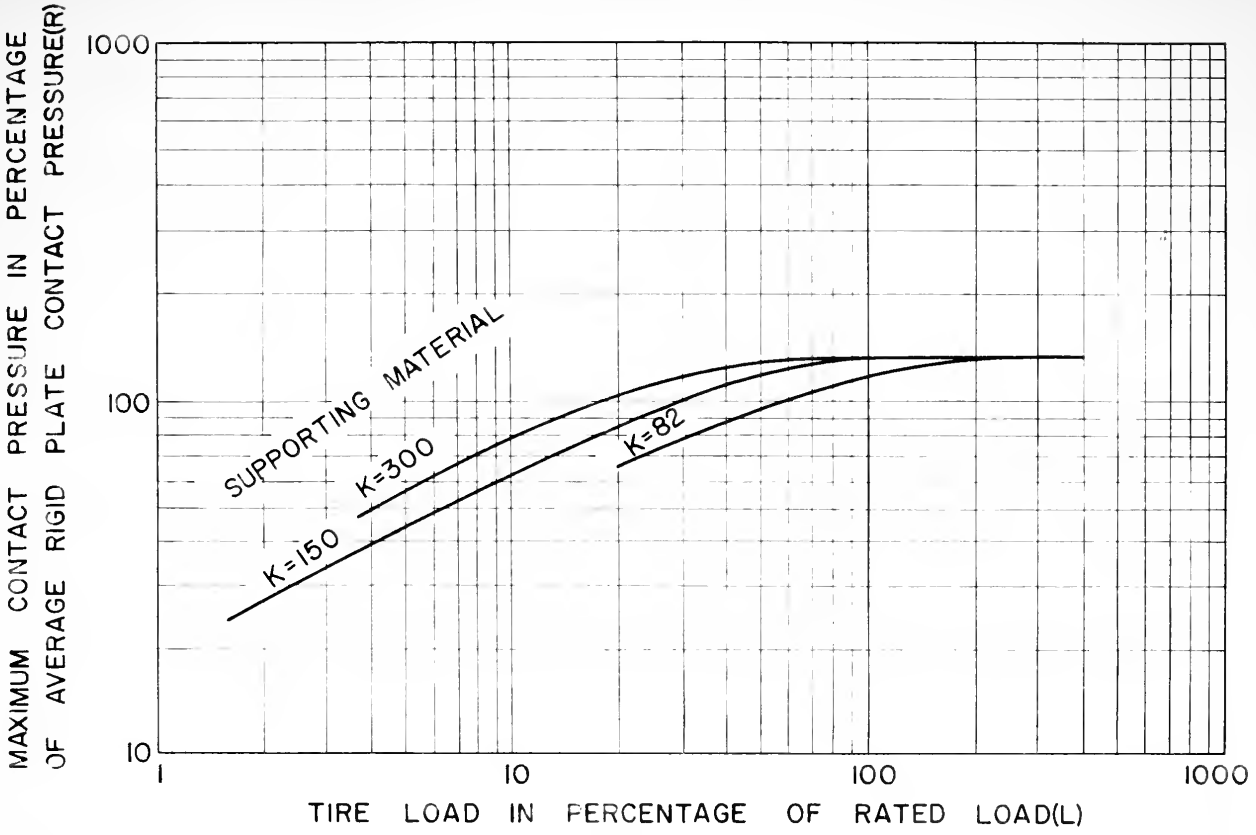

FIGURE 4. MAXIMUM CONTACT PRESSURE AT CENTER OF TIRE (FROM LAWTON, PROCEEDINGS, HIGHWAY RESEARCH BOARD, 1957)

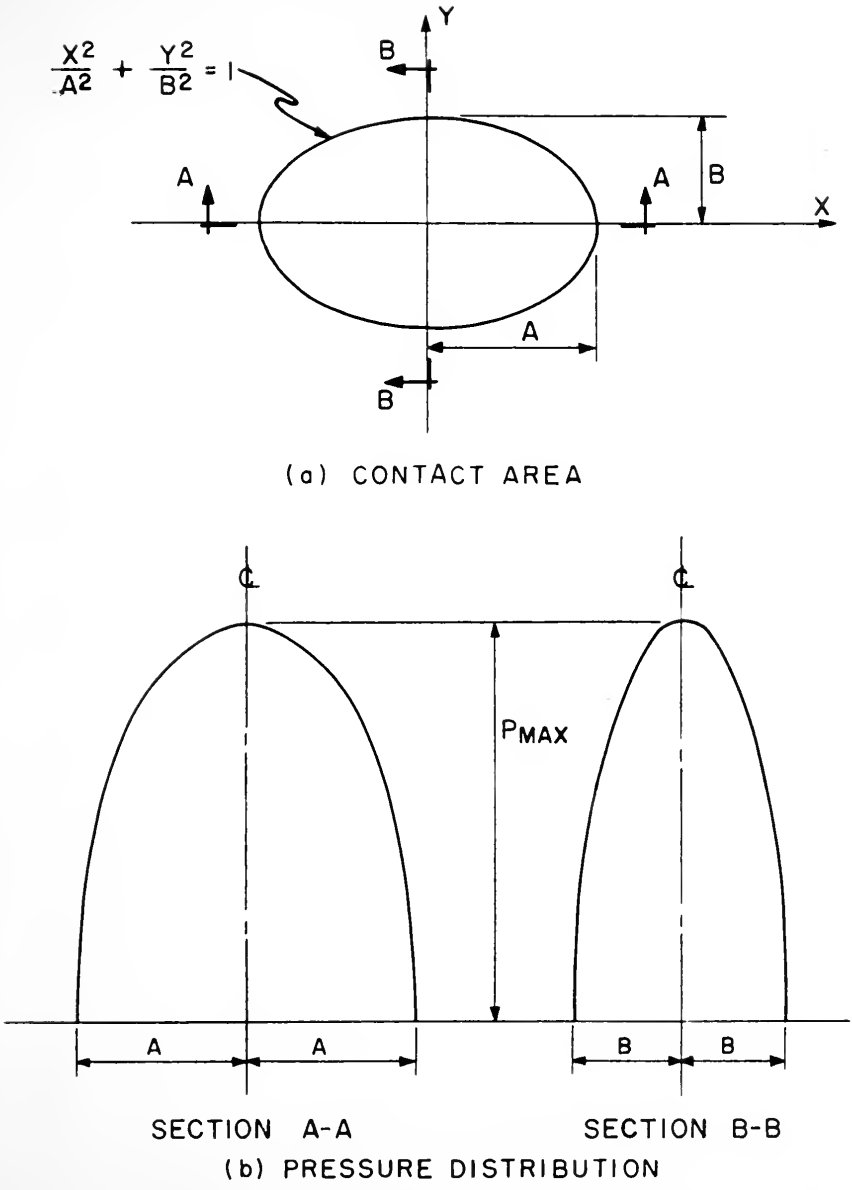

FIGURE 5. CONTACT AREA AND PRESSURE DISTRIBUTION

$$P_{IJ} = P_{MAX}\sqrt{1 - X_{IJ}^2 - \frac{Y_{IJ}^2}{A^2}} \qquad (10)$$

No attempt was made in this study to evaluate Poisson's ratio for any particular condition. While the computer program provides for any value between 0 and 0.5, the development of the curves was in conformance with the general practice of taking $\mu = 0.5$. The curves for vertical stress are not dependent on μ, of course, so are valid for any soil. The curves for deflection factor are dependent on μ as is seen in equations 2, 3, and 5, and are, therefore, limited to the assumption of $\mu = 0.5$ which implies no volume change.

The question of orientation is not as easily resolved. Because the load is not distributed symmetrically, the stress, and therefore deflection, a given distance from the center in one direction is different from that in another direction. For single or dual wheels, one set of curves would be adequate since all points of interest would be under the center of the load or on a plane through the transverse axis. When considering tandem axles, however, two more planes are immediately necessary - one along the longitudinal axis of one wheel and one through the centers of two diagonal wheels. Theoretically, this would require a different diagonal plane for each geometrically different arrangement of tandem axles in use. It would be possible to develop a complete set of charts for planes oriented say every five or ten degrees from the transverse axis. However, since one wheel of a tandem gear has a relatively small effect on stresses under the diagonally opposite wheel, the result would seem to be unwieldly and confusing, without adding any great usefulness to the charts. There-

fore, one diagonal plane was selected which would give a reasonable approximation of the diagonal for standard dual-tandem geare. It is expected that for most practical situations the actual stresses and deflections determined from this family of curves will give values correct within the precision of the curves. When more precise work is needed, of course, the computer program may be used directly or a new set of curves may be produced for the required orientation.

The four major problems are thus resolved by assuming a semi-ellipsoidal load, evaluating curves in planes oriented in three directions, assuming Poisson's ration = 0.5, and taking the reference pressure as the maximum of the ellipsoidal distribution, which is related to the inflation pressure.

All curves are kept dimensionless by taking the characteristic dimension, B, as unity. By this technique, the curves are made valid for any load of the same proportions used here, regardless of size of contact area or magnitude of load. Depths and offsets measured in terms of one half the minor axis of the loaded area correspond to depths and offsets in the curves. Results are plotted for depths and offsets up to ten units. Deflections were calculated by integrating strains to a total depth of 500 units.

The completed curves appear in Figures 6 through 11. The orientation of the plane represented by each chart is shown on the figure, Figures 6 and 7 being for the transverse axis of load, Figures 8 and 9 for the diagonal and Figures 10 and 11 for the longitudinal axis. Vertical stresses are shown in Figures 6, 8 and 10. Stress in per cent of maximum contact pressure, P_{MAX}, is plotted to a logarithmic scale

on the horizontal axis, and depth to an arithmetic scale on the vertical axis. Each curve represents stress at a distance R from the center of the load along the line indicated on the figure. Numbers on the curves indicate the value of R in terms of B, one half the minor axis of the contact area.

Figures 7, 9 and 11 present deflection factors in a similar manner. Actual total deflection for a given point is determined by equation 8. To determine stress or deflection at some point under a multiple arrangement of wheels, the appropriate factors are read from the curves for each wheel, and added. The sum gives the effect of the load group. An example determination of stress and deflection under one wheel of a tandem axle is shown in Appendix B.

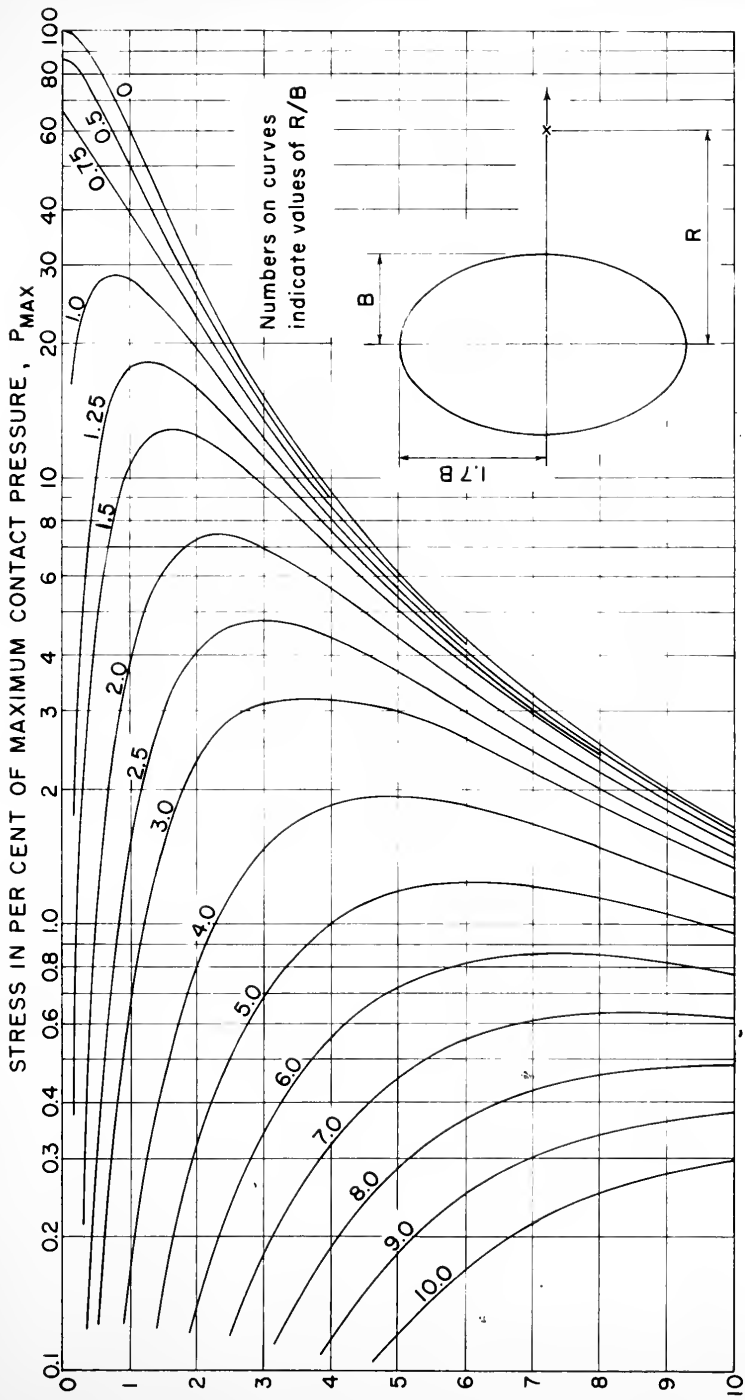

FIGURE 6. VERTICAL STRESS, σ_z. TRANSVERSE PLANE.

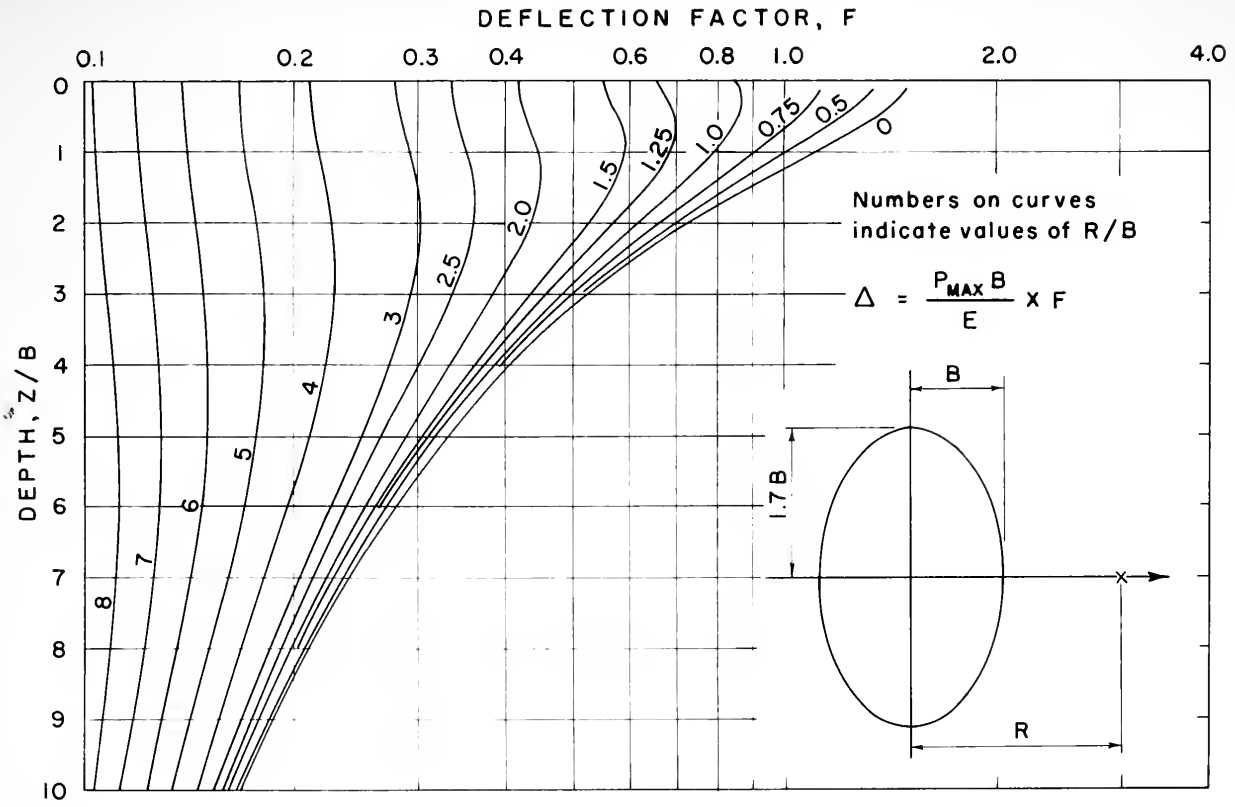

FIGURE 7. VERTICAL DEFLECTION, Δ. TRANSVERSE PLANE. (POISSON'S RATIO = 0.5).

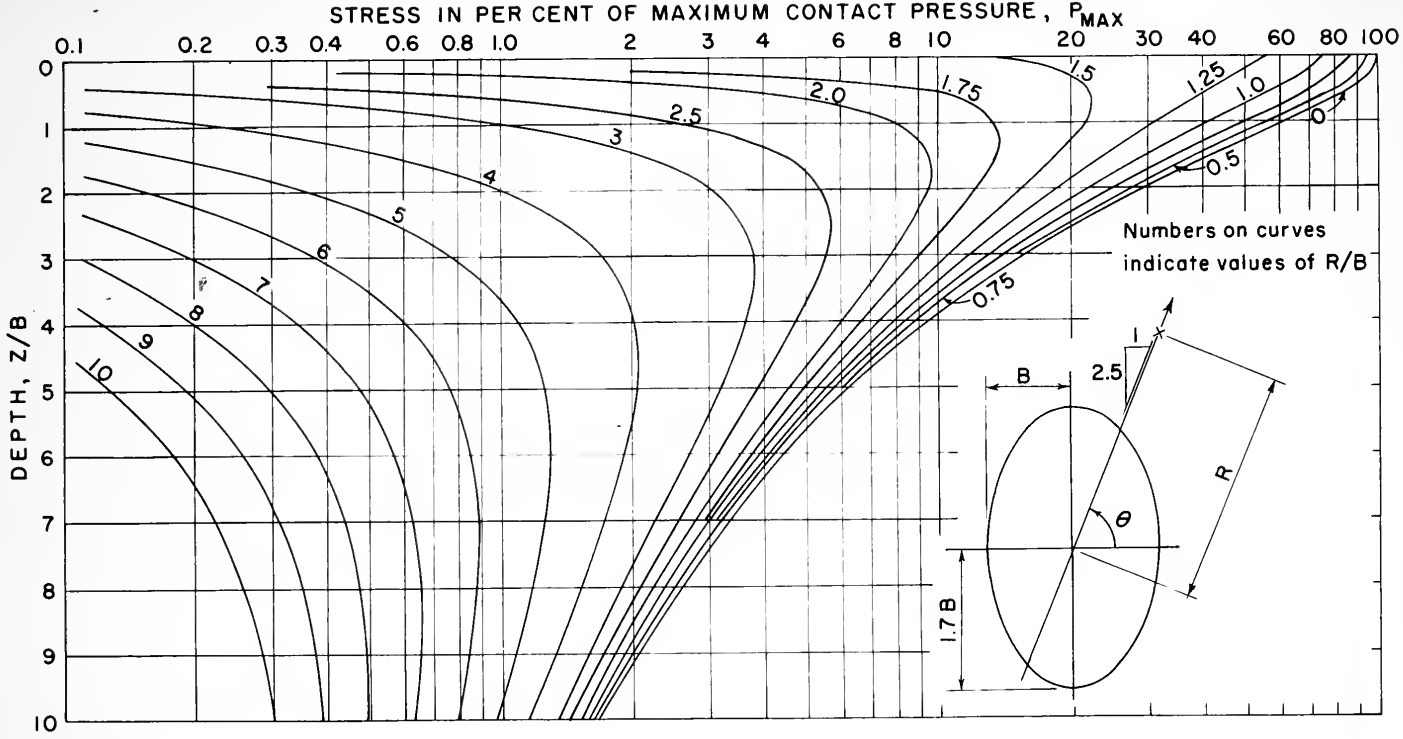

FIGURE 8. VERTICAL STRESS, σ_z. DIAGONAL PLANE ($\theta = 68.2°$).

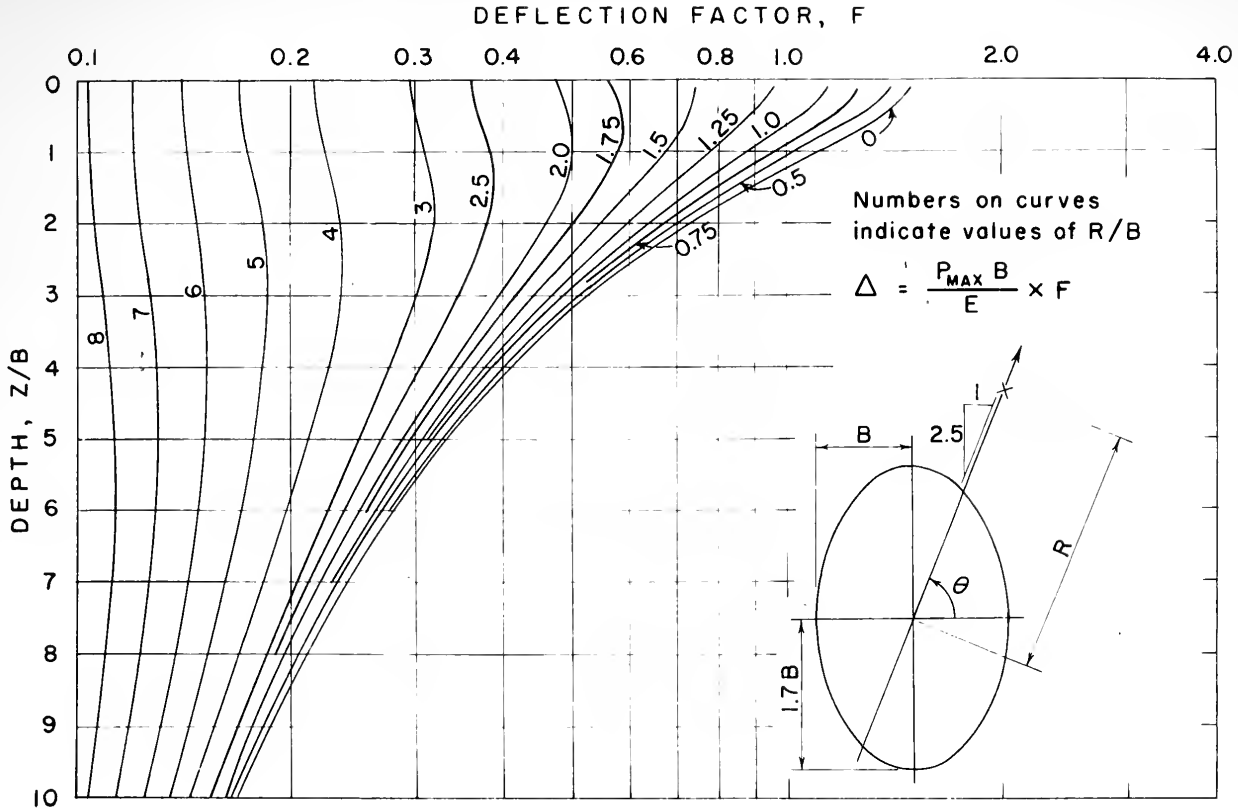

FIGURE 9. VERTICAL DEFLECTION, Δ. DIAGONAL PLANE ($\theta = 68.2°$). (POISSON'S RATIO = 0.5).

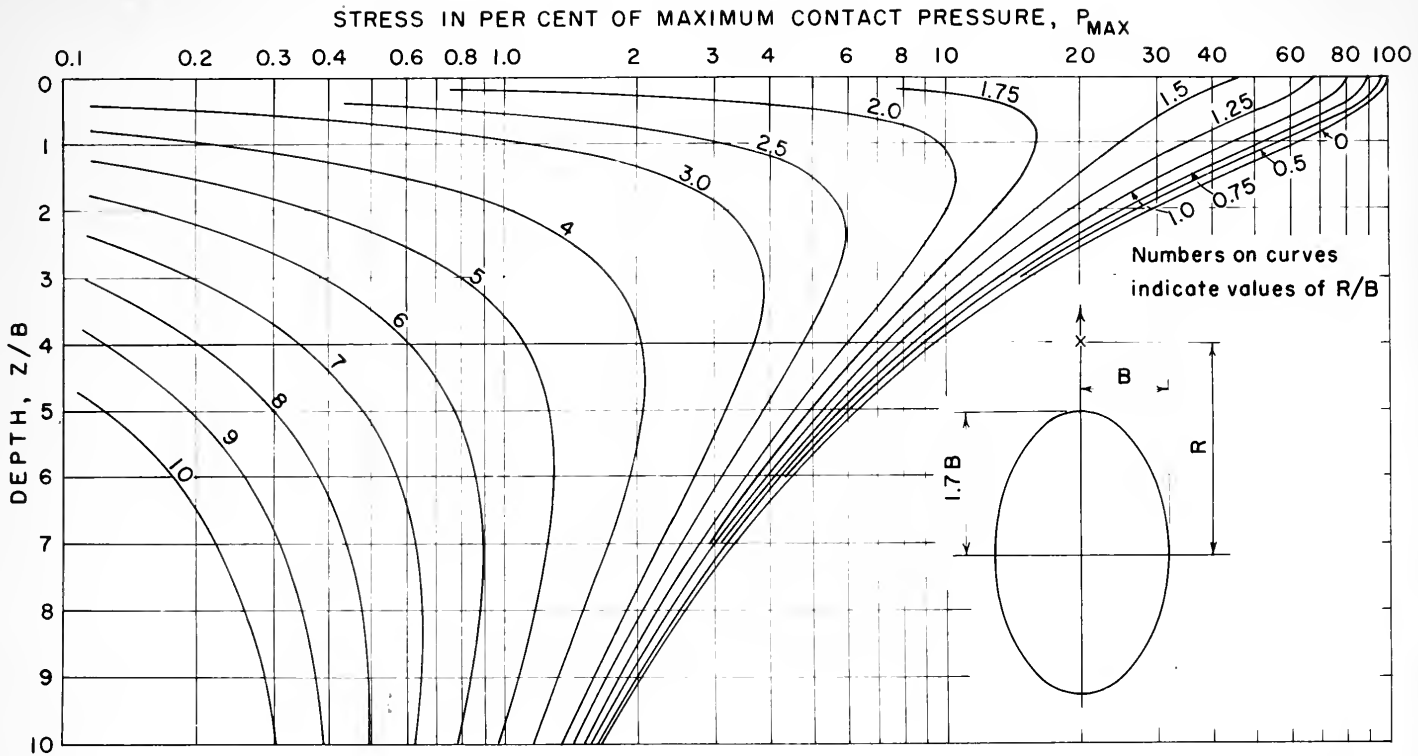

FIGURE 10. VERTICAL STRESS, σ_z. LONGITUDINAL PLANE.

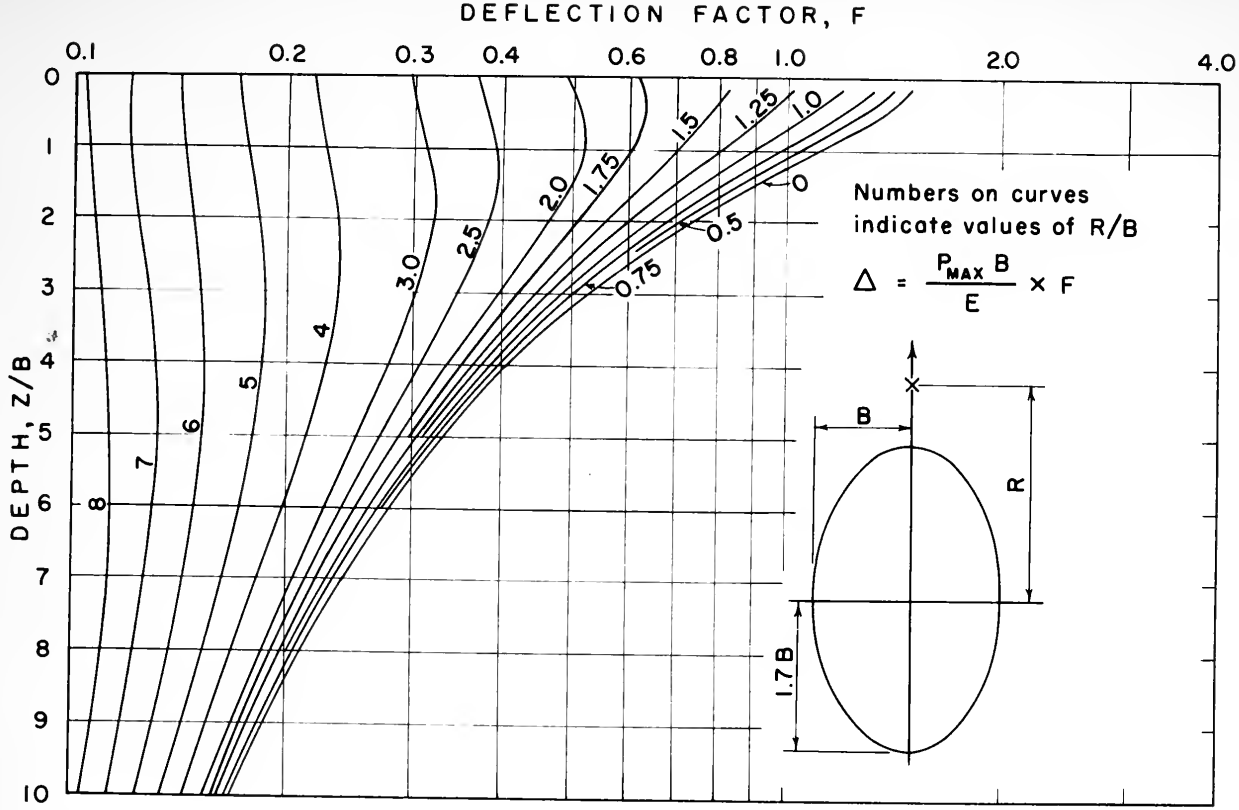

FIGURE 11. VERTICAL DEFLECTION, Δ. LONGITUDINAL PLANE. (POISSON'S RATIO = 0.5).

SUMMARY AND CONCLUSION

Summary

This study has produced a digital computer program to perform a numerical integration for determination of vertical stresses and deflections in pavements under wheel loads.

Loads were treated as semiellipsoidal distributions of pressure over the tire contact area. Boussinesq theory of stress distribution was applied, using Simpson's rule to integrate the effect of the entire loaded area. Elastic strains were calculated from the stresses, and integrated along vertical lines to determine total deflection factors.

Using the program reported here, curves of stress and deflection factor vs. depth were plotted for three different orientations of a vertical plane through the center of the load - transverse and longitudinal axes and one diagonal direction. The ratio of major to minor axis of load was taken as 1.7. The maximum pressure, at the center of the load, was used as a reference pressure. Poisson's ratio was taken as 0.5. Curves are provided for depths and offset distances up to five times the width of the load.

Recommendations

The following recommendations are made as a result of the study reported herein:

1. That further study be made of the distribution of pressure over the contact areas of tires -especially of truck tires.

2. That the computer program be used for further comparisons of different load distributions - in particular, the effect of uniform loads over elliptic contact areas compared to semi-ellipsoidal loads.

3. That a study of theoretical pavement deflections be made comparing results of three layer theory with those of this report.

BIBLIOGRAPHY

BIBLIOGRAPHY

1. Baker, R. F., and Papazian, H. S., "The Effect of Stiffness Ratio on Pavement Stress Analysis", Proceedings, Highway Research Board, 1960.

2. Brahma, S. P., "Design of Flexible Pavements", Masters Thesis, University of Wisconsin, 1958.

3. Burmister, D. M., "The Theory of Stresses and Displacements in Layered Soil Systems and Application to the Design of Airport Runways", Proceedings, Highway Research Board, 1943.

4. Foster, C. R., and Ahlvin, R. G., "Stresses and Deflections Induced by a Circular Load", Proceedings, Highway Research Board, 1954.

5. Foster, C. R., and Fergus, J. M., "Stress Distribution in Homogeneous Soil", Research Bulletin #12F, Highway Research Board, January, 1951.

6. Fox, L., "Computation of Traffic Stresses in a Simple Road Structure", Road Research Technical Paper No. 9, Department of Scientific and Industrial Research, Road Research Laboratory, 1948.

7. Heldt, P. M., "Ground Contact Area of Tires Varies Directly with Deflection", Automotive Industries, Vol. 64, No. 4, 23 July, 1932.

8. Herner, R. C., and Aldous, W. M., "The Load Transmission Test for Flexible Paving and Base Courses - Part I", Technical Development Report No. 108, Civil Aeronautics Administration Technical Development and Evaluation Center.

9. Jones, A., "Tables of Stresses in Three-Layer Elastic Systems", Paper presented at Highway Research Board Annual Meeting, January, 1962.

10. Lawton, W. L., "Static Load Contact Pressure Patterns Under Airplane Tires", Proceedings, Highway Research Board, 1957.

11. McLeod, N. W., "Influence of Tire Design on Pavement Design and Vehicle Mobility", Proceedings, Highway Research Board, 1952.

12. Newmark, N. M., "Influence Charts for Computation of Stresses in Elastic Foundations", Bulletin No. 338, University of Illinois Experiment Station, 1942.

13. Newmark, N. M., "Influence Charts for Computation of Vertical Displacements in Elastic Foundations", Bulletin No. 367, University of Illinois Experiment Station, 1947.

14. Palmer, L. A., and Barber, E. S., "Soil Displacement Under a Circular Loaded Area", Proceedings, Highway Research Board, 1940.

15. Stoll, U. W., "Computer Solution of Pressure Distribution Problem", Journal of Soil Mechanics and Foundations Division, American Society of Civil Engineers, December, 1960.

16. Taylor, D. W., Fundamentals of Soil Mechanics, John Wiley & Sons, Inc., New York, 1958.

17. Teller, L. W., and Buchanan, J. A., "Determination of Variation in Unit Pressure Over the Contact Area of Tires", Public Roads, Vol. 18, No. 10, December, 1937.

18. Timoshenko, S., and Goodier, J. N., Theory of Elasticity, McGraw-Hill Book Company, Inc., New York, 1951.

19. Walker, R. D., "Significance of Layer Deflections in Evaluating Flexible Pavements", Ph. D. Thesis, Purdue University, 1961.

20. Yoder, E. J., Principles of Pavement Design, John Wiley & Sons, Inc., New York, 1959.

21. Yoder, E. J., "Flexible Pavement Deflections - Methods of Analysis and Interpretation", Paper presented to the American Association of Asphalt Paving Technologists, January, 1962.

APPENDIX

APPENDIX A

Fortran Program for IBM 7090 Computer

```
      DIMENSION P2PI(25,25),R(25,25),U(25),V(25),W(25),U2(25),DY(25)
  110 FORMAT (F5.2,2I4,2F7.2,F5.2,I3)
  111 FORMAT (F5.2,5F7.2)
  112 FORMAT (1H ,F15.2,2F15.5)
  113 FORMAT (1H ,F15.2,3F15.5)
    3 READ INPUT TAPE 7,110,A,N,M,H,G,RATIO,IDENT
      IF(IDENT)2,4,4
    2 READ INPUT TAPE 7,111,DZ1,DZ2,DZ3,ZF1,ZF2,ZF3
    4 WRITE OUTPUT TAPE 6,110,A,N,M,H,G,RATIO
      DZ =DZ3
      PDELT = 0.0
      DELTA = 0.0
      SUMD = 0.0
      K = 1
      IZ = 1
      E = M+1
      F = N+1
      DX = 2.0*A/F
      X = DX-A
      DO 11 I=1,N
      YMAX = SQRTF(1.0-X*X/(A*A))
      DY(I) = 2.0*YMAX/E
      Y = DY(I)-YMAX
      DO 10 J=1,M
      P2PI(I,J) = (SQRTF(1.0-X*X/(A*A)-Y*Y))/(2.0*3.1416)
      R(I,J) = SQRTF((X-H)*(X-H)+(Y-G)*(Y-G))
   10 Y = Y+DY(I)
   11 X = X+DX
      M1 = M-1
      N1 = N-1
      Z = ZF3
    1 DO 16 I=1,N
      DO 15 J=1,M
      Q = SQRTF(Z*Z+R(I,J)*R(I,J))
      Q3 = Q*Q*Q
      Q5 = Q3*Q*Q
      S = R(I,J)*R(I,J)+Z*Z+Z*Q
      V(J) = 3.0*P2PI(I,J)*Z*Z*Z/Q5
      V2 = P2PI(I,J)*(3.0*R(I,J)*R(I,J)*Z/Q5-(1.0-2.0*RATIO)/S)
      V3 = P2PI(I,J)*(2.0*RATIO-1.0)*(Z/Q3-1.0/S)
      W(J) = V(J)-RATIO*(V2+V3)
   15 CONTINUE
```

```
      I2 = 1
 69   EVENS = 0.0
      DO 5 J=2,M1,2
  5   EVENS = EVENS+V(J)
      ODDS = 0.0
      DO 6 J=1,M,2
  6   ODDS = ODDS+V(J)
      SUM = DY(I)/3.0*(4.0*ODDS+2.0*EVENS)
      GO TO (72,73),I2
 72   U(I) = SUM
      I2 = 2
      DO 74 J=1,M
 74   V(J) = W(J)
      GO TO 69
 73   U2(I) = SUM
 16   CONTINUE
      I3 = 1
 79   EVENS = 0.0
      DO 7 I=2,N1,2
  7   EVENS = EVENS + U(I)
      ODDS = 0.0
      DO 8 I=1,N,2
  8   ODDS = ODDS + U(I)
      SUM = DX/3.0*(4.0*ODDS + 2.0*EVENS)
      GO TO (77,78),I3
 77   SIGZ = SUM
      I3 = 2
      DO 80 I=1,N
 80   U(I) = U2(I)
      GO TO 79
 78   DDELT = SUM
      GO TO (50,51),K
 50   SUMD = SUMD+DDELT
      DELTA = SUMD*DZ/3.0+PDELT
      SUMD = SUMD+DDELT
      K = 2
      WRITE OUTPUT TAPE 6,113,Z,SIGZ,DDELT,DELTA
      GO TO (90,91,92),IZ
 51   SUMD = SUMD+4.0*DDELT
      WRITE OUTPUT TAPE 6,112,Z,SIGZ,DDELT
      K = 1
      GO TO 41
 90   IF(Z-ZF2)100,100,41
100   DZ = DZ2
      PDELT = DELTA
      SUMD = DDELT
101   IZ = IZ+1
 41   Z = Z-DZ
      GO TO 1
 91   IF(Z-ZF1)102,102,41
102   DZ = DZ1
      PDELT = DELTA
```

```
      SUMD = DDELT
      GO TO 101
92    IF(Z-DZ)3,3,41
      END
```

APPENDIX B

Example Determination of Stress and Deflection

As an example of the use of the curves presented in this report, the vertical stress and deflection at a depth of 36 in. beneath one wheel of a dual-tandem aircraft gear, at rated load, is determined. The gear configuration, as shown in Figure 12, consists of dual wheels spaced at 31-1/4 in. center to center and tandem axles at 61-1/4 in. center to center. Total gear load is 178,000 lb, inflation pressure is 176 psi, and contact area is 267 sq in. The modulus of elasticity of the subgrade is 2700psi.

Contact area $= 1.7\pi B^2 = 267$ sq in.

$$B = \sqrt{\frac{267}{1.7\pi}} = 7.07 \text{ in.}$$

$$\frac{Z}{B} = \frac{36}{7.07} = 5.1$$

$$P_{MAX} = 1.32 \times 176 = 232 \text{ psi}$$

$$R_c = \sqrt{(31.25)^2 + (61.25)^2} = 68.7 \text{ in.}$$

Wheel	R	R/B	$z(\%P_{MAX})$	F
A	0.0	0.0	6.00 (Fig. 6)	0.33 (Fig. 7)
B	61.25	8.7	0.23 (Fig. 10)	0.1± (Fig. 11)
C	68.7	9.7	0.15 (Fig. 8)	0.0± (Fig. 9)
D	31.25	4.4	1.70 (Fig. 6)	0.19 (Fig. 7)
		Σ	8.08	0.62

$$\sigma_z = \frac{8.08}{100} \times 232 = 18.7 \text{ psi}$$

$$\Delta = \frac{232 \times 7.07}{2700} \times 0.62 = 0.38 \text{ in.}$$

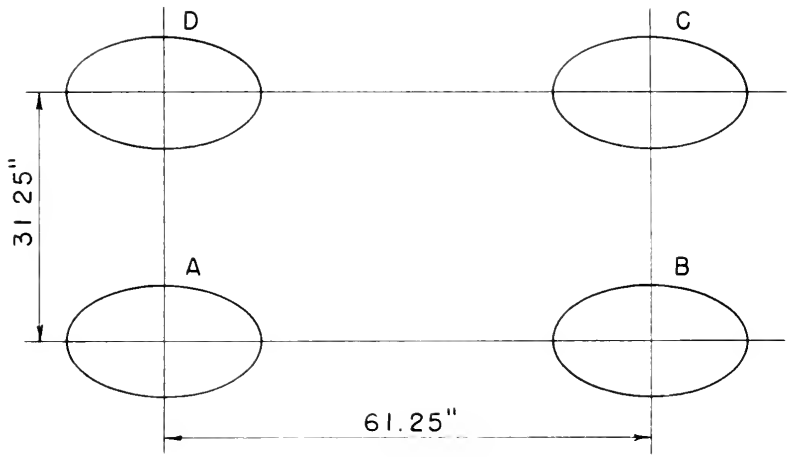

FIGURE 12. EXAMPLE GEAR CONFIGURATION.

AERIAL PHOTOGRAPHY APPLIED TO TRAFFIC STUDIES

MAY 1963
NO. 14

Joint Highway Research Project

PURDUE UNIVERSITY
LAFAYETTE INDIANA

by

W.F. HOWES
and
R.D. MILES

Technical Paper

AERIAL PHOTOGRAPHY APPLIED TO TRAFFIC STUDIES

TO: K. B. Woods, Director
Joint Highway Research Project

May 8, 1963

FROM: H. L. Michael, Associate Director
Joint Highway Research Project

File: 1-4-19
Project: C-36-32S

Attached is a technical paper entitled "Aerial Photography Applied to Traffic Studies" by W. F. Howes, Graduate Assistant, and R. D. Miles, Research Engineer. The paper was presented at the Research Session of the 49th Annual Purdue Road School on March 25, 1963.

The paper discusses the potential uses of time-lapse aerial photography in the study of highway traffic flow phenomena. Procedures for photographically obtaining basic data on traffic speeds, volumes, densities and headways are described. The method's ability to record driver acceleration, merging, diverging, weaving and passing practices is noted. The precision, accuracy, efficiency and limitations of the method are cited.

This paper is presented to the Board for the record.

Respectfully submitted,

Harold L. Michael

Harold L. Michael, Secretary

HLM/lko

Attachment

Copy:

F. L. Ashbaucher
J. R. Cooper
W. L. Dolch
W. H. Goetz
F. F. Havey
F. S. Hill
G. A. Leonards
J. F. McLaughlin
R. D. Miles
R. E. Mills
M. B. Scott
J. V. Smythe
J. L. Waling
E. J. Yoder

Technical Paper

AERIAL PHOTOGRAPHY APPLIED TO TRAFFIC STUDIES

by

W. F. Howes
Graduate Assistant

and

R. D. Miles
Research Engineer

Joint Highway Research Project
File No: 1-4-19
Project No: C-36-32S

Purdue University
Lafayette, Indiana
May 8, 1963

AERIAL PHOTOGRAPHY APPLIED TO TRAFFIC STUDIES

W. F. Howes
Graduate Assistant

R. D. Miles
Research Engineer

SYNOPSIS

This paper reports on a study of the applicability of aerial photography to the collection and analysis of highway traffic flow data. Specifically, time-lapse aerial photographs were investigated relative to their accuracy and efficiency in securing speed, volume, headway and other pertinent information on vehicle movement.

The aerial photographic method, although impractical for the conventional fixed location, limited scope traffic survey (e.g. a volume count or "spot" speed study), demonstrated a significant potential in the task of recording a wide variety of traffic phenomena over "space" as well as time. Time-lapse photography, with its ability to record a driver's behavior in a series of exposures, was judged to be the most accurate and practical way to analyze vehicle acceleration, merging, diverging, weaving and passing patterns over an extended length of roadway. These are important traffic flow elements which are all but impossible to study by conventional ground methods.

Among the most important assets of the aerial photographic method is its ability to pictorially record the environment in which traffic data are obtained. This attribute enhances the value of the data by affording the investigator with possible reasons for unusual traffic behavior.

AERIAL PHOTOGRAPHY APPLIED TO TRAFFIC STUDIES

[illegible]

[illegible] billion dollars will be spent [illegible] construction of [illegible] officials [illegible] of [illegible] affords, [illegible]

[illegible] only little is [illegible] of motor vehicles on the [illegible] data [illegible] and headway [illegible] been [illegible] at a fixed location [illegible] a complete "view" of flow [illegible] characteristics [illegible] between [illegible] have been made [illegible] various [illegible] by means of mathematical models and computer [illegible] capacity [illegible] control [illegible] These efforts, however, have been [illegible] by a lack of [illegible] field

data; i.e., data collected over "space" as opposed to the conventional "spot", or fixed location, studies.

Four general data gathering techniques are presently in use. By far the most common are the various manual and automatic methods. These, however, are applicable principally to "spot" studies of speed, volume and headways and, thus, are of limited value in the study of vehicle flow. Moving test vehicle procedures, while affording spacial data, are quite limited in the accuracy and variety of information obtainable.

Photography has often been suggested as a valuable tool in the collection of spacial traffic data. As early as 1927, the speed, volume and headway components of vehicle flow were being studied with the aid of aerial photography (8). By 1933, Bruce Greenshields had developed a terrestrial time-lapse motion picture technique which yielded accurate speeds and headways (4). Greenshields noted in 1947 the potential uses of aerial photography in traffic research (6). In recent years, Chicago Aerial Survey has pioneered the application of stereo continuous strip photography to the study of traffic flow (11, 9).

PURPOSE AND SCOPE

It was the purpose of this research to study, in terms of applicability, accuracy and efficiency, the time-lapse vertical aerial photography method of collecting traffic flow data. The technique was investigated relative to its ability to detect and record volume, speed, vehicle spacing and lane use information. Consideration was also given its use in gathering density, acceleration, vehicle placement, minimum passing distance, and other pertinent flow data.

DESCRIPTION OF THE METHOD

The vertical view of all points on a horizontal plane surface yields an object image of unchanging scale provided a single height of observation above the surface is maintained. The aerial photography technique permits a recording, with certain inherent distortions, of this image on a photographic film. The scale of the photographic image is a function of the lens focal length (f) and the above ground elevation (H) of the camera (aircraft) as equated by

$$\text{Scale} = s = \frac{H(\text{feet})}{f(\text{inches})}$$

Through a partial overlapping in the fields of view of two vertical photos taken at slightly different, but known, points in time and space, the motion of ground objects, such as motor vehicles, can be measured and recorded in terms of distance per unit time. In addition, measurements of headways between moving objects and their positions relative to fixed points may be obtained directly from the aerial photographs.

Procedure - Data Gathering

The Indiana State Highway Commission, Bureau of Photogrammetric and Electronic Processes, secured and processed the aerial photography used in this research. Employing a K-17C aerial camera adapted for a high speed recycling of two seconds or better and mounted in a State owned Piper Apache aircraft, nine inch by nine inch photography was obtained at five level and tangent highway locations in Hammond and Indianapolis, Indiana. By virtue of a 12-inch focal length lens and an 1800 foot flight elevation, a photo scale of approximately 150 feet per inch was maintained.

As estimated by the following relationship, a 72 percent overlap was considered sufficient to assure the appearance of nearly all vehicles in at least two photographs when a time interval of three seconds between exposures was used.

$$Q = \frac{\frac{1}{2} ls + S_V^t (t)}{ls} \quad (100)$$

where

Q = percent overlap

l = the photograph's dimension, in inches, parallel to the flight line

s = scale of photography in feet per inch

S_V^t = maximum expected vehicle speed in feet per second

t = time interval between exposures in seconds

Settings:

l = 9 inches, s = 150 feet per inch,

S_V^t = 100 feet per second and t = 3 seconds,

a Q of 72 percent results.

This interval-overlap combination was achieved by maintaining an aircraft ground speed of approximately 65 mph.

From four to eight tangent flight runs of one to two miles in length were made at each site during evening periods of high traffic volume in the Summer and Fall of 1962. By flying in a direction opposite to the major flow, the amount of data obtained per run was maximized. Four of the sites were recorded on Aerographic black and white film:

The Tri-State Expressway, a four-lane freeway in northwestern Indiana (Figure 1).

The Indiana East-West Toll Road, a four-lane freeway in northwestern Indiana (Figure 2).

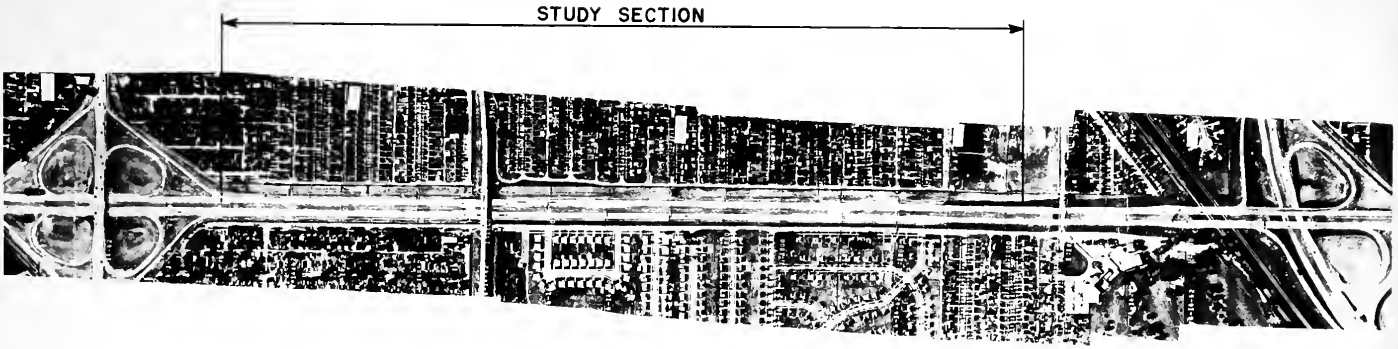

FIGURE 1. TRI-STATE EXPRESSWAY, HAMMOND

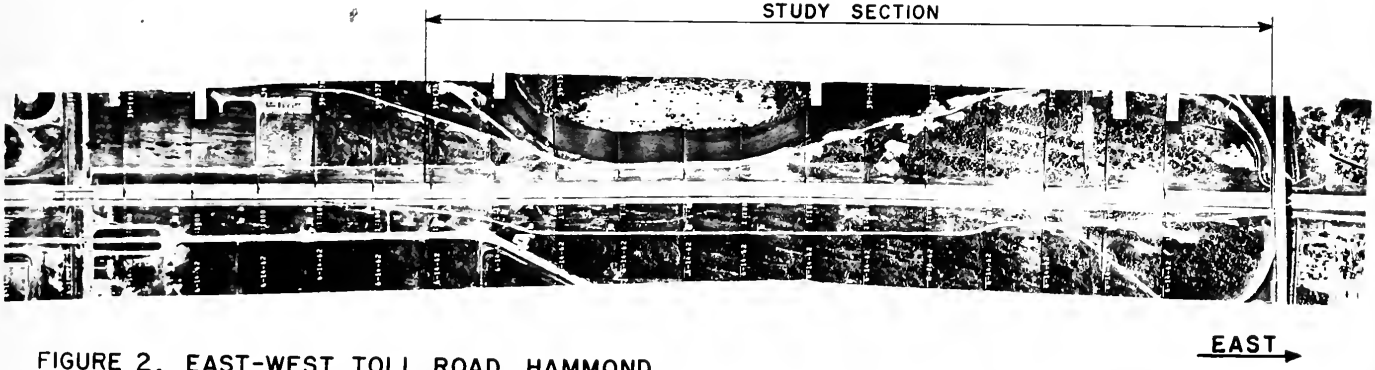

FIGURE 2. EAST-WEST TOLL ROAD, HAMMOND

Shadeland Avenue, a major arterial in [illegible] Indianapolis (Figure [illegible]).

[illegible] Indianapolis [illegible]

A fi[illegible] locati[illegible] [illegible]

[illegible]

[illegible]

[illegible]

da[illegible]

[illegible]

[illegible]

[illegible]

[illegible]

aerial [illegible]

[illegible]

was [illegible]

[illegible]

representing [illegible] Each exposure [illegible] the [illegible] segregation of [illegible]

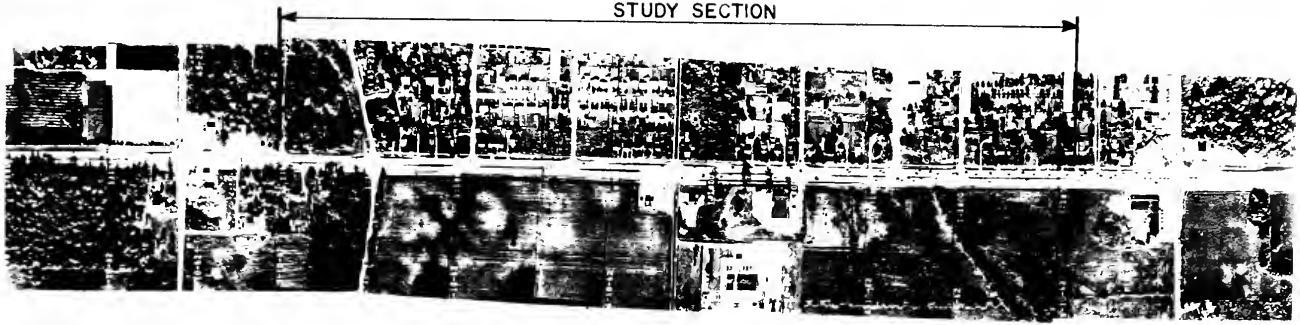

FIGURE 3. SHADELAND AVENUE (S.R. 100), INDIANAPOLIS

SOUTH

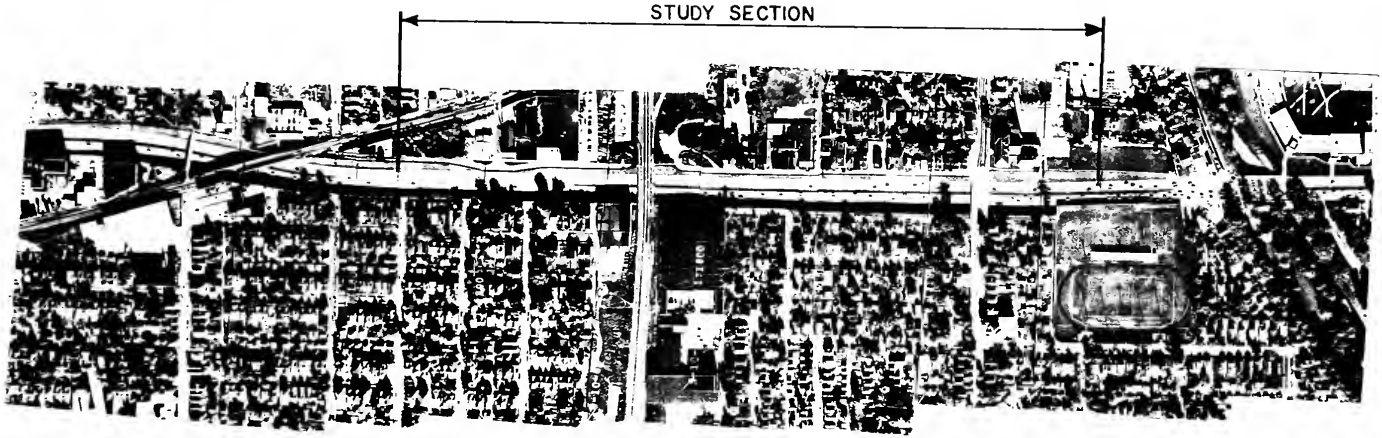

FIGURE 4. MADISON AVENUE (U.S. 31), INDIANAPOLIS

SOUTH

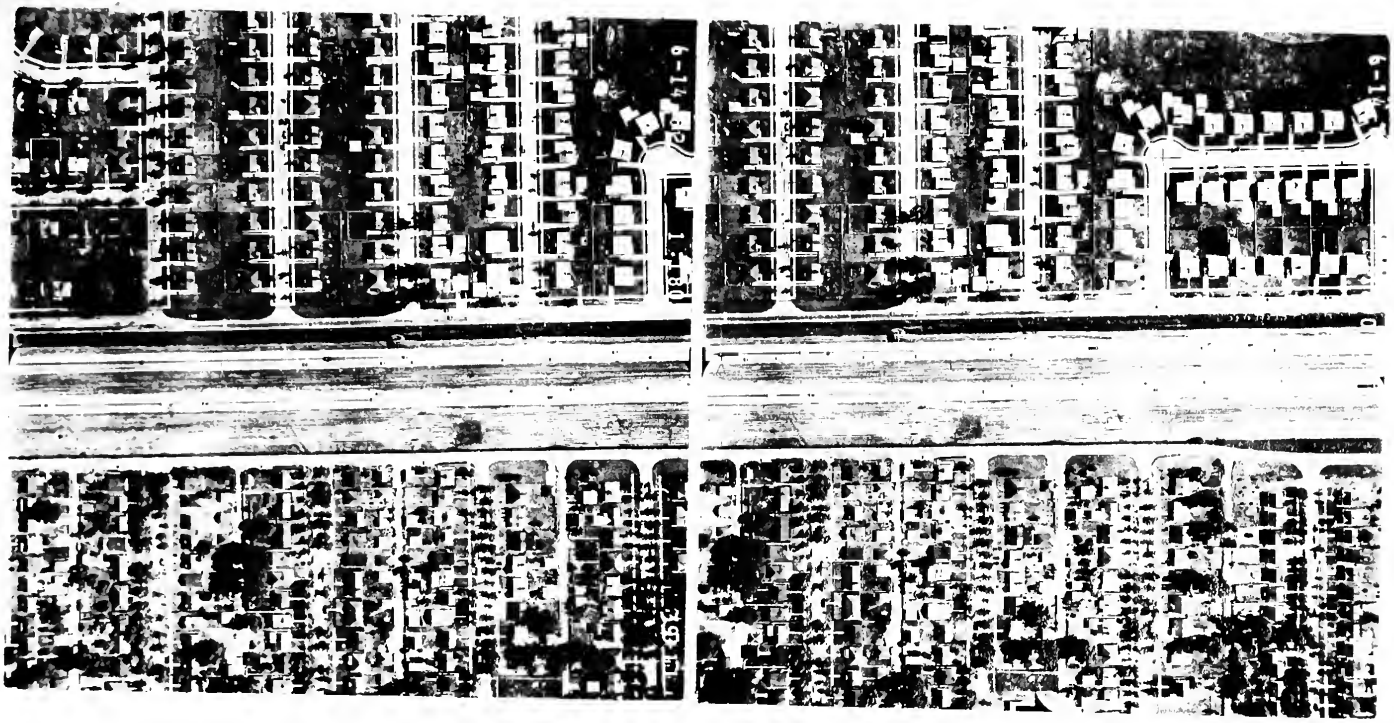

9 inch x 9 inch Exposures Reduced To Half Size

FIGURE 5. STANDARD VERTICAL AERIAL PHOTOGRAPHY

Each photo set was reduced independently. First, the scale of photography was determined from ground control afforded by the pavement expansion joints. Any significant change in scale over the length of flight was noted. Barring major variations, the mean scale value for all photos of a given site and day was used in the data analysis.

Viewing the photo pairs with a lens stereoscope permitted an approximately level section of tangent highway to be accurately defined for each site. The time duration of each flight run having been established in the field, the average time interval between successive exposures was readily computed. This quantity was then averaged over all the flight runs made at a given site and intervalometer setting.*

The vehicles of interest - those flowing freely on the through travel lanes - were identified on the photographs and numbered successively, by direction of flow, from the start of the photo run. Numbering was done directly on the prints with a lead or grease pencil.

Each vehicle appeared in at least two photographs. This permitted its speed to be obtained by measuring its progress along the roadway during the time interval between photos. A location on the highway common to both photographs served as a reference point to which the measurements could be scaled from the front bumper of the

---

* The assumption that the photographs for a given intervalometer setting were equally spaced in time was verified by tests conducted on the aircraft-camera-intervalometer system under simulated flight conditions. Variations about the mean interval were found to be less than $\pm$ 0.05 seconds.

vehicle in question (see Figure 6). The procedure yielded two values which were then added algebraically so as to give the distance traveled (D_v) in the photo interval.

"Headway" is commonly defined in traffic engineering as being the elapsed time between the passing of a fixed location on the highway of a common point (e.g. the front bumper) on two successive vehicles. The intermittent aerial photographic technique, being essentially a moving point that is recording vehicle positions as it surveys a route, cannot yield this quantity directly. Therefore, headways were initially determined from distance measurements as shown in Figure 6. A division of the distance headway by the speed of the "following" vehicle (S_f) yielded a time headway (h_t):

$$h_t = \frac{h}{S_f}$$

Traffic density (P) was established by simply counting the number of vehicles depicted in a photograph on either a "by lane" or "directional" basis.

Since each exposure was made at a slightly different point in time, traffic volumes could not be determined directly from a count of the vehicles pictured. However, a simple relationship between vehicle and aircraft velocities forms the basis of the "Speed Ratio" technique for estimating route volumes. This procedure considers volume as a function of average vehicle speed and route density.

Utilizing manual or automatic ground techniques, volumes are secured by recording the number of vehicles passing a fixed location during a specified period of time. However, when determining route volumes from aerial photographs, one must be cognizant of the fact

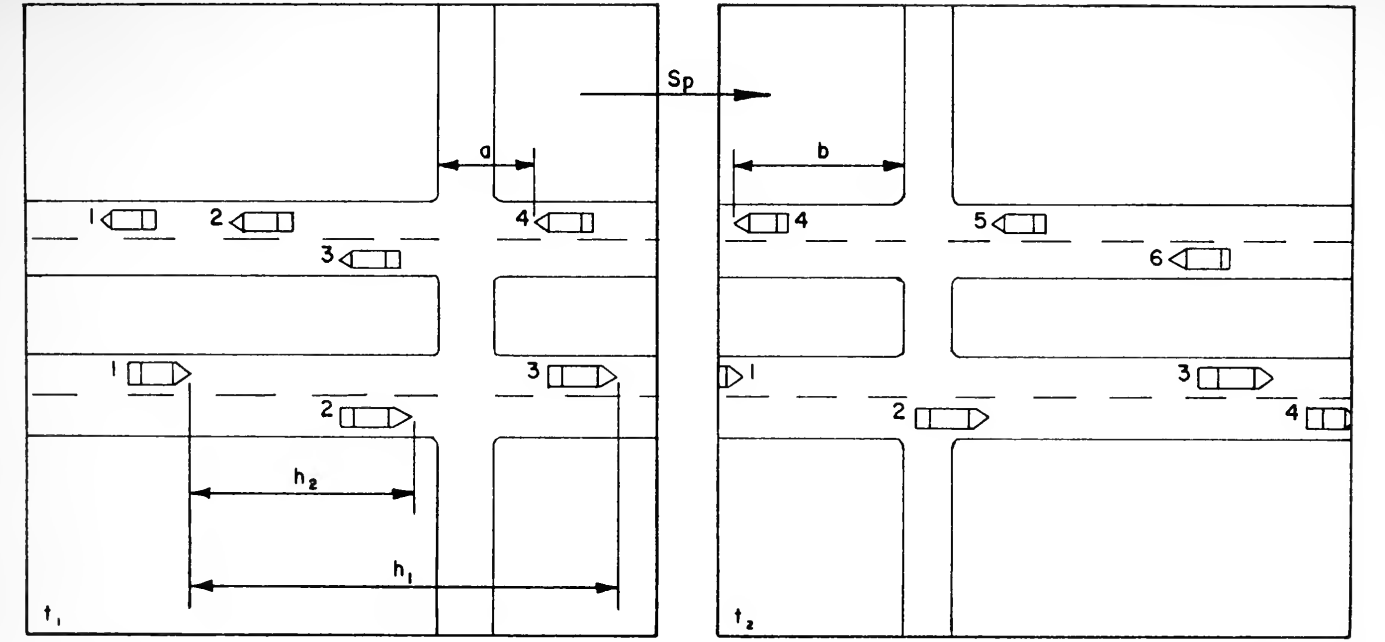

$a + b = D_V$ = distance vehicle travels in $(t_2 - t_1)$

h_1 = lane headway

h_2 = directional headway

FIGURE 6. TRAVEL DISTANCE AND HEADWAY MEASUREMENTS FROM TIME - LAPSE AERIAL PHOTOGRAPHY

that both the reference point (or aircraft) and the vehicles were in motion. Since the airborne camera did not photograph the entire section of highway, A-B, at the same instant in time, the total number of distinct vehicles depicted in a series of exposures represented not only those vehicles in the study section at the flight start, but also those which passed point B over the duration of the flight run (see Figure 8). It was this volume at B during a time t_p which the Speed Ratio method approximated by equation 1 when the aircraft was flying opposite the direction of traffic:

$$V_{t_p} = \frac{\bar{S}_v}{S_p + \bar{S}_v} \quad (n_{t_p}) \text{ . . . . . } \quad \text{Eq. 1}$$

where V_{t_p} = volume of traffic passing a fixed point in time t_p.

$\bar{S}_v$ = average vehicle speed in miles per hour.

S_p = aircraft ground speed in miles per hour.

n_{t_p} = the number of vehicles appearing between principal points A and B.

Two assumptions were inherent in the development of equation 1. All vehicles were considered to be traveling at: (1) the calculated average speed ($\bar{S}_v$); (2) equal distance headways.

If the aircraft was moving directionally with the traffic but at a speed greater than $\bar{S}_v$, the volume of traffic passing location B in time t_p was found from the relationship:

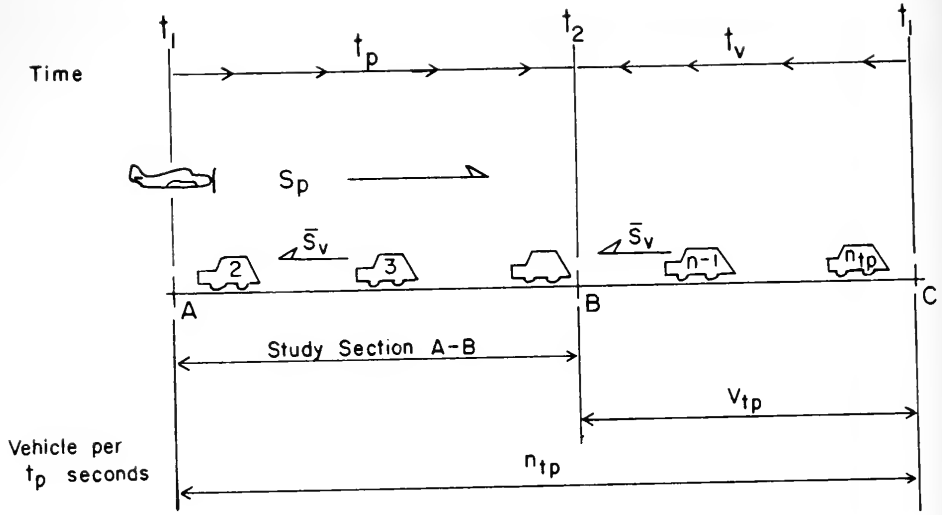

A = starting point of flight (photo principal point)

B = end point of flight (photo principal point)

BC = distance vehicles travel in time t_p

n_{t_p} = total number of distinct vehicles appearing on the airphotos between A and B (vehicles per t_p seconds)

S_p = speed of plane in feet per second

$\bar{S}_v$ = average vehicle speed in feet per second

$t_p = (t_2 - t_1)$ = time duration for flight from A to B in seconds

$t_v = (t_2 - t_1)$ = time, in seconds, required for vehicle n at point C to reach point B when traveling at $\bar{S}_v$. Defined as being equal to t_p.

V_{t_p} = vehicles passing point B in time t_p

FIGURE 7. "SPEED RATIO" CONCEPT FOR TRAFFIC VOLUMES FROM STANDARD AIRPHOTOS

VEHICLES AND PLANE MOVING IN OPPOSITE DIRECTIONS

$$V_{t_p} = \frac{\bar{S}_v}{S_p - \bar{S}_v} \quad (n_{t_p}) \quad \text{Eq. 2}$$

It should be noted that equation 2 is meaningless when $S_p < \bar{S}_v$.

Data reduction from the Ektachrome aerial photography was accomplished in essentially the same manner as described above. In this case, however, positive transparencies were viewed on a light table. All numbering and marking was done with a grease pencil directly on the "glossy" side of the photos.

TRAFFIC FLOW RELATIONSHIPS STUDIED WITH TIME-LAPSE AERIAL PHOTOGRAPHY

Nearly five hundred aerial photographs were taken as a part of the present research. The nature of the data obtained prohibited a thorough statistical analysis of any particular traffic characteristic or highway site. However, a wealth of information revealed itself on the aerial exposures, indicating the potential of time-lapse aerial photography in the study of traffic flow. To be of use to highway officials, procedures must be capable of yielding basic information on traffic speeds, headways and volumes.

Speeds

Figure 8 depicts a cumulative frequency graph of individual vehicle speeds compiled from aerial photographs of the Tri-State Expressway. The data were gathered over a one mile long homogeneous section of the highway so as to afford information comparable to a "spot" speed study. The vehicle speeds of Figure 8 were plotted for

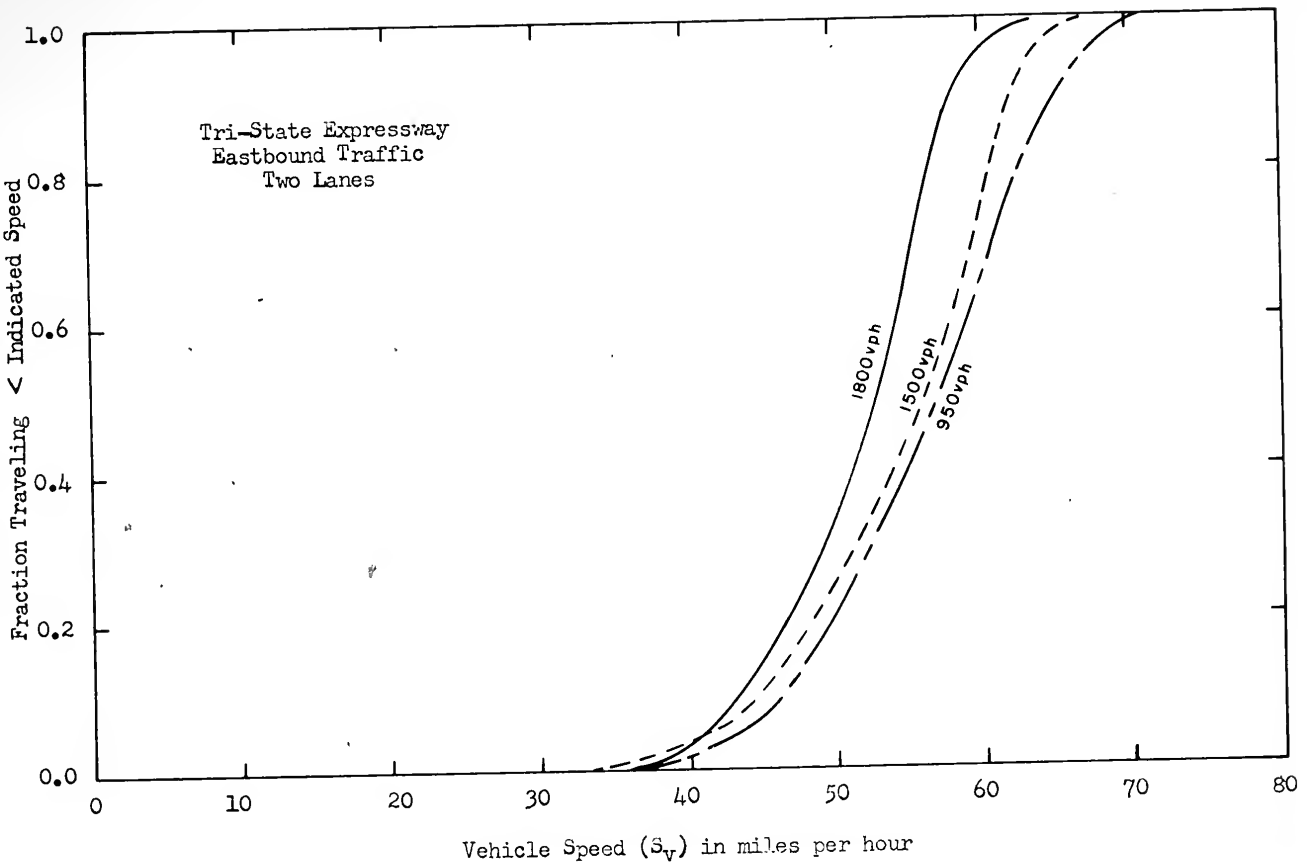

FIGURE 8. VEHICLE SPEED DISTRIBUTION AT VARIOUS DIRECTIONAL TRAFFIC VOLUMES ON A FOUR-LANE FREEWAY AS MEASURED ON AERIAL PHOTOGRAPHS

several directional volumes to illustrate the tendency for velocities to decrease in magnitude and range with increasing traffic.

Many investigators have noted that average speed tends to vary as a function of the traffic volume. Mean speeds for various directional volumes of traffic on the Tri-State Expressway are shown in Figure 9, along with a best fitting straight line constructed by the method of least squares. A slight decrease in speed with increasing volumewas indicated.

Time Headways

Cumulative frequency distributions of time headways for two lanes of unidirectional traffic at three different free flowing volumes were constructed from the Tri-State Expressway photography (see Figure 10). A comparison of these curves with the Poisson distribution seems to confirm the popular belief that vehicles are randomly distributed on the open highway. As expected, the frequency of short headways increased with mounting traffic volumes.

Lane Distributions

When studying highway capacity on multilane facilities, the investigator is often interested in lane usage characteristics. Figure 11 relates the number of vehicles per hour traveling in the median, or passing, lane as a fraction of the total, two-lane directional volume.

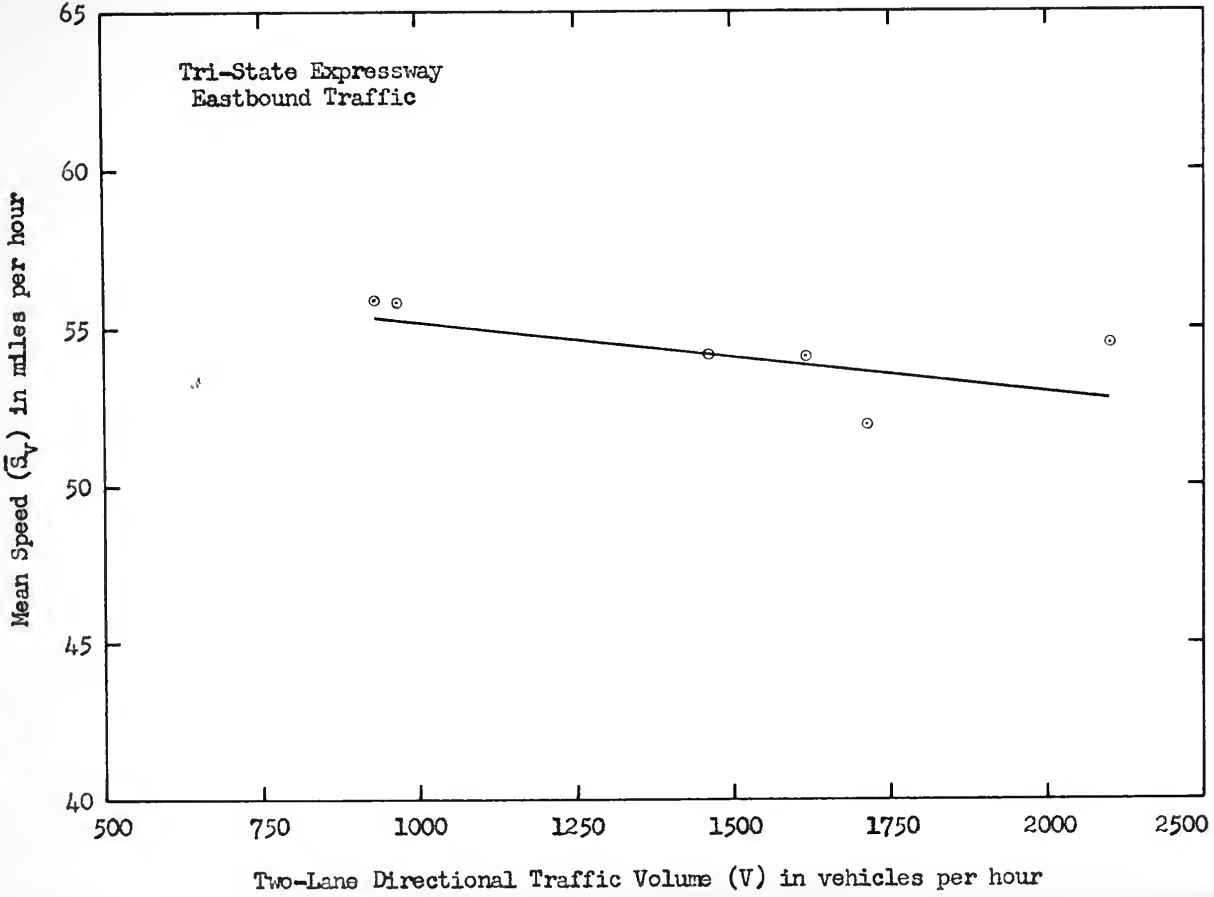

FIGURE 9. MEAN SPEED AS A FUNCTION OF DIRECTIONAL TRAFFIC VOLUME ON A FOUR-LANE FREEWAY AS MEASURED ON AERIAL PHOTOGRAPHS

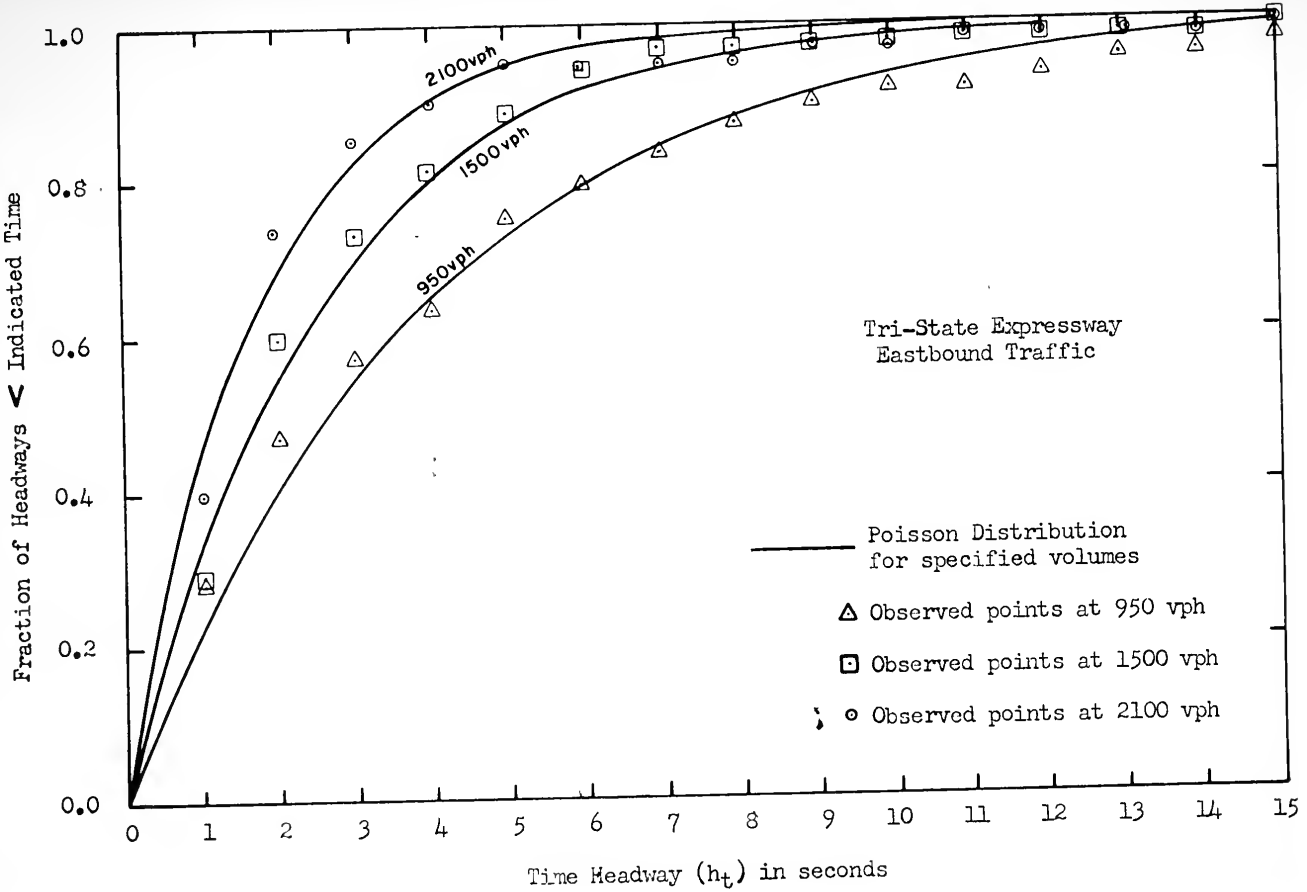

FIGURE 10. CUMULATIVE FREQUENCY DISTRIBUTION OF VEHICLE TIME HEADWAYS AT VARIOUS DIRECTIONAL VOLUMES ON A FOUR-LANE FREEWAY AS MEASURED ON AERIAL PHOTOGRAPHS

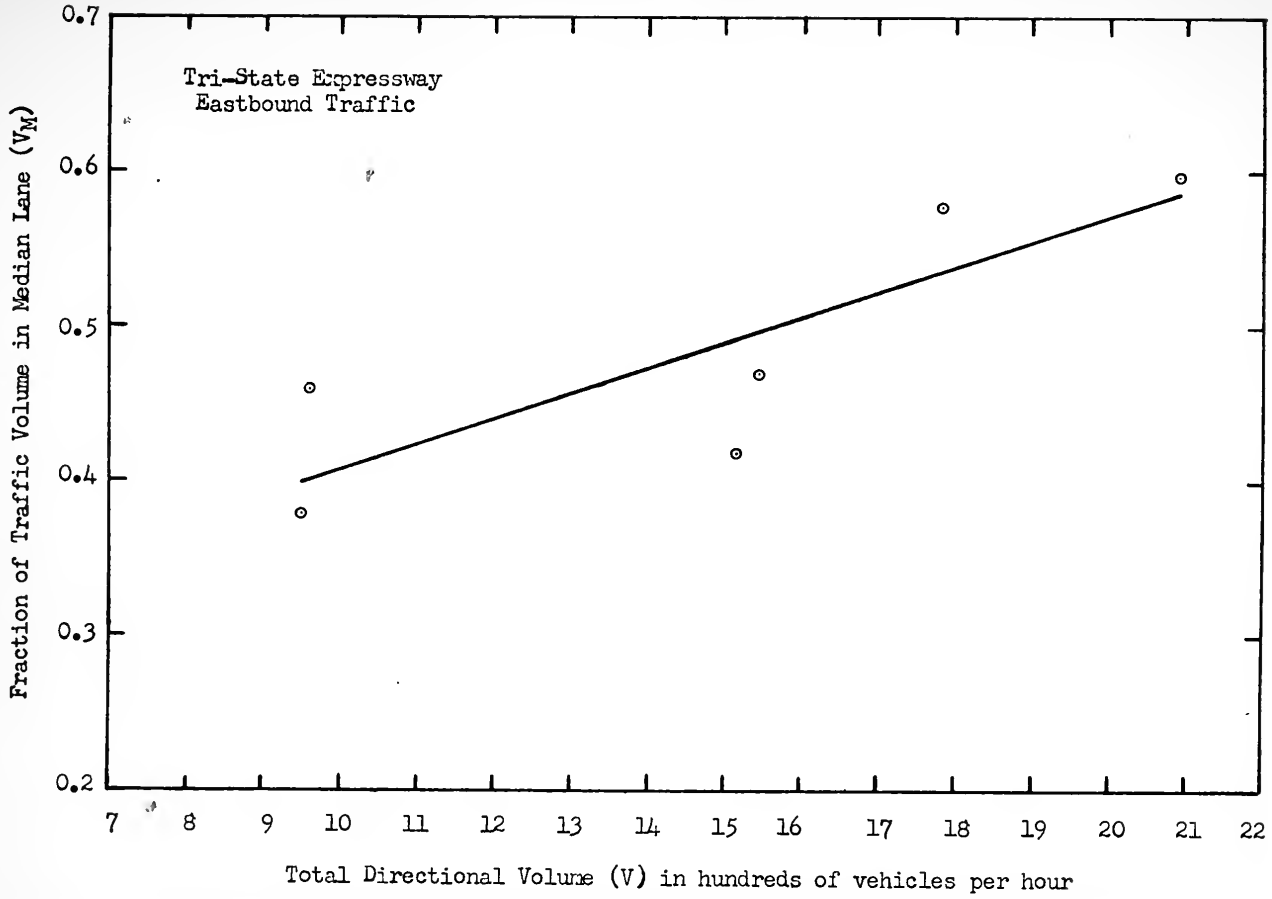

FIGURE 11. FRACTION OF THE DIRECTIONAL TRAFFIC VOLUME IN THE MEDIAN LANE AT VARIOUS VOLUMES ON A FOUR-LANE FREEWAY AS MEASURED ON AERIAL PHOTOGRAPHS

The preceding discussion has been confined to relationships involving only the basic traffic flow quantities of speed, volume, and time headway. However, several investigators (5, 7, 10, et al.) have suggested the use of "spacial" variables as being more meaningful and accurate representations of traffic flow phenomena. Data for two of these variables — traffic density and acceleration— are readily obtained with time-lapse aerial photography.

Traffic Density

Wagner and May (10) have suggested a graphical method for pin-pointing, in terms of traffic density, locations along an extended length of roadway which are particularly susceptible to congestion, and to determine, in units of time, the duration of these high density conditions. Utilizing time-lapse vertical photography, flight runs were made over the route at intervals throughout the study period. Every exposure afforded a density for each direction of traffic. These densities were plotted as functions of time and distance much as one would construct a topographic contour map. Connecting points of equal density, Figure 12 depicts contour lines at intervals of 20 vehicles per lane mile.

For the Madison Avenue example illustrated, high densities, indicative of extreme congestion, occurred near the Pleasant Run Parkway signalized intersection. This condition was particularly severe at about 5:30 P.M. when vehicles were backed up nearly 1000 feet.

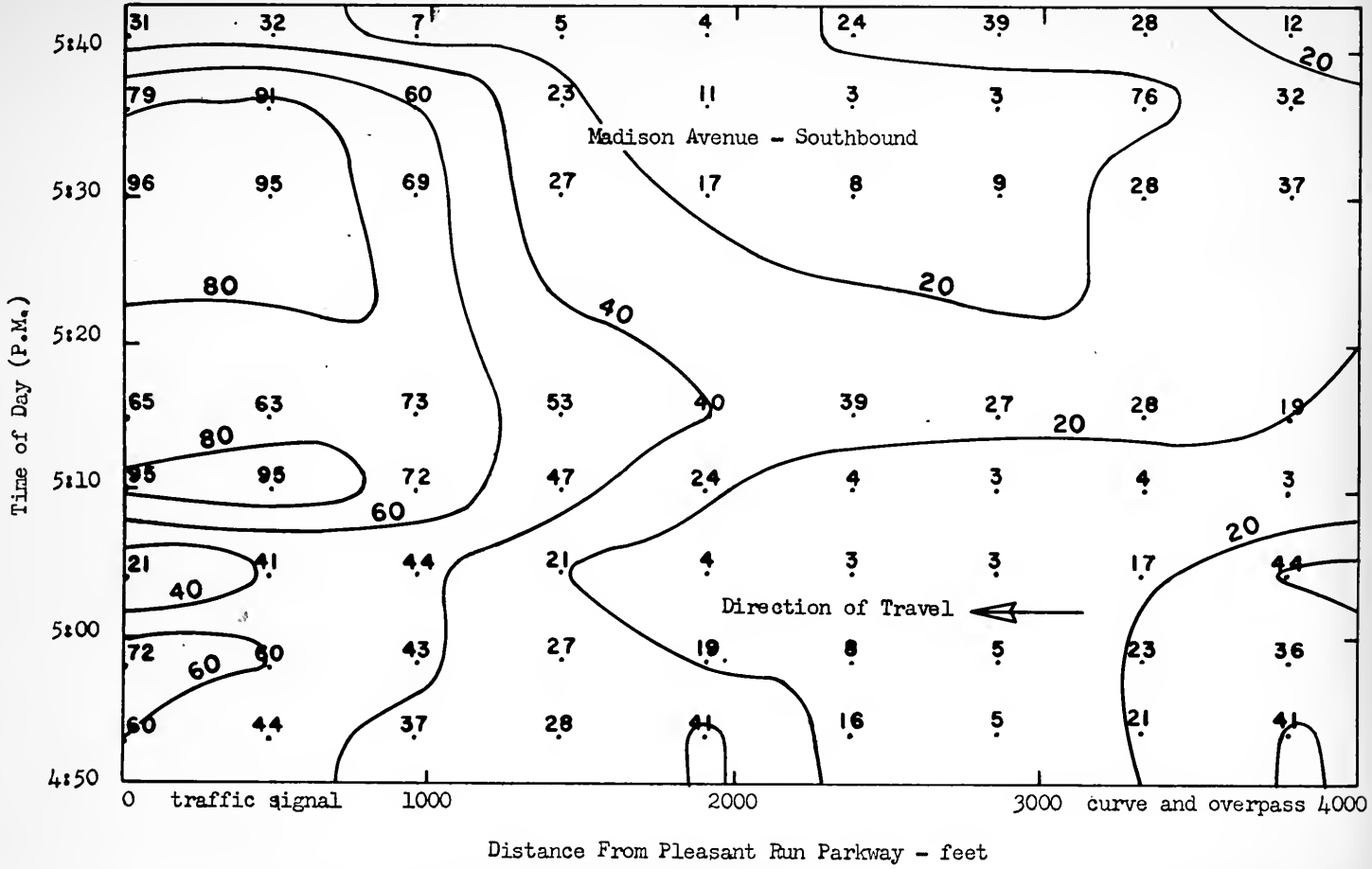

FIGURE 12. TRAFFIC DENSITY CONTOUR MAP PREPARED FROM AERIAL PHOTOGRAPHY

Figure 13 presents average speed as a function of route density for eastbound movements on the Tri-State Expressway. Traffic densities were recorded on aerial photographs and converted into vehicles per direction mile (all lanes in one direction) for analysis. A slight decrease in speed was observed to accompany moderate increases in density.

Acceleration

Although traffic density is a function of both speed and route volume, it alone cannot adequately describe the nature of vehicle flow. At any given density, the facility is either approaching congestion or emerging from congestion. This dynamic component of traffic flow is probably best described by vehicle acceleration patterns. A net acceleration of vehicle speeds foretells a decrease in density, the absence of acceleration reveals an unchanging density, and a net deceleration is indicative of increasing density.

The time-lapse aerial photography technique is an ideal means for observing the acceleration patterns of individual motorists as they progress along the highway. Figure 14 diagrammatically depicts the variations in speed for each of five vehicles traveling westbound on the Tri-State Expressway. Although in this example no vehicle was tracked for more than 2500 feet, longer traces could have been achieved by minimizing the speed of the aircraft relative to the vehicle's velocity and/or by increasing the flight elevation.

Figure 15 relates the positions of the five vehicles in point of time as well as space. Each vehicle's movement is represented by a line with the slope being a measure of speed as expressed in the equation,

$$\text{Tan } \theta = \frac{\triangle \text{distance}}{\triangle \text{ time}} = \text{vehicle speed}$$

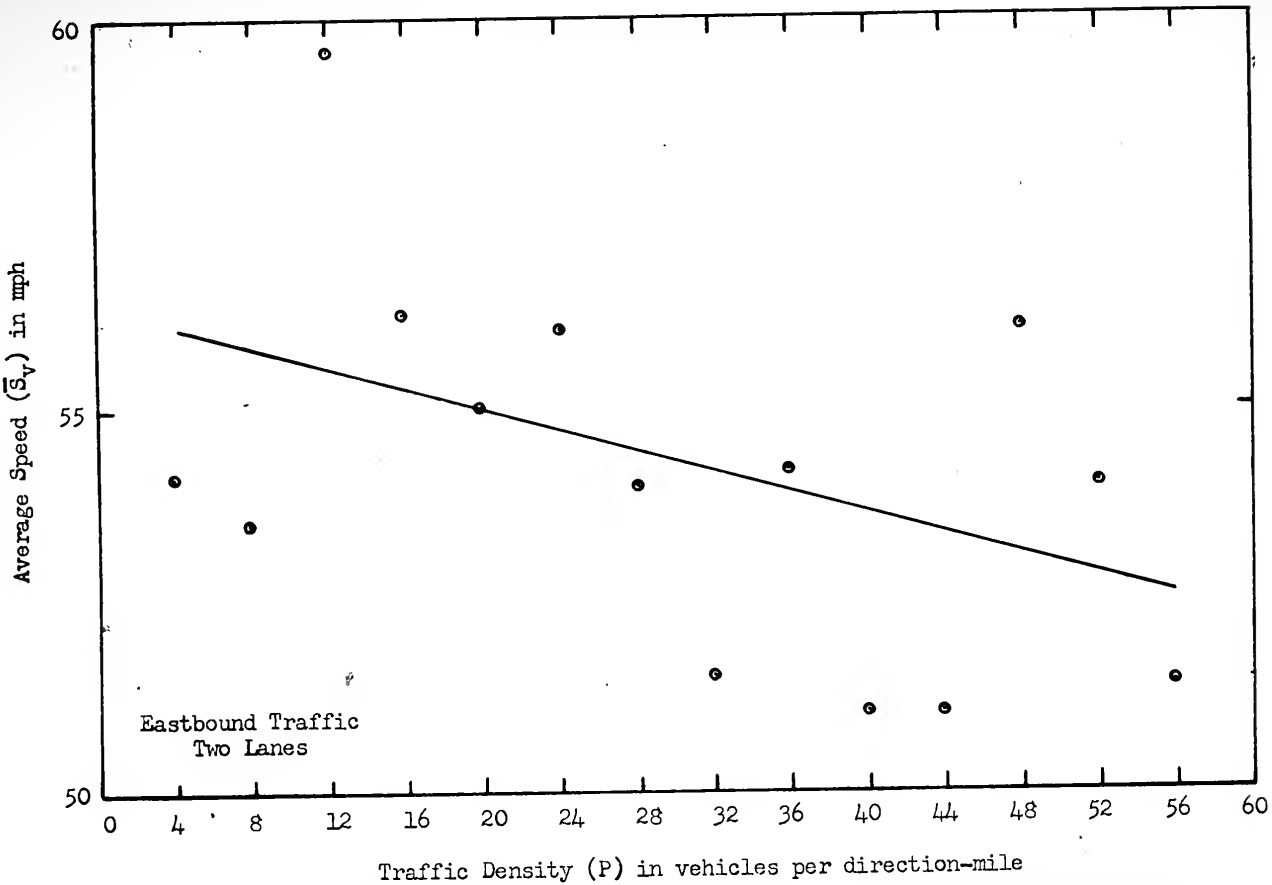

FIGURE 13. SPEED-DENSITY RELATIONSHIPS ON A FOUR-LANE FREEWAY AS MEASURED ON AERIAL PHOTOGRAPHS

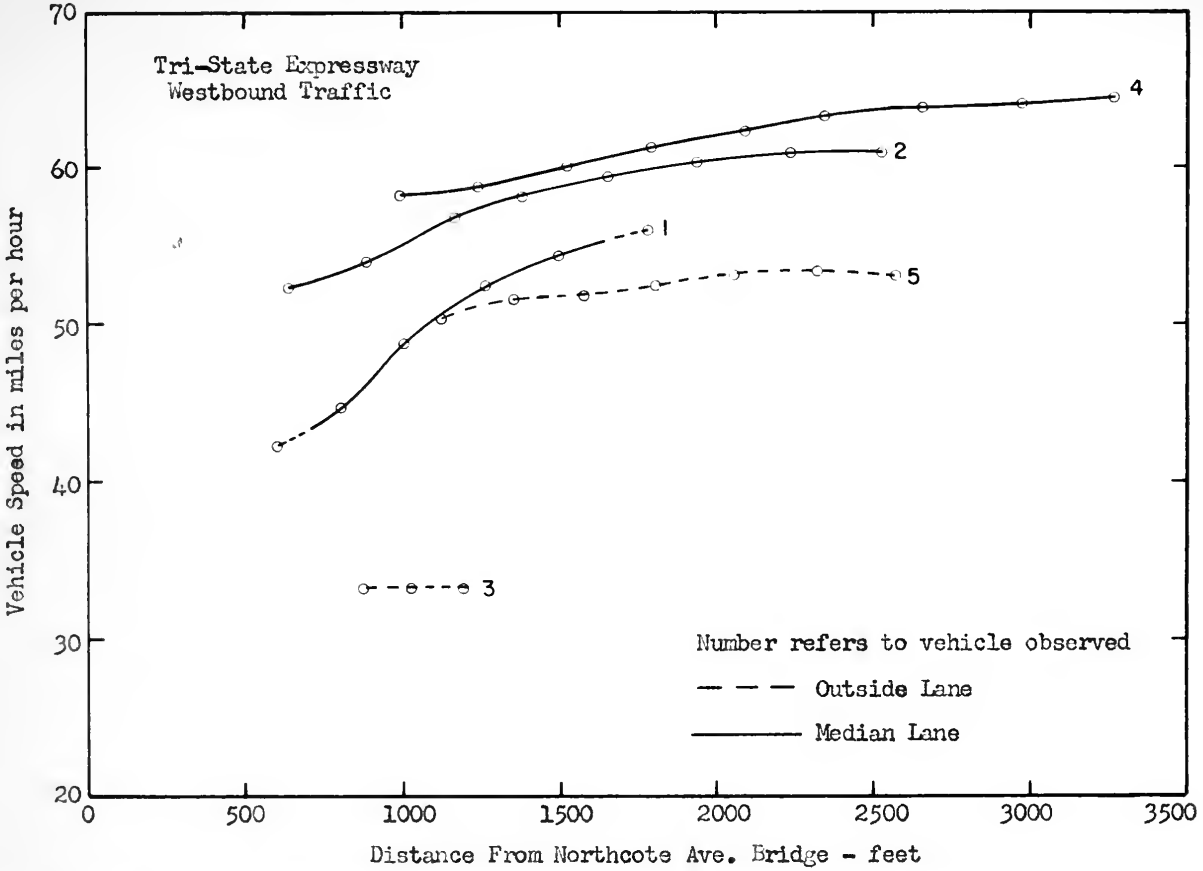

FIGURE 14. VEHICLE ACCELERATION AND SPEED PATTERNS ON A FOUR-LANE FREEWAY AS MEASURED ON AERIAL PHOTOGRAPHS

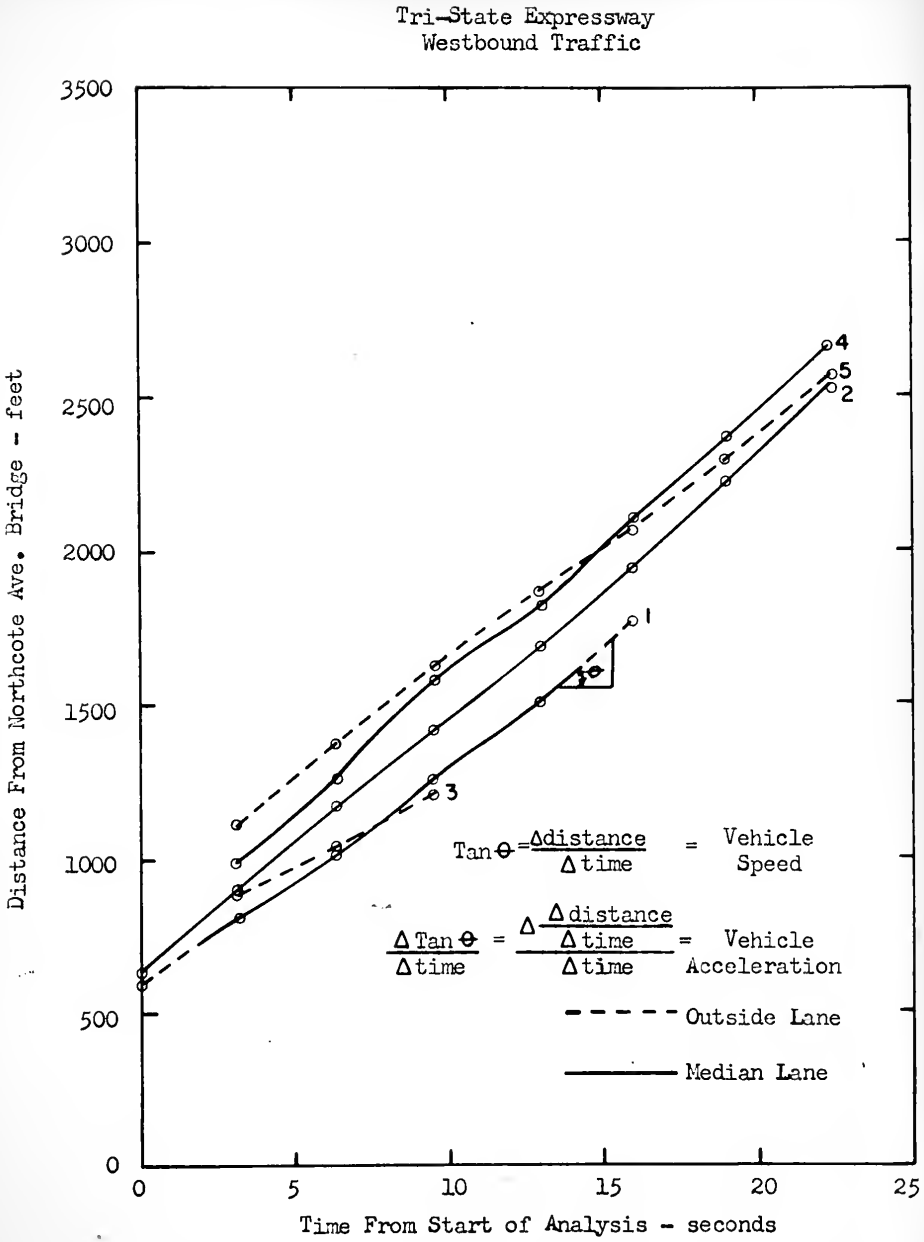

FIGURE 15. TRACKING THE MOVEMENT OF INDIVIDUAL VEHICLES IN TIME AND SPACE BY THE USE OF AERIAL PHOTOGRAPHY

Changes in slope (speed) yield vehicle accelerations:

$$\frac{\Delta \text{Tan } \theta}{\Delta \text{Time}} = \frac{\Delta \frac{\Delta \text{distance}}{\Delta \text{time}}}{\Delta \text{time}} = \text{vehicle acceleration}$$

Lines crossing one another indicate that the vehicles in question were at the same longitudinal location on the highway at a concurrent moment in time. Thus, either the vehicles had collided or one was passing the other. The plot shows that vehicle number 1 accelerated from 41 mph to 56 mph in passing vehicle number 3 eight seconds after the start of the photo analysis and 1100 feet West of Northcote Avenue. The passing maneuver of vehicle number 1 involved its moving from the outside lane to the median lane and then returning. This was completed in approximately 13 seconds and in somewhat over 950 feet.

Average Speed

Traffic speeds also may be expressed in spacial terms by plotting the average speed of the vehicles appearing in each exposure as a function of the aerial photograph's location on the route. This is shown in Figure 16 for the Shadeland Avenue (State Route 100) site and reveals a decided increase in the average velocity of vehicles traveling south from the Pleasant Run Parkway intersection. The peak average speed occurred about 1,700 feet beyond the Parkway, followed by a reduction in speed as the drivers approached and passed 16th Street.

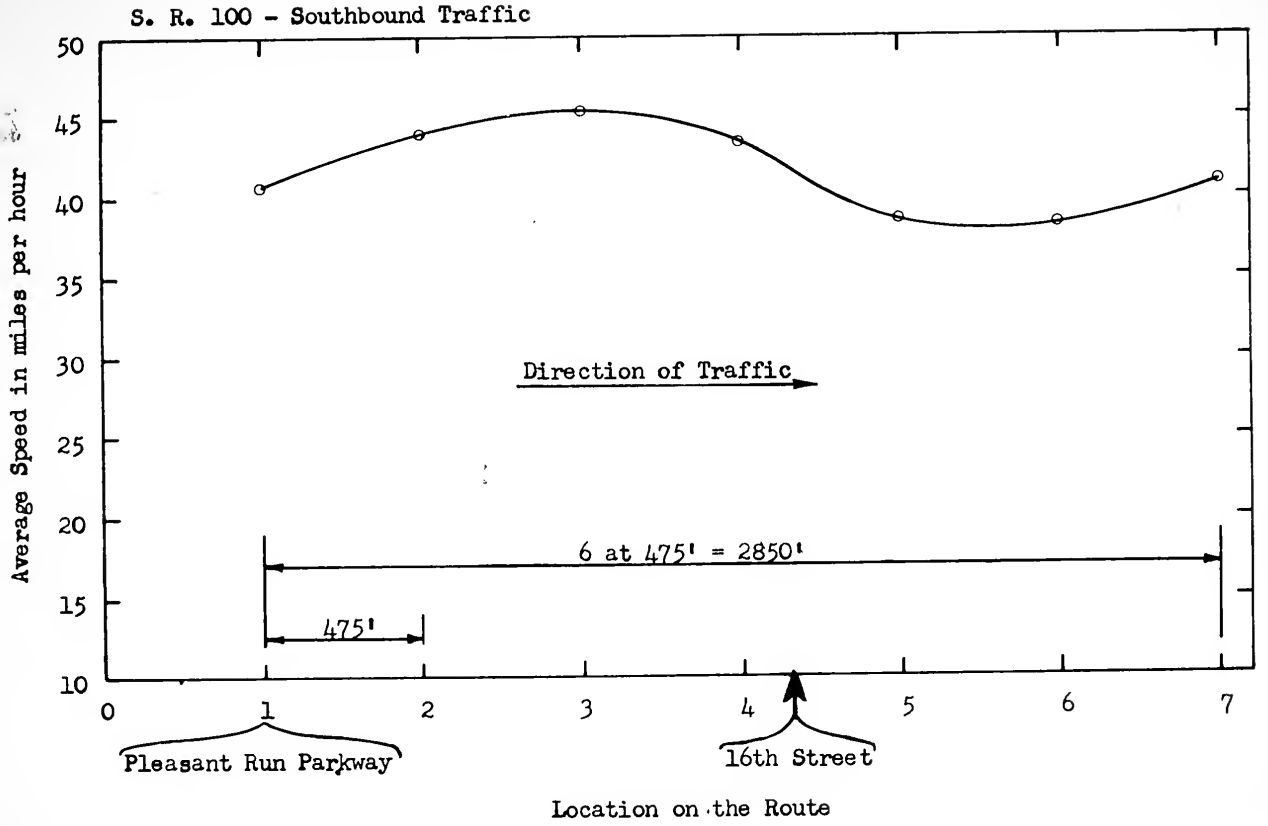

FIGURE 16. AVERAGE VEHICLE SPEED FOR DIRECTIONAL TRAFFIC AS A FUNCTION OF THE LOCATION ON THE ROUTE AS MEASURED ON AERIAL PHOTOGRAPHS

Distance Spacing

An analysis of vehicle spacing patterns assists the investigator in describing the character of traffic density and, as such, represents an important part of any traffic flow study. Since the gap (g) between successive vehicles is a spacial quantity, aerial photography is particularly applicable to this type of survey. Figure 17 depicts the mean minimum vehicle spacings allowed by passenger car motorists when following vehicles at various speeds.

Lane Changing

Figure 18 illustrates the results of a study of lane changing as a function of directional traffic volume on the Tri-State Expressway. The data were obtained from aerial photographic coverage of the site by noting the number of vehicles changing lanes as a fraction of the total vehicle count for each flight run. A regression line was statistically fitted to a few scattered points and indicated an increase in the frequency of lane changing with increasing traffic flow for the volumes shown.

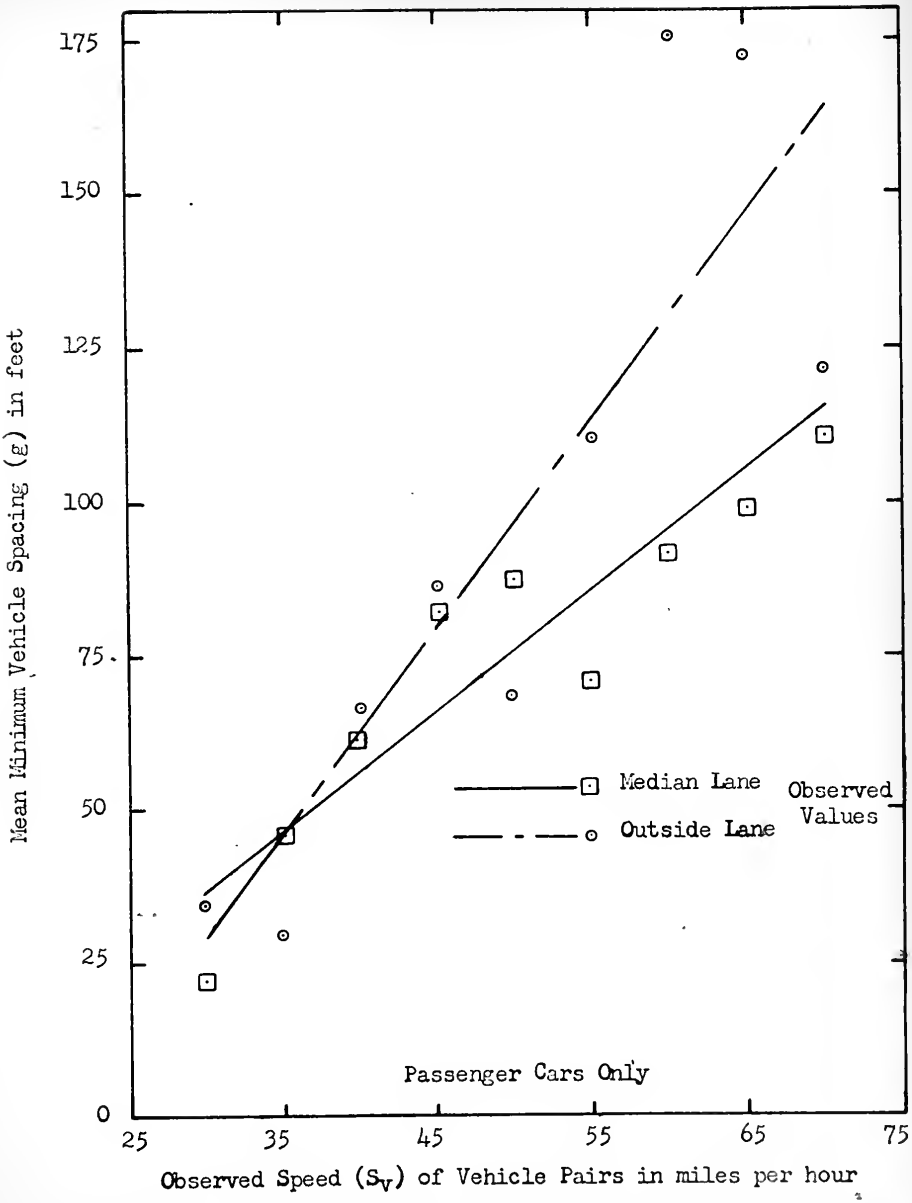

FIGURE 17. MINIMUM SPACINGS ALLOWED BY THE AVERAGE DRIVER WHEN TRAILING ANOTHER VEHICLE AT VARIOUS SPEEDS ON FOUR-LANE DIVIDED HIGHWAYS AS MEASURED ON AERIAL PHOTOGRAPHS

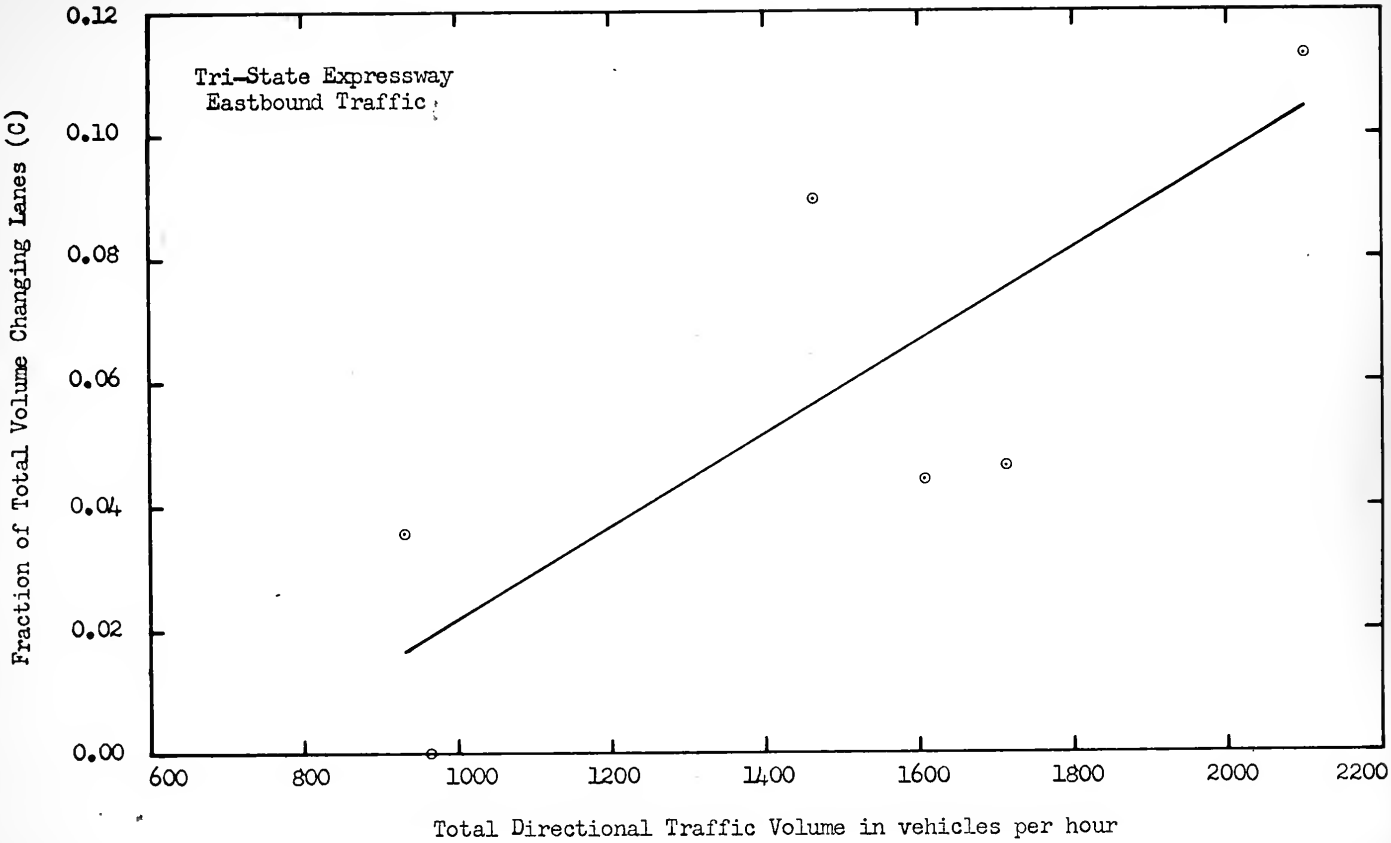

FIGURE 18. LANE CHANGING AS A FUNCTION OF DIRECTIONAL VOLUME ON A FOUR-LANE FREEWAY AS MEASURED ON AERIAL PHOTOGRAPHS

GENERAL ANALYSIS OF THE AERIAL PHOTOGRAPHY METHOD

Data Gathering Characteristics

Data gathering, as the term is employed here, encompasses two components of any traffic surveying method: a detecting device and the recording technique. It is toward an analysis of the efficiency, accuracy and measurement precision of the aerial photographic method that the following discussion is directed. Although the analysis deals primarily with the collection of speed, volume and headway data, it is applicable to the study of all traffic flow characteristics recorded on the photographs.

Equipment, Supplies and Personnel

The previous discussion on methodology has indicated the equipment, supplies and personnel employed in collecting data by the use of aerial photographs. These items are summarized, along with estimated costs, in Tables 1 and 2.

Costs may be expected to vary somewhat with the nature and scope of the study. For example, the costs per unit of data gathered would undoubtedly decrease as the survey period is lengthened.

Aerial photography can be employed to study, with a single complement of equipment and personnel, a large number of sites within close proximity of each other at essentially the same time. The method, therefore, becomes increasingly economical as the study locations become more numerous. Color photography, however, remains significantly more expensive than the standard black and white aerial photography.

TABLE 1

EQUIPMENT, SUPPLIES AND PERSONNEL USED IN

GATHERING TRAFFIC DATA - BLACK AND WHITE

TIME-LAPSE AERIAL PHOTOGRAPHY

Basic Equipment:

Piper Apache PA-23 aircraft
K-17C aerial camera
12" precision lens
B-3B intervalometer (2-120 seconds)
Morse B-5 rewind type film processing unit

Major Supplies:

Eastman Kodak Super XX Aerographic 1623 black and white film
(or Plux X Aerographic)
Film processing chemicals
Photographic paper

Personnel:

Aircraft pilot
Photographer
Film processor
Photo index compiler

Unit Costs:

Aircraft (with camera system and pilot)	-	$30.00/hour*
Photographer	-	$ 3.00/hour*
Film (150' roll)	-	$57.75/roll*
1175 exposures	-	$ 0.33/exposure*
Film processing (labor, chemicals, etc.)		
heavyweight 9"x9" prints	-	$ 0.26/print*
lightweight 9"x9" prints	-	$ 0.23/print*
Compilation of index sheet (approx. 50 prints)	-	$ 5.00/sheet**

---

* Costs estimated by the Indiana State Highway Commission, Bureau of Photogrammetric and Electronic Processes, 1962.

** Does not include cost of the 9"x9" prints making up the index.

TABLE 2

EQUIPMENT, SUPPLIES AND PERSONNEL USED

IN GATHERING TRAFFIC DATA - COLOR

TIME-LAPSE AERIAL PHOTOGRAPHY (TRANSPARENCIES)

Basic Equipment:

Piper Apache PA-23 aircraft
K-17C aerial camera
12" precision lens
B-3B intervalometer (2-120 seconds)
Morse B-5 rewind type film processing unit with seven 6 gallon tanks and reel

Major Supplies:

Eastman Kodak Aero-Ektachrome color film
Color film processing chemicals and supplies

Personnel:

Aircraft pilot
Photographer
Film processor

Unit Costs:

Aircraft (with camera system and pilot)	-	$30.00/hour*
Photographer	-	$ 3.00/hour*
Film (40' roll)	-	$72.00/roll*
@ 45 exposures	-	$ 1.60/exposure
Film processing for transparencies	-	$46.90/roll*
@ 45 exposures	-	$ 1.04/exposure

* Costs estimated by the Indiana State Highway Commission, Bureau of Photogrammetric and Electronic Processes, 1962.

Precision of Recorded Data

For the procedures described in earlier sections of this report, the aerial photographic technique afforded precisions of ± 0.6 feet for travel distances, ±0.3 feet for distance headways and approximately ±0.1 seconds for the photo interval. For meeting the requirements of a normal traffic study these levels of precision are considered adequate.

Accuracy of Data Gathering Methods

The aerial photographic method, when properly executed, affords the ±10% accuracy required of most traffic surveys. Knowledge of the true interval between successive photographs and a precise determination of the scale of photography are fundamental to an accurate measurement of speeds, volumes and headways from time-lapse photography. In the present study, the interval between exposures was approximately three seconds, with a maximum variance over a given flight run of ±0.05 seconds or less than ±2 percent.

The scale of photography was most accurately determined by frequent reference to established ground control points. In the present studies of level highway sections, the employed scale ratio of approximately 1:1800, once precisely defined, was found to vary less than ±5 percent over the one to two mile flight run or across any individual photograph.

The normal pitch and roll effects associated with standard aerial photography are not considered significant sources of error in scale determinations provided the pilot is experienced in aerial mapping and has made a conscientious effort to minimize motion about these axes. It seems probable, however, that atmospheric conditions

during the flight would have a profound effect on the degree of scale variations related to pitch, roll and changes in flight altitude.

Operational Problems and Limitations

During the course of the research, the operational problems and limitations associated with data gathering by aerial photography were noted. Chief among these were delays due to inclement weather, the method's restriction to daylight hours, obstructions to the aerial view, the necessity of maintaining a tangent flight path, and a fluctuating photo scale caused by changes in topography and/or flight elevation. In addition, variations in plane speed occasionally resulted in insufficient exposure overlap, the critical factor in assuring each vehicle's appearance in two successive photographs.

Data Reduction Characteristics

The reduction and tabulation of data is usually the most time consuming and costly phase of a traffic study. Thus, it is appropriate that some attention should be devoted to an analysis of the economics, precision and time efficiency of the data reduction techniques investigated. For discussion purposes, the analysis is limited to the reduction of speed, volume and headway quantities.

Equipment and Supplies

In designing the data reduction procedures employed in this study, every effort was made to minimize the amount of special equipment and skilled labor required. Therefore, the methods described can be readily adopted by any highway organization with the hiring of an adequate clerical staff.

The use of grease pencils, drafting [illegible]les, appropriate [illegible] and a magnifying glass [illegible] the cost of reduction equipment [illegible] and white aerial photographic prints to about $13.00 per man. The necessity of a light table for viewing the [illegible] $30 per man when obtaining [illegible]

of the black and white versus the color aerials. Tests (F-test) were made, at a 0.05 level of significance, of the hypothesis,

$$U_A = U_B$$

where U_A = true mean rate of data reduction from black and white aerial photographs

U_B = true mean rate of data reduction from the color aerial photographs.

Vehicle numbering, type classification and velocity measurement rates were combined and a single "speed data" reduction rate computed in minutes per vehicle. At a 0.05 level of probability, the color and the black and white time-lapse aerial photographic methods were not found to differ significantly in their efficiency of speed data reduction. The mean rates for the black and white photographs and color exposures were 2.73 and 2.74 minutes per vehicle respectively.

Testing the efficiency of the headway measuring task at a 0.05 level of significance, the black and white and the color photographs differed significantly, with the former being the more efficient. The respective reduction rates were 1.05 and 1.30 minutes per vehicle.

Variances in the rates of volume determinations were analyzed and both aerial photographic methods were found to have an average rate of data reduction of 0.53 minutes per vehicle.

Problems and Limitations

Many problems unique to the aerial photographic method were observed during the data reduction phase of the research. In addition to "leaning" vehicles under bridges, the pronounced tree and building

shadows of the late afternoon often complicated vehicle identification and impaired the precision of measurements from the photographs. Similarly, on routes running east-west shadows cast by the vehicles themselves rendered measurements to the darkened bumpers difficult to obtain. Shadowed vehicles were only slightly more distinct on the color transparencies than on black and white prints.

Most of the workers found a small magnifying glass helpful in identifying vehicles and measuring distances on the photos. However, several complained of eye strain and attributed it to optical distortions in the lens. Tiring of the eyes was also reported following a prolonged viewing of the color transparencies on a light table.

All of the workers admitted being distracted by the roadside culture depicted on the photos (e.g., a large outdoor swimming pool adjacent to the Tri-State Expressway), and each found the judgments required in deciding questionable cases of vehicle type or land usage to be time consuming. The individual black and white prints were somewhat cumbersome to work with and required tedious orientation before measurements could be obtained. Considerable care was required when measuring distances on the photographs so as to minimize distortions due to parallax; the safest procedure [illegible] to measure only between points on or very near the ground.

CONCLUSION

The aerial photographic method proved capable of effectively detecting and recording the basic traffic flow elements of speed, volume and headway.

In obtaining a wide variety of additional data, the time-lapse aerial photographic technique, when adopted to a specific survey's requirements, would appear to be particularly useful. Such physical characteristics as vehicle classification and roadway geometry and condition are readily and permanently recorded by the photographic method. Since intermittent aerial photographs afford a "view" of a vehicle's movement over both space and time, the combined physical and psychological phenomena in traffic flow may be studied in terms of traffic density, acceleration and deceleration practices, passing behavior, lateral placement, spacing habits and merging, diverging and weaving patterns.

Among the most important assets of the aerial photographic method is its ability to pictorially record the environment in which traffic data is obtained. This attribute enhances the value of the data by affording the investigator with possible reasons for unusual traffic behavior.

Standard aerial photography, however, cannot be efficiently employed for a "spot" study of but one or two elements of traffic flow at a few sites. Photography begins to have practical application only when it is desired to procure concurrently a permanent record of a variety of traffic and roadway information at a large number of locations.

The use of standard aerial photography is impeded by the necessity of having daylight, good flying weather, and an absence of major obstructions to the vertical view. In addition, the cost of collecting and reducing basic traffic data on aerial photographs is considerably greater than with conventional ground techniques in all but the most complex and extensive surveys.

Color photography yields in the greatest detail a complete view of the study route, its vehicles and the surrounding culture. The advantages of color over black and white exposures, however, rarely justify the additional cost.

Aerial photography is not the "ultimate" in techniques for surveying vehicle traffic characteristics. In common with the more conventional methods, photography suffers from several practical limitations. Nevertheless, the technique affords the traffic engineer a valuable tool for investigating many of the most important and complex elements of traffic flow.

BIBLIOGRAPHY

1. Manual of Photogrammetry. [illegible] Society of [illegible]
Washington, D. C., 2nd Edition, [illegible]

2. Committee on Highway Capacity, [illegible] Capacity
U. S. Department of Commerce, Bureau of Public [illegible]
D. C., 1950.

3. Duncan, A. J., Quality Control and Industrial [illegible]
R. Irwin, Inc., Homewood, Illinois. [illegible]

4. Greenshields, B. D., "The Photographic Method of [illegible] Behavior", Proceedings, Highway Research Board, V[illegible] 1933.

5. Greenshields, B. D., "A Study of [illegible]
Highway Research Board, Vol. 14, p[illegible]

6. Greenshields, B. D., "The Potential [illegible] in Traffic Analysis", Proceedings, [illegible] 27, pp[illegible]

7. Greenshields, B. D., "The Density [illegible]
Traffic Engineering, Vol. 30, No. [illegible] 26-32, [illegible]

8. Johnson, A. N., "Maryland Aerial Survey of Highway [illegible] Baltimore and Washington", Proceedings, Highway [illegible] Vol. 8, pp. 106-115, 1928.

9. "Aerial Study of Tunnel Approach [illegible]
Magazine, Vol. 92, No. 7, pp. 97-[illegible]

10. Wagner, F. A., and May, A. D., Jr., [illegible]
in Freeway Traffic Operations Study, [illegible]
42nd. Annual Meeting of the Highway [illegible]

11. Wohl, M. and Sickle, S. M., "Combining Short Cut [illegible] Approach to Traffic Studies", [illegible] No. 3, pp. 397-403, June 1959 and Vol. [illegible] December 1959.